EXERGO-ENVIRONMENTAL ANALYSIS OF A COMBUSTION GAS TURBINE SYSTEM SUBJECTED TO INLET AIR COOLING AND EVAPORATIVE AFTER COOLING OF THE COMPRESSOR DISCHARGE

BY

Suleman Mohammed

A Thesis Presented to the

DEANSHIP OF GRADUATE STUDIES

KING FAHD UNIVERSITY OF PETROLEUM & MINERALS

DHAHRAN, SAUDI ARABIA

In Partial Fulfillment of the
Requirements for the Degree of

MASTER OF SCIENCE

In

MECHANICAL ENGINEERING

May 2017

KING FAHD UNIVERSITY OF PETROLEUM & MINERALS

DHAHRAN- 31261, SAUDI ARABIA

DEANSHIP OF GRADUATE STUDIES

This thesis, written by **Suleman Mohammed** under the direction his thesis advisor and approved by his thesis committee, has been presented and accepted by the Dean of Graduate Studies, in partial fulfillment of the requirements for the degree of **MASTER OF SCIENCE IN MECHANICAL ENGINEERING.**

Dr. Abdul Khaliq
(Advisor)

Dr. Zuhair M. Gasem
Department Chairman

Dr. Luai M. Alhems
(Member)

Dr. Salam A. Zummo
Dean of Graduate Studies

Dr. Haitham M. Bahaidarah
(Member)

Date 25/05/2017

This work is dedicated to my beloved parents, wife and children

ACKNOWLEDGMENTS

All the praises and thanks to Allah (Subha na hu wataala) for blessing me with the power of knowledge and guidance to carry out this work for completion of my M.Sc. in Mechanical Engineering in King Fahd University of Petroleum and Minerals.

I would like to express my greatest gratitude to my advisor, Dr. Abdul Khaliq, who expertly guided me through my graduate education and shared the excitement of three years of discovery. His unparalleled support helped me solve the hurdles in my research work.

I would like to extend my appreciation to all my committee members, Dr. Luai M. Al-Hadhrami and Dr. Haitham M. Bahaidarah for their valuable insights and guidance throughout my thesis work.

My thanks to the Dean, all the faculty and staff members of mechanical engineering departments, KFUPM and all the working members of the prestigious university specially Mr. Asif Sayani with whom I had interacted during my stay.

Above ground, I am indebted to my parents, without whom, the destination of a graduate student would never have been possible. I am grateful to my parents who supported me psychologically and financially. I would also acknowledge my wife, Afrin, and my children who blessed me with a life of joy when nothing appeared joyful in my life.

Lastly, I would thank the Indian friends specially Ata Ur Rahman, Faisal, Basheer, Amir, Raaghib, Inayath from KFUPM who made my stay joyful than it could have ever got.

Thanks to them for any support or help I have taken from them. I would also like to thank all my other friends from and outside of KFUPM. May Allah bless them all.

TABLE OF CONTENTS

LIST OF TABLES

LIST OF FIGURES

LIST OF ABBREVIATIONS

Symbols

$a_1, a_2, ..$	coefficients of polynomial determining specific heat
C_p	specific heat at constant pressure, kJ/kg-K
$\bar{C}_p$	molar specific heat at constant pressure, kJ/kmol-K
$\bar{C}_v$	molar specific heat at constant volume, kJ/kmol-K
e_x	specific exergy, kJ/kg
$\bar{e}_x$	molar specific exergy, kJ/kmol
f	specific general quantity
g	gibbs function, kJ/kg
h	specific enthalpy, kJ/kg
$\bar{h}$	molar specific enthalpy, kJ/kmol
$\dot{I}$	irreversibility rate, kW
k	polytropic ratio
MW	molecular weight, kg/kmol
$\dot{m}$	mass flow rate, kg/s
n	number of moles, kmol
P	pressure, kPa
$\dot{Q}$	heat transfer rate, kW
R	gas constant, kJ/kg-K
$\bar{R}$	universal gas constant, kJ/kmol-K
s	specific entropy, kJ/kg-K
$\bar{s}$	molar specific entropy, kJ/kmol-K

T	temperature, K
$\dot{W}$	work done rate, kW
v	specific volume, m^3/kg
$\dot{X}$	flow exergy rate, kW
x, r	pressure ratios
y	mole fraction
( )	'a function of' a quantity

Greek Letters

α	mass rate ratio
δ	percentage of air in different zones
θ	percentage of pressure drop
Δ	difference of a quantity
$\Delta\bar{H}_r$	molar enthalpy of reaction, kJ
$\Delta\bar{G}_0$	molar gibbs function of reaction, kJ
ε	effectiveness
ϕ	relative humidity
Φ	equivalence ratio
η	efficiency
ω	humidity ratio, kg/kg of air
$\bar{\omega}$	molar humidity ratio, kmol/kmol of air

Abbreviations

AC	after cooler
AH	air humidifier
LPC	low pressure compressor
CC	combustion chamber
Ex	expander
gen	generator
HE	heat exchanger
HPC	high pressure compressor
HPGT	high pressure gas turbine
IC	intercooler
LHV	lower heating value of the fuel kJ/kg
LPGT	low pressure gas turbine
MC	mixing chamber
PC	plant capacity, m^3
Re	recuperator
RH	reheater
TIT	turbine inlet temperature, K
WAR	water-to-air ratio, kg/kg of air
WH	water heater

Subscripts

0	ambient condition
1,2,3,	state points

a	air
ch	chemical
f	fluid
i	iterating parameter
in	input
mix	mixture
out	output
pump	pump
ph	physical
R	reactants
r	reaction
sat	saturation condition
t	turbine
v	vapor
W	work
w	water

Supercripts

o	standard state or formationi
cfw	cooling fluid water
aha	air humidifier air
ahw	air humidifier water
whw	water heater water

ABSTRACT

Full Name : Suleman Mohammed

Thesis Title : Exergo-environmental analysis of a combustion gas turbine system subjected to inlet air cooling and evaporative after cooling of the compressor discharge

Major Field : Mechanical Engineering

Date of Degree : May 2017

Gas turbines, which are greatly used for electric power generation, faces a problem of power output reduction at peak ambient conditions. Application of Brayton refrigeration cycle along with the evaporative after cooling in combustion turbines was found to be a promising option for power augmentation and NOx emission reduction. Therefore, in the current research, a gas turbine fueled by natural gas and integrated with the Brayton refrigeration cycle for inlet air cooling along with the evaporative after cooling was studied. The performance of the proposed cycle was assessed theoretically from energy, exergy and environment point of view. To this effect, first a detailed exergy analysis was conducted to identify the causes and locations of thermodynamic imperfection and then the exergetic variables, viz; cycle exergetic efficiency and component irreversibility were calculated. Semi-analytical relations for the theoretical measurement of two key emissions namely; NOx and CO were studied and applied. The effects of some influencing parameters such as the turbine inlet air temperature, ambient relative humidity, ambient air temperature, extraction pressure ratio, extracted mass rate, overall pressure ratio, water to air ratio and fuel-air equivalence ratio on energetic, exergetic, and environmental performance of the cycle was observed. Efforts have been made to

determine the values of all these design parameters at the point of minimum exergy destruction and minimum CO and NOx emissions. It was found that the proposed gas turbine cycle can bring down the emission levels to the regulatory standards (less than 35 ppm). It was also able to increase the power output by 31% with a slight drop in its efficiency. Also, the exergy lost to the environment was considerably reduced from 18% to 9%. Therefore, the results of this research may be used to determine the range of operating parameters at which the gas turbine could be operated which can provide a considerable reduction in the emissions while maintaining a higher performance.

ملخص الرسالة

الاسم الكامل: سليمان محمد هارون

عنوان الرسالة: تأثير التوربينات التي تعمل على العمواد البارد عند الدخول والمبخر عند الخروج على البيئة وكفاءة

التخصص: هندسة المكانكية

تاريخ الدرجة العلمية: مايو 2017

ن مولدات الطاقة (الطوربينات) تستخدم في اغلب الأحيان لإنتاج الطاقة الكهربائية. ولكن كفاءة هذه المولدات تكون منخفضة حين ترتفع درجة الحرارة والرطوبة في المحيط. ولكن الدراسات السابقة أوضحت ان طريقة(براتيون للتبريد الدوري) تساعد في زيادة الكفاءة. لذلك في هذه الأطروحة سيتم دراسة مولدات الطاقة (الطوربنات) التي تعمل على الغاز الطبيعي مضاف إليها طريقة (براتيون) للتبريد حيت يتم إدخال الهواء البارد وعند الخروج يتحول إلى بخار ماء. وقد تمت دراسة هذا النظام نظرياً من حيث الكفاءة ومدى تأثيرها على البيئة. ولتحقيق ذلك، أولا تم إجراء تحليل للطاقة بشكل مفصل لتحديد أسباب ومواقع النقص في الديناميكا الحرارية. ومن ثم تم حساب المتغيرات في الطاقة وأثر النقص في كل مكون. بعد ذلك تم تحليل اثنين من الانبعاثات الرئيسية – أكاسيد النيتروجين وأول أكسيد الكربون (NOx and CO). بعض العوامل المؤثرة كانت مثل درجة حرارة الهواء الداخل للتوربينات ونسبة الرطوبة ودرجة حرارة الهواء المحيط ونسبة الضغط ومعدل الكتلة المستخرجة. ايضا تمت دراسة تأثير نسبة ضغط الهواء ونسبة الهواء الى الماء ونسبة الوقود للهواء وتأثيرها على الكفاءة والإنبعاثات الضارة على البيئة بسبب انبعاث ثاني أكسيد الكربون وأكاسيد النيتروجين. واما النتائج المستفاده من اضافة دورة التبريد بطريقة (برايتون)، انها قللت من الغازات المنبعثة الى المستويات المقبوله والمتعارف عليها دوليا. كما انها استطاعة زيادة كمية الطاقه المستفاد من التوربين بنسبة ٣١ بالمئة وزيادة االكفاءة من ٩ الى ١٨ بالمئة. ولذلك نأمل ان شاء الله ان يتم استخدام هذا البحث بشكل عملي في تصنيع التوربينات لما فيه من مميزات.

CHAPTER 1

INTRODUCTION

1.1 Background

Energy is a key for economic growth of every nation and energy conversion from given into desired form in an efficient and environment friendly manner is still a challenge. Majority of power production comes from the combustion of fossil fuels which results in the fast depletion of fossil fuel reserves and environment degradation which creates a need to enhance the fuel efficiency utilization and emissions reduction. The climate of the Kingdom of Saudi Arabia is harsh and extreme especially in the summer and can rise up to 53^{o}C during summer [1]. Having a desert climate in the Kingdom, large ambient temperature variations are observed on daily and seasonal basis. Seasonal temperature variations causes the power demand to fluctuate and its peak is observed in summer afternoons due to the air conditioning loads. Combustion turbines are extensively used in the gulf region for meeting out the increasing demand of electric power at peak summer conditions due to their thermodynamic, economic and environmental benefits [2]. Saudi Electric Company (SEC), which provides power generation, transmission and distribution to Saudi Arabia has revealed that, until 2012, 51% of its total power was been generated using Gas Turbines while 18% of the total power is produced in a combined cycle mode of gas and steam shown in Figure 1 (a). In addition, cumulatively 12000 MW plants (Gas Turbine and Combined cycle mode) are still under construction which would be ready by

the year 2021 which would make gas turbines and combined cycle mode contribution to reach 56% of its total generation capacity as can be seen from Figure 1 (b) [3].

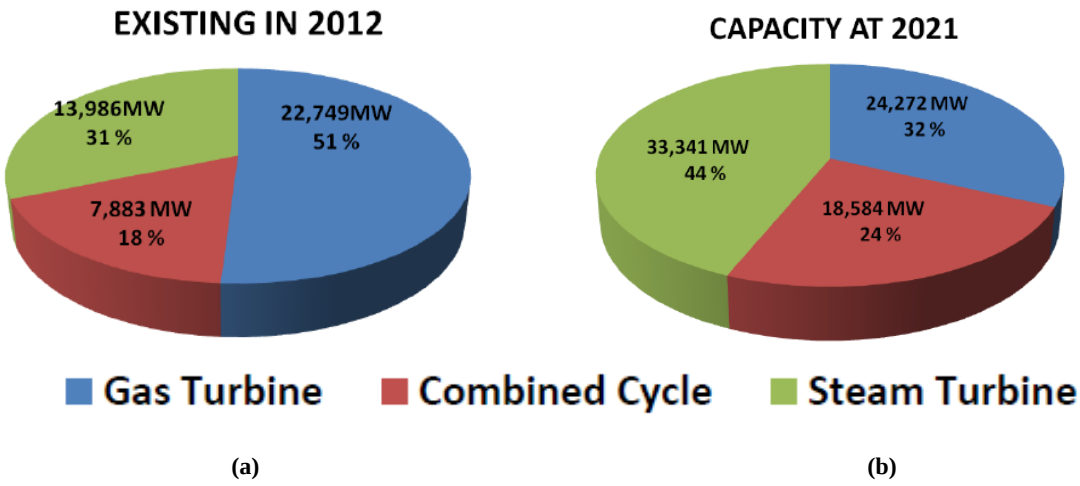

Figure 1 Distribution of Electricity Generation by SEC (a) Existing until 2012 (b) Planned by 2021 [3]

In SEC's annual report of 2014 as shown in the Figure 2, they reported that 50.4% of their power was generated using gas turbines alone and 14.2 % using the combined-cycle mode [4]. This shows the popularity of the gas turbines in the gulf and how beneficial would it be to increase 1% each turbine's output without expanding its size.

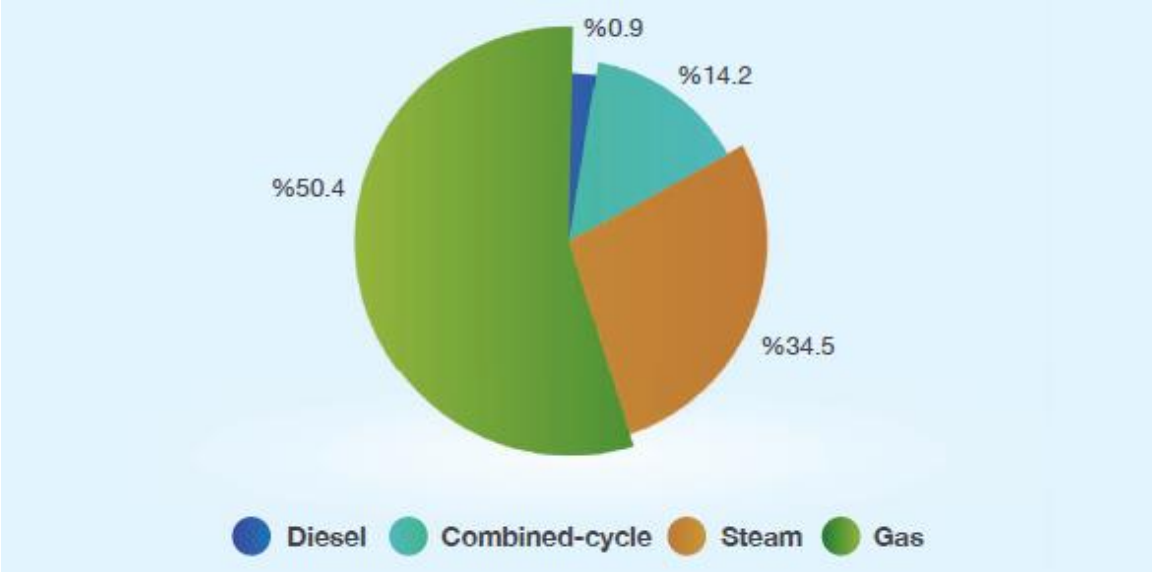

Figure 2 Relative distribution of the capacity of the SEC's generating units in 2014 [4]

1.2 Principle of Operation of a Simple Gas Turbine System

A simple gas turbine system consists of a compressor, combustion system and a turbine usually mounted on a single shaft as shown in the Figure 3. The compressor draws air into the engine, increases the pressure of the air and feds it to the combustion chamber. A steady stream of fuel is injected into the combustion chamber where high pressure and high temperature gas stream (~2000 K) is obtained. The hot combustion gases then expands through the turbine developing power and as well, drives the compressor. [5], [6]

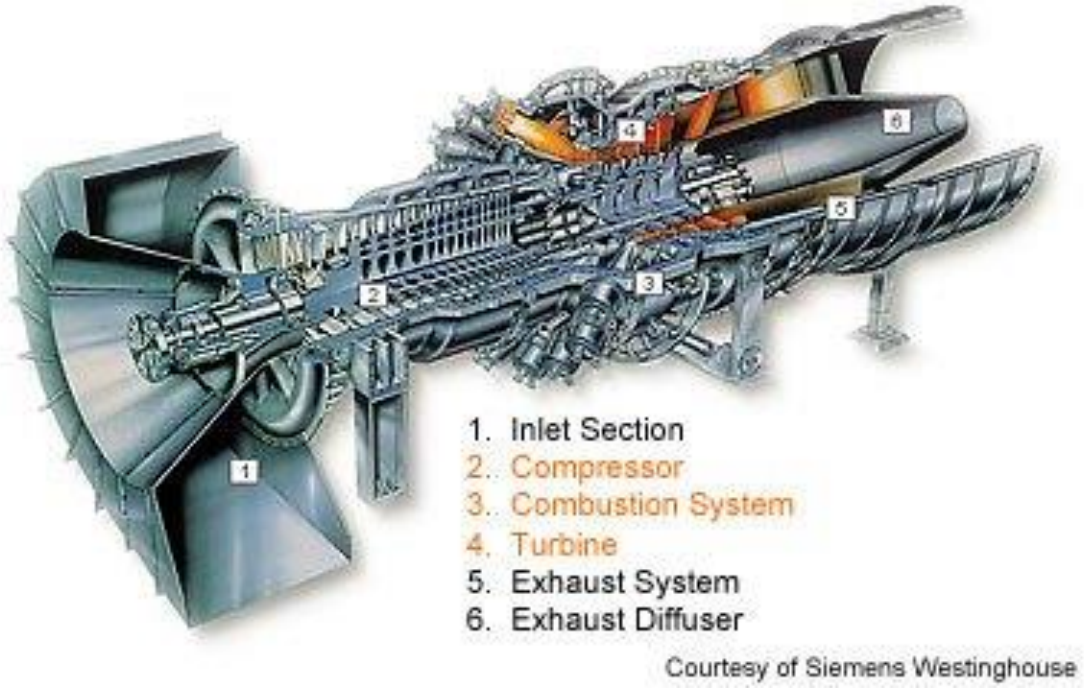

Figure 3 Principle of Operation of a Simple Gas Turbine System [7]

1.3 Need for Inlet Air Cooling

The intake air density decreases when the ambient temperature increases as can be seen from Figure 4 [8]. The gas turbines operate at constant speed and are constant volume flow combustion machines [9]. This causes a decrease in the intake mass flow rate as the temperature increases and hence, the power developed by the gas turbines. The increase in ambient relative humidity also reduces the density of air, as vapor is lighter than the dry air. Therefore, the power developed by gas turbines is adversely affected by the atmospheric temperature and humidity. Thermal efficiency of gas turbines also reduces due to the decreased power. During the period of peak power demand, it is seen that 1^{o}C rise in atmospheric temperature may reduce the gas turbine power output by 0.57% [10]. It is reported that up to 35 % power output may be enhanced if inlet air cooling technique is deployed [11]. Peak load demands higher power output which is counteracted by lower

power output of the turbines. These observations create a need of compressor inlet air temperature reduction for the efficient operation of gas turbines in summer ambient conditions. In addition to performance improvement obtained using inlet air cooling, it can also reduce the harmful NOx emissions.

To summarize, the advantages of inlet air cooling include [12]

1. Increased production
2. Higher efficiency
3. Compliance with environmental regulations
4. Life extension

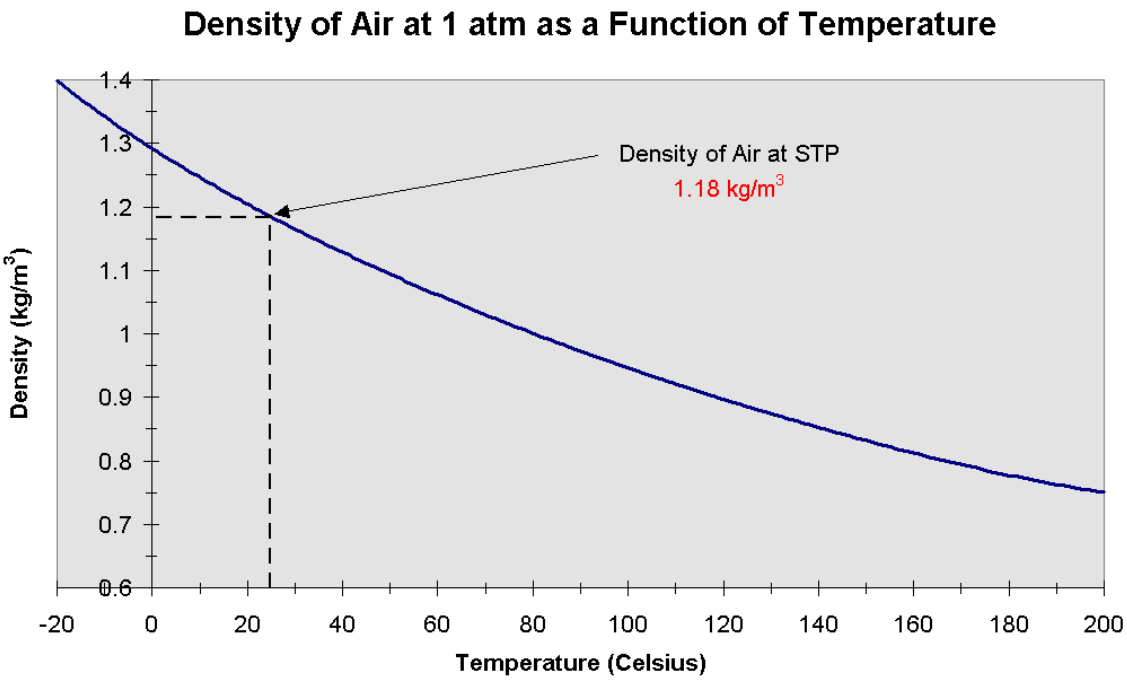

Figure 4 Effect of Temperature on the density of air [8]

1.4 Working Principle of Conventional Inlet Air Cooling Techniques

In this context, various inlet air cooling technologies have been tried for enhancing the gas turbine performance which are described in the aforementioned subsections.

1.4.1 Evaporative Air Cooling System

In this method, evaporation is used to cool the air. A pump is used to circulate water over the cooling pad or wetted media. Air is drawn through this wetted media using a fan. As the air passes, it cools down resulting in the evaporation of water. This cooled air is then passed over to the compressor of the gas turbine cycle as shown in the Figure 5. An upper limit for the power augmentation exists for this type of cooling technique in addition to the need of water treatment pre inlet cooling [13,14].

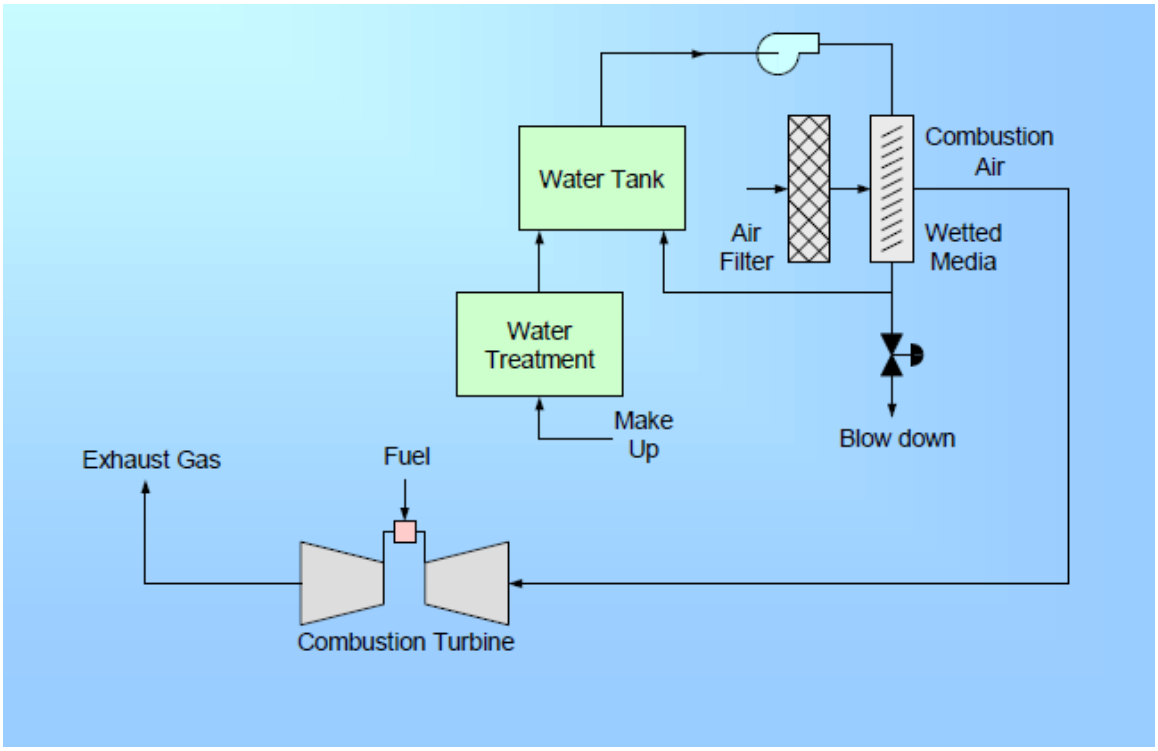

Figure 5 Evaporative Air Cooling System

1.4.2 Fogging System

This method also works on the evaporative cooling principle. In these systems, a high pressure demineralized water passes through a fog spray system, where fine droplets are produced. These droplets float in air and evaporate. The latent heat absorbed by the water is supplied by the air causing the temperature to drop. The air gets cooled and humidified, which is then passed to the inlet of compressor of the gas turbine cycle as shown in the Figure 6 [15]

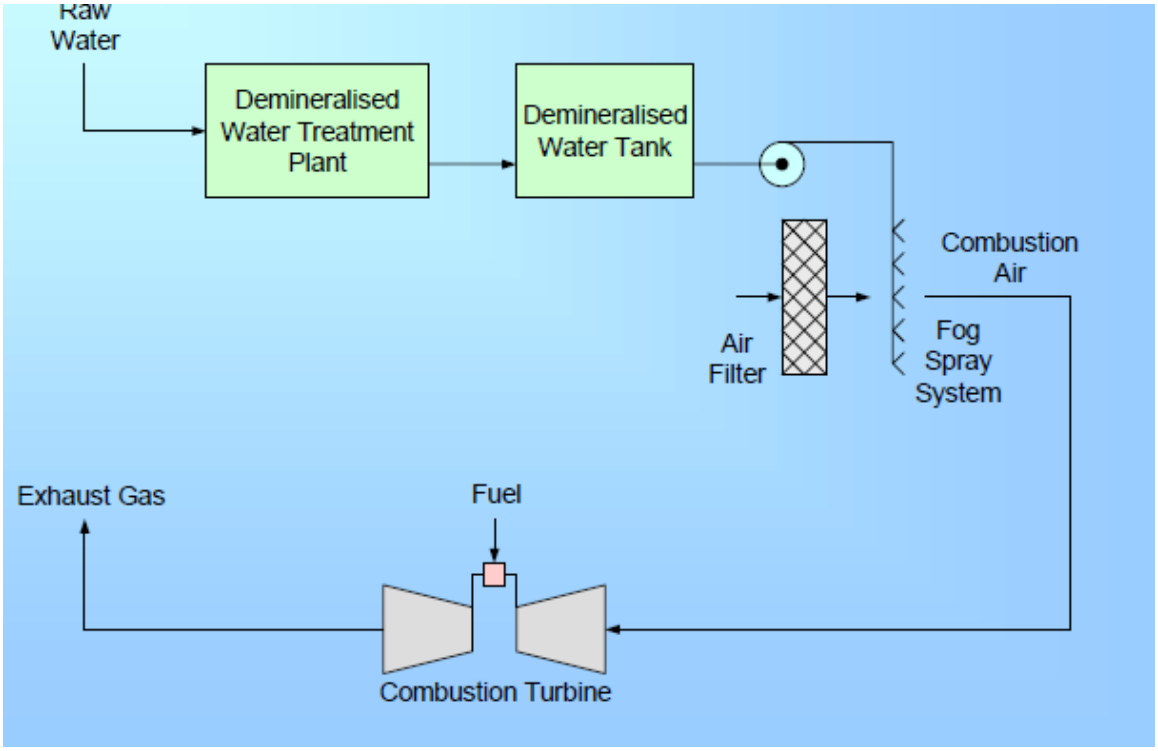

Figure 6 Fogging Cooling System

1.4.3 Vapor Compression Cooling System/Mechanical Chilling

These systems employ the vapor compression refrigeration system to cool down the temperature of the air. A mechanical chiller is usually employed where water acts as an

intermediate heat exchange fluid or coolant between the refrigerant and the air due to the high heat capacity of air. The refrigerant absorbs the heat from the water and cools it down in the mechanical chiller. This cooled water is then circulated through the air cooling coil above which passes the air reducing its temperature, which can then be supplied to the compressor of the gas turbine cycle as shown in the Figure 7. This system involves an increase in the parasitic load due to the addition of a compressor which is driven mechanically. It also involves the use of Chlorofluorocarbons (CFCs) and are considered to be non-ecofriendly [16]. The operating principle of vapor compression refrigeration cycle is given in the Appendix A.1 Vapor Compression Refrigeration Cycle.

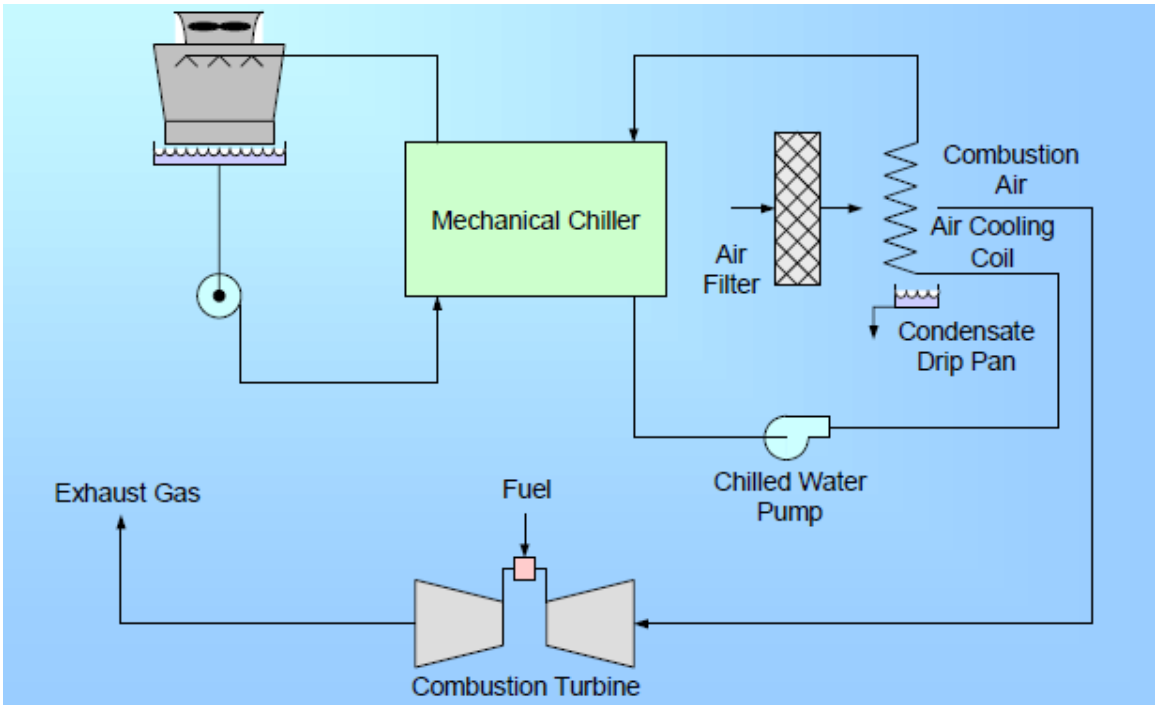

Figure 7 Vapor Compression Cooling System/Mechanical Chilling

1.4.4 Vapor Absorption Cooling System/Absorption Chilling

The mechanical energy needed to run the compressor in the vapor compression system is replaced with the thermal energy in vapor absorption cooling system. This system usually employ steam from the combined gas turbine cycle or from a separate source which acts as the thermal energy source to the vapor absorption refrigeration cycle. The operation of vapor absorption cooling system is as shown in the Figure 8 [17]. These systems are much more expensive than any other cooling systems. They involve the use of large cooling towers to reject the waste heat and also not suited, if no source of steam is available in the cycle. They are not cost effective and efficient due to the requirement of many heat exchangers and in general vapor absorption refrigeration system has low COP.

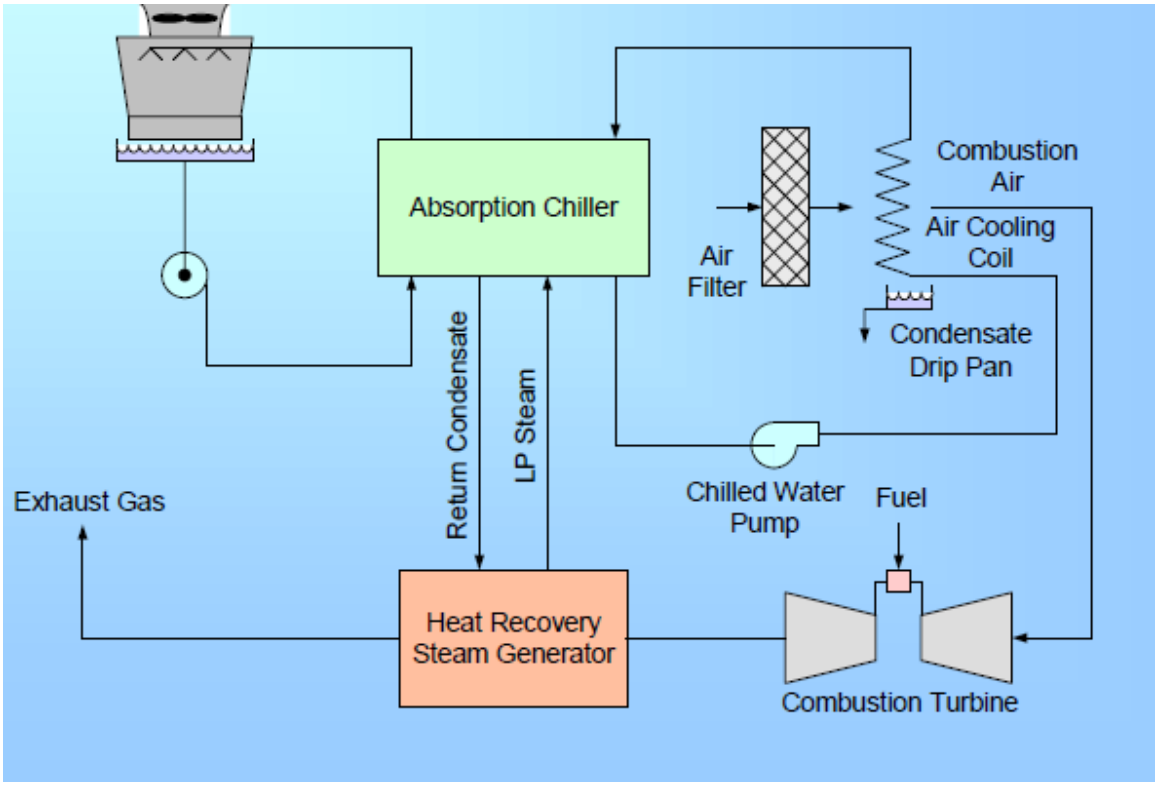

Figure 8 Vapor Absorption Cooling System [17]

1.5 Need for Evaporative After Cooling of the Compressor Discharge

The advantages of the above stated inlet cooling has an upper limit below 280 K when the vapor present in the air could freeze and form ice crystals which can affect the compressor's performance as the air temperature drops [18]. Evaporative after cooling is injecting water at the exit of the compressor. This water gets converted into steam and is absorbed by the air. This reduces the air temperature but increases the mass flow rate through the gas turbine which raises the power output. If a recuperator or heat exchanger follows the compressor, then the heat recovered from the exhaust gases would be more with evaporative after cooling compared to no water injection [19]. It is reported that, employing evaporative after cooling could increase the power of the gas turbine by as much as 55% with a slight increase in the efficiency [20].

1.6 Impact of emissions from the gas turbine

The exhaust from a gas turbine is composed of carbon monoxide (CO), carbon diaoxide (CO_2), water vapor (H_2O), unburned hydrocarbons (UHC), particulate matter (mainly carbon), NOx, and excess atmospheric oxygen and nitrogen. H_2O and CO_2 are not regarded as pollutants because they are a result of complete combustion of fuel but do contribute to the global warming. Improving thermal efficiency can reduce these emission which is as a consequence of less fuel being burned. The pollutants can cause extreme health risks and are regulated from country to country to keep them under limits [21].

If CO is inhaled by human beings in excess amounts, it can reduce the capacity of blood to absorb oxygen resulting in asphyxiation and even death sometimes. UHC can combine

with NOx to form photochemical smog in addition to be toxic. Particulate matter reduces the exhaust visibility and soils the atmosphere [22]. Recent studies indicate that, it also contribute to respiratory diseases such as Asthma [23]. NOx ($NO + NO_2$) is responsible to form photochemical smog at ground level. It also damages plant life and is the main culprit in happening of acid rain [24]. In United States, The Environmental Protection Agency (EPA) has set regulations that depend on its power output which controls the emissions which are in the range of 15-45 ppm for natural gas firing turbines referenced to 15% oxygen on a dry basis [25]. As per the data received from the Royal Commission Environmental Regulations, Kingdom of Saudi Arabia, the most harmful pollutants Carbon Monoxide and Particulate matters emitting from the boilers and industrial furnaces are permissible in the range of 0 – 100 ppmv [26].

CHAPTER 2

LITERATURE REVIEW

In the previous chapter, the need for evaporative after cooling and inlet air cooling, the conventional types of inlet air cooling systems followed by impact of emissions from the gas turbines were discussed. It was evident that an alternative technology for inlet air temperature reduction is highly desirable to enhance the power output of gas turbines operating in hot climates of the Kingdom. The following chapter presents key researches carried out in the field of evaporative after cooling and inlet air cooling driving towards increased power output, efficiency and reduced emissions. The energetic, exergetic and environmental analyses carried out in the literature has also been presented in this chapter that forms a foundation towards the present research.

2.1 Exergy

It is important to differentiate between energy and exergy before it could cause any confusion. Exergy is a thermodynamic parameter that identifies the quality of energy but not its quantity of energy. Therefore, exergy uses the combination of both first and second laws of thermodynamics [27]. Exergy is considered as a common attribute to which heat, work input or output can be compared. Another important point about exergy is, exergy is not conserved but destroyed during the process [28]. Method of exergy analysis is very much capable to predict the magnitude of thermodynamic losses which are responsible to deteriorate the performance of an energy conversion system. To carry

out exergetic analysis, an energy balance method for energy quantity and principle of increase of entropy for quality of energy was applied which reflects and quantify the thermodynamic losses occurred due to irreversible nature of the component of the proposed system and provides information about the potential targets for technology improvement. The information obtained from exergy analysis can be used to work for decisions that weigh which research efforts will minimize the undesired losses in the components of energy transformation system in order to obtain the desired energy gain [29]. Many different approaches to second law analysis have been reported in literature of which exergy is the most common way followed by entropy analyses [30].

Based on the investigations carried out in the recent past, the superiority of second law analysis over the conventional first law approach is well established. Application of second law of thermodynamics along with the first law clearly pin point the major exergy destructive components which are responsible to deteriorate the system performance [31]. There is a considerable literature on second law analysis of combustion turbines integrated with the inlet air cooling system and evaporative after cooling of which some of the studies are well reported.

2.2 Effect of temperature on gas turbines

It is reported that a simple cycle combustion gas turbine in the central Qasem region of Saudi Arabia experienced a drop of 24 % in its power output during the midday ambient temperatures in summers [32].

2.3 Impact of Inlet Air Cooling on gas turbines

Dawoud et al. [33] after incorporating four techniques to achieve inlet air cooling namely evaporative cooling, fogging cooling, absorption cooling and vapor compression cooling, showed that for a natural gas operated combustion turbine, reduction in compressor inlet temperature from 45^{o}C to 15^{o}C, enhanced the power output from 69 MW to 84.4 MW. It means the power output is increased by 20% by cooling the incoming air considerably. This shows the compressor inlet temperature is essential to reduce for increasing the power augmentation in gas turbines at peak summer. Various inlet air cooling technologies have been applied and the outcomes are well reported in the literature. Al-Ibrahim and Varnham [32] documented an interesting review of methods for inlet air cooling to increase the power production in combustion gas turbines during noon time. They highlighted the importance of evaporative cooling over the other methods which needs large amount of pure water resulting in limiting its use in a country that is scarce in water resources. Santos and Andrade [9] compared three cooling techniques mechanical chiller, absorption chiller and evaporative cooling with the basic gas turbine. They found that evaporative cooler offered the lowest energy cost followed by absorption chilling and lastly mechanical chilling. Alhazmy et al. [34] employed the methods of mechanical chilling and evaporative cooling to reduce the inlet temperature of air going to gas turbines that operate in extreme ambient conditions in Jeddah. Power output with the mechanical chilling increased by 6.77% versus 2.57% for the spray evaporative cooling. Yang et al. [35] introduced various inlet air cooling technologies for the gas turbines operate in combined cycle mode and analyzed their performance analytically. Al-Amiri and Zamzam [36] investigated the combustion gas turbine where compressor inlet air is

cooled through both refrigerative and evaporative cooling systems in view of assessing the net power increase. Their findings reveal that evaporative inlet air cooling method is suitable for the power increase of 8% to 15%..

2.3.1 Evaporative Inlet Air Cooling

Mohapatra and Sanjay [37] studied the air transpiration cooled gas turbines subjected to evaporative inlet cooling from exergetic analysis point of view. Their analysis reveals that such configuration of gas turbines increase the specific work by 9.98% and efficiency 4.34%, respectively. Pandelidis et al. [38] studied the cascaded effect of and indirect evaporative cooling and desiccant cooling with three different configurations on the output of gas turbine cycle and discussed their detailed thermodynamic advantages.

2.3.2 Fogging Inlet Air Cooling

Sanaye and Tahani [39] studied the effect of inlet fogging to the compressor inlet and as well inside the compressor, known as wet compression, on the power output, turbine exhaust temperature and cycle efficiency. The results of three fogging types, saturated, 1 % overspray, and 2% overspray were reported which displayed an increase in power output. Kim and Kim [40] carried out exergetic performance investigations of gas turbine cycle subjected to over spray process which consists of inlet fogging and wet compression to obtain inlet air cooling reported few interesting findings.

2.3.3 Vapor Compression Inlet Cooling/Mechanical Chilling

Comodi et al. [41] worked on reducing the sensitivity of atmospheric conditions on the gas turbine performance and clearly highlighted the gains in power output and thermal

efficiency achieved after the adoption of direct expansion mechanical vapor compression method.

2.3.4 Vapor Absorption Inlet Cooling/Absorption Chilling

Mohapatra and Sanjay [42] conducted the parametric analysis of gas turbine plant where inlet air was done through vapor absorption cooling cycle. They showed that an improvement of 7.48% in efficiency and 1.8% in specific power can be achieved, respectively with the employment of absorption system for inlet air cooling. Mahmoudi et al. [43] presented the exergetic analysis of gas turbine integrated with absorption system for inlet air temperature reduction. They estimated that the power output of gas turbines rises from 6% to 12% when the inlet temperature decreases by 10^{o}C. The irreversibilities in the absorption refrigeration cycle were found to be very low as compared to the gas turbine.

2.3.5 Novel Inlet Air Cooling Techniques

The techniques of compressor inlet air cooling utilized by the aforementioned investigators are limited to the following:

1- Evaporative inlet air cooling has an upper limit to the cooling achieved and requires demineralized water for corrosion free operation.

2- Fogging technique cannot be employed in highly humid conditions. The demineralization of water also adds complexity in using this method.

3- Mechanical chillers due to the use of CFC's and electric power consumption are not eco-friendly and thermodynamically less beneficial.

4- Vapor absorption cooling systems commonly use LiBr-H_2O are not cost effective and efficient due to the requirement of many heat exchangers and low COP.

To overcome with the aforementioned disadvantages, some of researchers came forward with new methods to achieve inlet air cooling. One of them was discovered by Zhang et al. [44] in which liquefied natural gas (LNG) cryogenic energy was utilized. They observed power augmentation up to 11.6 % when compared to without inlet air cooling but no significant difference in efficiency was obtained. Farzaneh-Gord and Deymi-Dashtebayaz [45] proposed a unique method which involved utilization of refinery gas pressure drop which can then reduce the inlet air temperature and enhance the performance of one of the Khangrian refinery gas turbines. The novel method had the upper hand when compared to two conventional methods. They observed the improvement of 1%-3.5% in the energy efficiency of gas turbines when the inlet air temperature decreases from 4^{o}C to 25^{o}C.

Khaliq et al. [46] considered a new method for reducing the compressor inlet air in gas turbines operates in hot climatic regions. They utilized the reverse Brayton cycle for inlet air temperature reduction and based on investigation reported that maximum irreversibility is associated with the combustor in the cycle and the magnitude of irreversibility strongly depends on combustion temperature and extraction pressure ratio. Jassim et al. [47] further highlighted the use of Brayton refrigeration cycle in gas turbines for inlet air temperature reduction and theoretically analyzed their performance from both first and second law point of views. Their theoretical investigation was focused on the optimal design of combustor and heat exchanger. Khaliq [48] examined the operation of gas turbine engine in cogeneration mode and presented additional results that further

supported the benefits of Brayton refrigeration cycle as a promising method of inlet air temperature reduction.

2.4 Impact of Evaporative After Cooling on gas turbines

Evaporative after cooling is achieved by injecting water after the compressor or before the recuperator where it converted into steam and mixes with the compressed air stream. Decrease in the temperature of mixed air results in the gaining of energy by injecting water which in turn increases heat rejection in the recuperaor if included. It results in an increase in the capacity of recuperator which helps in improving the thermal efficiency. Heppenstall [49] reviewed several advanced gas turbine cycles which have been developed over time to improve the gas turbine's performance. Emphasis of different cycles was to recover the heat from the gas turbine's exhaust. He observed the effect of evaporation by injecting water into the air flow at the compressor exit. This arrangement produced 20% more specific output than that of basic cycle. Roumeliotis and Mathioudakis [50] highlighted the importance of water/steam injection techniques for gas turbine engine and gained some insights on gas turbine operation with water injection and they analyzed its performance from power enhancement point of view. They also investigated the risks associated with the water/steam injection, overspray or inlet fogging on the behavior of the gas turbine cycle.

2.5 Intercooling in Gas Turbines

Intercooling involves compressing the air in stages while it is cooled between each stage through a heat exchanger called an Intercooler [51]. Inter-cooling reduces the heat transfer problem and allows the recuperation with high efficiency in gas turbines [49].

Sanjay and Prasad [52] investigated the effect of intercooling on the performance of the cycle and observed that, power output increases significantly with intercooling in addition to the reduction in green-house gas emissions.

2.6 Recuperation in Gas Turbine

The temperature of the exhaust gases leaving the turbine is usually higher than the temperature of the air leaving the compressor. These hot gases can be used to transfer heat to the high pressure air leaving the compressor which is known as recuperation or regeneration [51]. Happenstall [49] observed that gas to gas recuperation offer reasonably efficiency without mechanical complexity at relatively low capital cost. Further, there is small water requirement needed during evaporative after cooling of the compressor discharge which facilitates the use of a recuperator in gas turbines. A study carried out by Mahmoudi et al. [43] showed enough energy content in the exhaust gases still remain after recuperation and necessary cooling system such as absorption refrigeration could be employed.

2.7 Combination of the above Performance Enhancement Techniques applied to gas turbines

Reduction of inlet air temperature to gas turbines, augment the power and enhance the efficiency to some extent. In order to obtain a simultaneous gain in power and to reduce the NOx emissions, concept of evaporative after cooling was introduced and is utilized by very few investigators simultaneously along with inlet air cooling, intercooling and recuperation. Shukla and Singh [53] investigated the combined effect of inlet evaporative cooling, steam injection and film cooling on the thermodynamic performance of steam

injected gas turbine cycle and reported that the energy efficiency is increased by 3.2% when the compressor inlet air temperature decreases from 45ºC to 9ºC.

For this reason, Khaliq and Chaudhary [54] presented the exergy analyses of intercooled, reheat and regenerative gas turbines subjected to evaporative after cooling and inlet air cooling of the compressed air. They found that thermodynamic losses in the key components are quite sensitive to the pressure ratio and combustor outlet temperature. Khaliq and Chaudhary [55] further investigated the regenerative gas turbines subjected to absorption evaporative after cooling and inlet air cooling and reported some promising results. Khaliq and Dincer [56] conducted the parametric analysis of regenerative combustion gas turbines in cogeneration mode where inlet air cooling was done through absorption refrigeration and compressed air was cooled through evaporative cooling. Their results showed that the variation in the overall pressure ratio and combustion temperature significantly affect both the thermal and second law efficiency of the cycle.

2.8 NOx formation in gas turbines

Gas turbines produce low levels of NOx when operated in lean premixed mode with natural gas as a fuel in addition to high cycle efficiency in the range of 50%. With the increasing concerns regarding acid rain and depletion of ozone layer, the standards regulate the amount of NOx that is released from the turbines. A target of 100 ppm can be met by easy management of thermal NOx but a goal of 10 ppm, which is a regulation of future gas turbines requires a detailed level of understanding [57]. To predict the amount of NOx, several semi-empirical and empirical correlations exist in the literature, which differ in their assumptions. Sullivan [58] compared the existing experimental data with

the correlation developed and found that each correlation agree over a range of inlet conditions only. The correlations presented in the literature predict the total amount of NOx, which includes NO and NO_2. In most flames, it is predominantly NO that is formed with oxidation to NO_2 occurring in a post flame process that does not affect total NOx. Cole and Summer hays [59] reviewed the techniques for the estimation of NO_2 concentrations resulting from NOx which are useful in predicting the composition of combustor exhaust in a gas turbine cycle.

Among the several researches carried out to predict the NOx emissions from a combustor, Lee et al. [60] employed combined Computational Fluid Dynamics (CFD) and Chemical Reactors Network (CRN) to predict NOx emissions from a lean premixed combustor and found that swirl angle has very little effect on emissions while he studied the effect of equivalence ratio and swirl angle. The results obtained were found to reasonably agree with the experimental results. Bussman and Baukal [61] investigated the effect of ambient conditions on NOx formation and found that ambient relative humidity reduces the amount of NOx where as it increases with ambient air temperature. Contrary results were obtained for coal fired furnace when Li et al. [62] where they found that increasing temperature reduced the NOx concentration with improved flame stability in the first zone. In the second burnout zone, NOx increased with an increase in air temperature.

2.9 CO formation in gas turbines

Carbon monoxide is always considered as one of the harmful pollutants and is formed due to the low temperature operation of a gas turbine. When the reactant oxygen is not

sufficient during a reaction, some of the carbon from the fuel remains in the form of CO. It has become mandatory by the regulations to restrict the levels of CO in the environment due to its health hazards. In this regard, Bussman and Baukal [63] assessed the effect of ambient conditions on the amount of CO formed and found that ambient conditions alter the CO levels considerably. They also found that a decrease in excess O_2 tends to reduce the mixing rate of the air and fuel, which can cause higher level of CO. Li et al. [62] studied effect of air temperature on the formation of CO in a coal-fired furnace, where they found that increasing air temperature increases CO formation. In an attempt to relate the formation of CO produced in gas turbines as a function of temperature, pressure and residence, some empirical relations exist in the literature which can predict accurately the emissions formed. In this context, Rizk and Mongia [64] developed a semi analytical correlation based on the kinetic theory that relate the formation of CO with the operating parameters of the reactors.

2.10 Overall Thesis Objective

From the aforementioned literature review, it was observed that, reverse Brayton cycle has been used by few of the investigators for inlet air cooling where an air compressor is commonly utilized by the gas turbine cycle and refrigeration cycle. Application of Brayton refrigeration cycle provides cooling of inlet air close to 0^{o}C in an eco-friendly manner. A considerable performance enhancement in terms of power output and energy efficiency was obtained after the employment of this inlet air cooling technology in combustion gas turbines. In order to further enhance the efficiency of gas turbines and to reduce the emissions, evaporative after cooling of the compressor discharge is introduced into the design. The increase in mass flow rate and reduction in temperature at the turbine

inlet due to the application of evaporative after cooling enhances the power output significantly and reduces the NOx emissions considerably. Therefore, introducing evaporative after cooling along with the inlet air cooling in combustion gas turbines is expected to have three-fold benefits:

1- Increases the power output significantly in an eco-friendly manner
2- Enhances the thermal efficiency
3- Reduces the NOx emissions considerably

Reported literature shows no exergo-environmental analysis has been done to theoretically examine the performance of intercooled, reheat and regenerative combustion gas turbines where inlet air cooling is achieved through the use of Brayton refrigeration cycle and evaporative after cooling of the compressed air. No preceding research to quantify the reduction in NOx and CO emissions was taken for the gas turbines where combined method of evaporative after cooling and inlet air cooling was applied. The gas turbine cycle proposed and analyzed fills a gap of the literature and added a contribution as the study is unique of its kind related to gas turbines which provide a significant increase in power output, better thermal efficiency, and reduced NOx emissions during peak summer ambient conditions.

Therefore, chief objectives of the present thesis were to

1- Formulate a theoretical model for evaluating the thermo-environmental performance of the natural gas fueled combustion gas turbine integrated with Brayton refrigeration cycle for reducing the inlet air temperature and evaporative after cooler for lowering down the temperature of compressed air.

2- To compute the second law efficiency of the major exergy destructive components along with the thermal and exergy efficiency of the overall cycle. In addition, the NOx and CO emissions were quantified and compared to the cycle without the application of evaporative after cooling and inlet air cooling.

3- To study the effects of some influencing parameters like extracted mass rate, turbine inlet temperature, extraction pressure ratio, overall pressure ratio, fuel-air equivalence ratio, ambient temperature, water-to-air ratio and ambient relative humidity that can ascertain energetic-exergetic-environmental performance of the proposed cycle.

4- Further, an effort was made to theoretically evaluate the degree of thermodynamic and environment imperfection related to the performance of gas turbine engine.

5- To determine the optimal operating conditions and to establish the basic design criteria for the proposed combustion gas turbine cycle using the method of exergo-environmental methodology

CHAPTER 3

SYSTEM DESCRIPTION, MATHEMATICAL MODELLING

3.1 Description of the System

In the current research, an intercooled regenerative reheat combustion gas turbine cycle is proposed where compressor inlet air cooling is achieved through the use of Brayton refrigeration cycle and evaporative after cooling is obtained with the use of injecting water. Figure 9 shows the schematic of the proposed system. The proposed cycle consists of compressors, heat exchangers, expander, turbines and the mixing chamber. Both the cycles, i.e., Gas Turbine cycle and Refrigeration cycle use a common compressor. Air at a pressure of P_2, is extracted from the low pressure compressor (LPC) and allowed to cool down in the heat exchanger (HE) to T_3 using a cooling fluid (Water). This cooled air is then passed to the humidity eliminator (HuE) where the vapour content is completely removed to avoid flashing in the expander. The air then passes through Expander (Ex) to the ambient pressure P_4 and temperature T_4 which is substantially lesser than ambient temperature T_0. The ambient air which is at high temperature T_o exchanges heat with the cold stream T_5 before entering the compressor. The air entering the compressor is cooled down to a temperature which is close to 0^oC. An indirect intercooler is employed to cool the compressed air from the low pressure compressor (LPC). This indirect intercooler uses ambient humidifier air (1^1) supplied by the air humidifier (AH) to cool down the

compressed air. The air humidifier works on the evaporation principle where water evaporates using the sensible heat of air and hence cooling it down. The pressure of cooled air further rises in high pressure compressor (HPC) where it's pressure and temperature changes to P_8 and T_8. The outlet of HPC is then passed to the after cooler (AC) where water is injected at the saturation temperature and pressure. Before injecting the water into the after cooler, it is warmed using the turbine exhaust through water heater (WH). Now, the humid cooled air 9 exchanges heat in a recuperator (Re) with the low pressure gas turbine (LPGT) exhaust 14. The turbine exhaust is utilized to warm up the injected water passing through the heat exchanger after which it is supplied to a combustion chamber (CC) where fuel-air are mixed and burned producing hot gases. These hot gases first expand in a high pressure gas turbine (HPGT) to pressure P_{12} and temperature T_{12} after which it is re-combusted in a reheater (RH) producing hot gases at a lower pressure P_{13}. These hot gases are passed to the low pressure gas turbine (LPGT) to produce work after converting the mechanical energy to electrical energy using a generator.

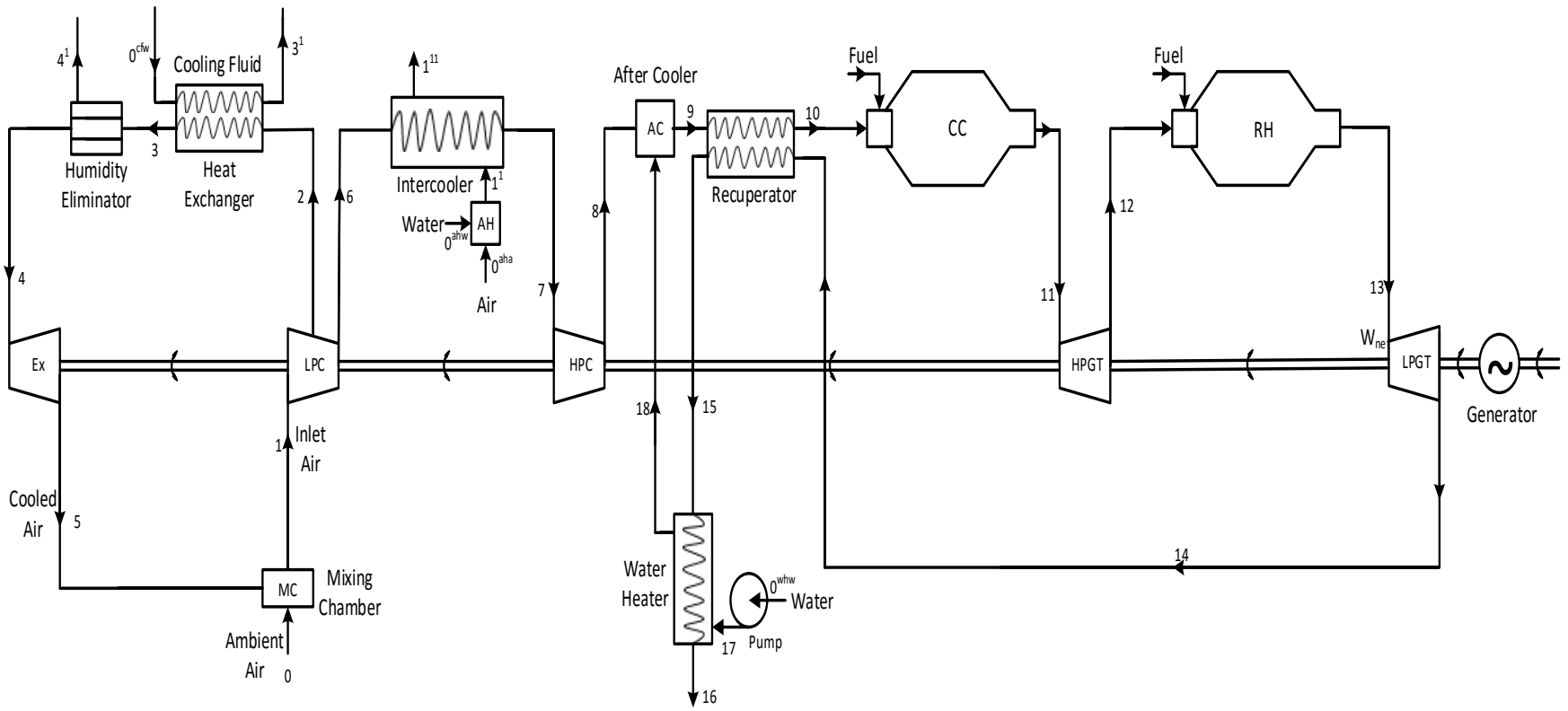

Figure 9 Schematic of the proposed gas turbine cycle

Large cooling demand of power of the Gulf region during peak summer ambient conditions can be met out effectively through the employment of the proposed innovative gas turbine cycle in an eco-friendly manner. Most of the gas turbines operating in the kingdom use natural gas as a fuel and despite all the development efforts, the natural gas-fired combined cycle is likely to remain, for many years, attractive as a new plant for utility scale applications. Therefore, natural gas is supplied as a fuel so that proposed model may be compared with the actually existing gas turbines in the kingdom, which is the advancement to the existing natural gas fuelled combustion gas turbine cycles in the following ways:

1- Integration of combustion gas turbine with the Brayton refrigeration cycle (1-2-3-4-5-1) provides cooling and increases the power output in an eco-friendly manner.

2- Integration of Brayton refrigeration cycle for reduction of compressor inlet air temperature in combustion gas turbine along with the use of evaporative after cooling enhances its thermal efficiency significantly and reduces the NOx emissions considerably.

3.2 Methodology

The mathematical model is developed using Engineering Equation Solver (EES), which is a numerical solver that provides a built-in-mathematical and thermodynamic property functions to solve a set of non-linear equations with an extensive data base of fluid thermodynamic properties. It is a unique software that identifies all the unknowns from a group of equations including arrays. The software is also able to solved differential and

complex equations, perform integration. For a detailed capabilities, it is advised to refer to the manual that can be downloaded from http://www.fchart.com [65].

3.3 Mathematical Model

The governing equations are developed based on the conservation of mass and energy principles along with some empirical correlations for predicting emissions in combustors. Basic thermodynamic equations are employed to determine thermo-physical properties of the elements and mixtures. Once the governing equations are modelled, they are solved simultaneously using EES [65] determining the condition at each state point which is dictated by temperature, pressure, and its composition. Then the exergy balance equation was applied to each component and it quantifies the exergy destruction and losses in the component concerned.

3.3.1 Assumptions

In order to simplify the analysis carried out, following assumptions were taken:

1- All the processes in the cycle are operating under steady state conditions

2- The specific heat of different species is taken as a pure function of temperature and curve fit coefficients up to the fourth order of temperature are considered. Other thermo-physical properties such as enthalpy, entropy, exergy, gibbs function are derived from specific heat.

3- All the components except combustion chamber and reheater are considered as adiabatic, since small heat transfer occurs through them. 5% of the total heat input to combustion chamber and reheater is assumed to be lost to the surroundings

4- Dry air is composed of nitrogen (N_2), oxygen (O_2), argon (Ar) and carbon dioxide (CO_2).

5- The fuel supplied is natural gas which is a mixture of methane (CH_4), ethane (C_2H_6), propane (C_3H_8), butane (C_4H_8), and nitrogen (N_2).

6- The dead state is same as ambient conditions which are taken as temperature (T_0) = 300 K (variable), relative humidity (ϕ_0) = 50% (variable) and pressure (P_0) = 101.3 kPa. The temperature of water supplied to the proposed cycle is the same as the air temperature.

7- The water at saturation temperature is supplied to the aftercooler corresponding to inlet pressure of aftercooler.

8- The heat exchangers in the cycle viz., Brayton refrigeration cycle heat exchanger, Intercooler between the compressors, Exhaust gas recuperator and after cooling water heater are cross flow unmixed type heat exchangers with fixed sizes.

9- The humidity eliminator removes all the moisture content without any pressure drop.

10- Air is fully saturated when it leaves the air humidifier (AH).

11- Combustion chamber and reheater are considered as conventional type of combustors where small fraction of air is used for combustion and the remaining is bypassed to other zones, i.e., intermediate and dilution zone.

12- Pressure drop in components such as heat exchangers, air humidifier, after cooler, combustion chamber, reheater, mixing chamber is taken as the small percentage

of the input pressure to those components. Percentage of pressure drops are tabulated in Table 1

Table 1 Pressure drop in various components [12], [19], [46], [48], [56]

Component	Pressure drop (θ)	Component	Pressure drop (θ)
Air humidifier (AH)	1 %	After cooler (AC)	1 %
Combustion chamber (CC)	4 %	Humidity eliminator (HuE)	1 %
Heat exchanger (HE)	0.5 %	Intercooler (IC)	1 %
Mixing chamber (MC)	0.5 %	Recuperator (Re)	2 %
Reheater (RH)	4 %	Water heater (WH)	1 %

13- Efficiency of the following components were taken as mentioned in Table 2

Table 2 Efficiencies of various components [19], [43], [46], [48], [55], [56], [66]

Component	Efficiency (η)
Isentropic efficiency of expander (η_{Ex})	97%
Isentropic efficiency of turbines (η_t)	95%
Pump efficiency (η_{pump})	88%
Generator efficiency (η_{gen})	98%
Efficiency of combustors (η_{CC} & η_{RH})	95%

3.3.2 General Mass, Energy and Exergy Balance

The general mass, energy and exergy balance equations applied to each component as a control volume, may be written as [28], [67]–[69]

$$\sum_{in} \dot{m} = \sum_{out} \dot{m} \quad (1)$$

$$\sum_{i=1}^{n} \dot{Q}_i - \dot{W} = \sum_{out} \dot{m}h - \sum_{in} \dot{m}h \quad (2)$$

$$\dot{X_W} = \sum_{i=1}^{n} (\dot{X}_{heat})_i + \sum_{in} \dot{m}e_x - \sum_{out} \dot{m}e_x - \dot{I} \quad (3)$$

For a single stream flow, exergy balance equation is written as

$$\dot{X_W} = \dot{X}_{heat} + \dot{m}.e_{x,in} - \dot{m}.e_{x,out} - \dot{I} \quad (4)$$

Exergy associated due to heat transfer $\dot{Q}$ may be determined from

$$\dot{X}_{heat} = \left(1 - \frac{T_0}{T}\right)\dot{Q} \quad (5)$$

3.3.3 Thermo-physical properties formulation

The proposed cycle involves number of fluids which include humid air, water, fuel and combustion gases. All these fluids are mixture of elements and compounds. All the necessary thermodynamic properties needed depends on a single property, which is specific heat.

3.3.3.1 Specific heat

The molar specific heat at constant pressure of the elements and compounds involved can be written as fourth order polynomial function of a temperature as [70,71]

$$\bar{C}_p(T) = \bar{R}(a_1 + a_2T + a_3T^2 + a_4T^3 + a_5T^5) \quad (6)$$

Where $\bar{R}$ is the Universal Gas constant and the coefficients a_1 to a_5 for the gases needed in the study are tabulated in Table 3 while for the hydrocarbons, it is tabulated in Table 4.

$\bar{C}_p(T)$ and $\bar{C}_v(T)$ are related by the equation $\bar{C}_v(T) = \bar{R} - \bar{C}_p(T)$ (7)

Table 3 Polynomial coefficients of equation (6) for various gases [70]

Species	T (K)	a_1	a_2	a_3	a_4	a_5
CO_2	250-1000	0.0228e2	0.0992e-1	-0.1040e-4	0.0687e-7	-0.0212e-10
	1000-5000	0.0445e2	0.0314e-1	-0.1278e-5	0.0239e-8	-0.1669e-13
H_2O (g)	250-1000	0.0339e2	0.0348e-1	-0.0636e-4	0.0697e-7	-0.0250e-10
	1000-5000	0.0267e2	0.0306e-1	-0.0873e-5	0.1201e-9	-0.0639e-13
N_2	250-1000	0.0330e2	0.1408e-2	-0.0396e-4	0.0564e-7	-0.0245e-10
	1000-5000	0.0293e2	0.1488e-2	-0.0569e-5	0.1010e-9	-0.0675e-13
O_2	250-1000	0.0321e2	0.1128e-2	-0.0576e-5	0.1314e-8	-0.0877e-11
	1000-5000	0.0370e2	0.0614e-2	-0.1259e-6	0.0178e-9	-0.1136e-14
CO	250-1000	0.0330e2	0.1512e-2	-0.0388e-4	0.0558e-7	-0.0247e-10
	1000-5000	0.0303e2	0.1443e-2	-0.0563e-5	0.1019e-9	-0.0691e-13
NO	250-1000	0.0338e2	0.1253e-2	-0.0330e-4	0.0522e-7	-0.0245e-10
	1000-5000	0.0325e2	0.1269e-2	-0.0502e-5	0.0917e-9	-0.0628e-13
NO_2	250-1000	0.0267e2	0.0784e-1	-0.0806e-4	0.0616e-7	-0.0232e-10
	1000-5000	0.0468e2	0.0246e-1	-0.1042e-5	0.0198e-8	-0.1392e-13
Ar	250-1000	0.0250e2	0.0000e0	0.0000e0	0.0000e0	0.0000e0
	1000-5000	0.0250e2	0.0000e0	0.0000e0	0.0000e0	0.0000e0

Table 4 Polynomial coefficients of equation (6) for various hydrocarbons [71]

Species	T (K)	a_1	a_2	a_3	a_4	a_5
CH_4	250-1000	5.1499e0	-1.3671e-2	4.9180e-5	-4.8474e-8	1.6669e-11
	1000-5000	1.6355e0	1.0084e-2	-3.3692e-6	5.3496e-10	-3.1552e-14
C_2H_6	250-1000	4.2914e0	-5.5154e-3	5.9944e-5	-7.0847e-8	2.6869e-11
	1000-5000	4.0467e0	1.5354e-2	-5.4704e-6	8.7783e-10	-5.2317e-14
C_3H_8	250-1000	4.2110e0	1.7160e-3	7.0618e-5	-9.1959e-8	3.6442e-11
	1000-5000	6.6679e0	2.0612e-2	-7.3655e-6	1.1844e-9	-7.0695e-14
C_4H_{10}	250-1000	4.4548e0	8.2606e-3	8.2989e-5	-1.1465e-7	4.6457e-11
	1000-5000	9.7699e0	2.5500e-2	-9.1414e-6	1.4733e-9	-8.8080e-14

3.3.3.2 Enthalpy

Once the molar specific heat of a species i is found, its molar enthalpy as a function of temperature T may then be calculated as [72]

$$\bar{h}_{i(T)} = \bar{h}^0_{i(T_0)} + \int_{T_0}^{T} \bar{C}_{p_i}(T)dT \qquad (9)$$

Where T_0 is the reference temperature and $\bar{h}^0_{i(T_0)}$ is the molar enthalpy of formation at that reference temperature. The molar enthalpy of formation at the reference temperature of 298.15 K for all the species needed in the study are tabulated in Table 5

3.3.3.3 Entropy

Molar specific entropy of a species i depends on temperature T and as well as pressure P or partial pressure y_iP if it is in a mixture, which is given as [72]

$$\bar{s}_{i\,(T,p)} = \bar{s}_{i_{(T_0,p_0)}} + \int_{T_0}^{T} \frac{\bar{C}_{p_i}(T)}{T} dT - \bar{R} ln\left(\frac{y_i p}{p_0}\right) \quad (10)$$

Where y_i is the mole fraction of the species in a mixture, T_0 and P_0 are reference temperature and pressure respectively and $\bar{s}_{i_{(T_0,p_0)}}$ is the value of entropy at reference temperature and pressure which are as well tabulated in Table 5.

Table 5 Molar enthalpy of formation, absolute molar specific entropy and standard chemical exergy at reference temperature and pressure of 298.15 K, 101.3 kPa [29,51,70,72]

Species (i)	Molar enthalpy of formation ($\bar{h}_i^0$)	Molar specific entropy ($\bar{s}_i$)	Standard chemical exergy ($\overline{e_{x_i}^0}$)
CO_2	-393546 kJ/kmol	213.7 kJ/kmol-K	19870 kJ/kmol
H_2O (g)	-241845 kJ/kmol	188.7 kJ/kmol-K	9500 kJ/kmol
O_2	0	205 kJ/kmol-K	3970 kJ/kmol
NO	90297 kJ/kmol	210.6 kJ/kmol-K	88900 kJ/kmol
NO_2	33098 kJ/kmol	239.9 kJ/kmol-K	55600 kJ/kmol
CO	-110541 kJ/kmol	197.5 kJ/kmol-K	275100 kJ/kmol
N_2	0	191.5 kJ/kmol-K	720 kJ/kmol
Ar	0	154.8 kJ/kmol-K	11690 kJ/kmol
CH_4	-74595 kJ/kmol	186.4 kJ/kmol-K	831650 kJ/kmol
C_2H_6	-83846 kJ/kmol	229.2 kJ/kmol-K	1495840 kJ/kmol
C_3H_8	-104673 kJ/kmol	270.3 kJ/kmol-K	2154000 kJ/kmol
C_4H_{10}	-134981 kJ/kmol	295.5 kJ/kmol-K	2805800 kJ/kmol

3.3.3.4 Thermo-physical properties for a mixture of gases

Once the thermo-physical properties of individual species in a mixture are known, the corresponding property of the mixture can be calculated after [51]

$$\bar{f}_{mix} = \sum_{i=1}^{n} y_i \bar{f}_i \quad (11)$$

The relation between molar specific thermodynamic property and specific thermodynamic property is [51]

$$f_i = \frac{\bar{f}_i}{MW_i} \quad (12)$$

Where f can be any property such as molar mass, gas constant for a substance, specific heat, enthalpy or entropy and n is the number of species in a mixture. MW is the molar mass in kg/kmol of the species.

3.3.4 Working fluid descriptions

There are three different kinds of mixtures in the given cycle. The composition of each one of it is described in this section.

3.3.4.1 Dry Air

Dry air in the atmosphere is known to contain N_2, O_2, Ar, CO_2, Ne, He, Kr and Xe as its constituent in the decreasing order. Ne, He, Kr and Xe are usually very less in magnitude and can be neglected. Hence, the following composition of dry air is taken [29,73]

$$y_{N_2} = 0.7803; \quad y_{O_2} = 0.2099; \quad y_{Ar} = 0.00933; \quad y_{CO_2} = 0.00047 \quad (13)$$

3.3.4.2 Combustion gases

Combustion gases when burnt completely will produce CO_2, H_2O, N_2, Ar with excess of O_2. One of the primary objectives of this research is to predict the emissions from the gas turbine. Hence, the combustion gases will contain variable amount of mole fractions of the following gases CO_2, H_2O, N_2, O_2, Ar, NO_2, NO and CO. The exact composition will change from case to case when the operating parameters such as equivalence ratio, ambient temperature changes.

3.3.4.3 Fuel

It is reported that 43.7 % of the total reserves of Natural gas in the world is held by Middle East. About 80% of the gas turbines in Saudi Arabia are using natural gas as a fuel to run the power plants. This has inspired us to investigate the performance of the gas turbine using the actual composition of natural gas. It is also found that its composition never remains constant. An approximate estimation of its composition considering the major components is selected from the literature [73, 74]

$$y_{CH_4} = 0.96; \quad y_{C_2H_6} = 0.02; \quad y_{C_3H_8} = 0.006; \quad y_{C_4H_{10}} = 0.003; \quad y_{N_2} = 0.011 \quad (14)$$

3.3.4.4 Humid Air

Thermodynamic properties of the humid air are calculated per dry air basis and hence, when the mass is being multiplied to the property, it should be of dry air. The humidity ratio is used to indicate the amount of moisture in the air denoted by ω. It is defined as the mass of vapor present in a unit mass of dry air. Hence, any thermodynamic property of humid air per kilogram of dry air can then be calculated after [75,76]

$$f_{humair} = f_{dryair} + \omega f_{vapor} \quad (15)$$

Where f can be any property such as specific heat, molar mass, specific enthalpy or specific entropy. Thermodynamic properties of dry air and vapor are calculated based on the above discussion and polynomial coefficients of Table 3.

Sometimes, the moisture content is indicated in relative humidity (ϕ) which is the ratio of amount of vapor m_v air is holding to the amount of vapor $m_{v,sat}$ air can hold when it is fully saturated at a given temperature T and pressure P. It is related to the humidity ratio as [51]

$$\phi = \frac{\omega P}{(0.622+\omega)P_{sat,T}} \quad (16)$$

Where $P_{sat,T}$ is the saturation pressure of water at a given temperature T which can be determined from Antoine equation as follows, [77]

$$P_{sat,T} = \exp\left(16.3872 - \frac{3885.7}{(T-273)+230.17}\right) \quad (17)$$

3.3.4.5 Water

Thermodynamic properties of water are taken from the library of EES which is formulated based on thermodynamic properties of water and steam, viscosity of water and steam and thermal conductivity of water and steam [78,79].

3.3.5 Combustor design

Combustion chamber and reheater are modelled as conventional combustors which have several inlets for air intake and a fuel nozzle [21,80,81]. The main components of a combustor are shown in the Figure 10.

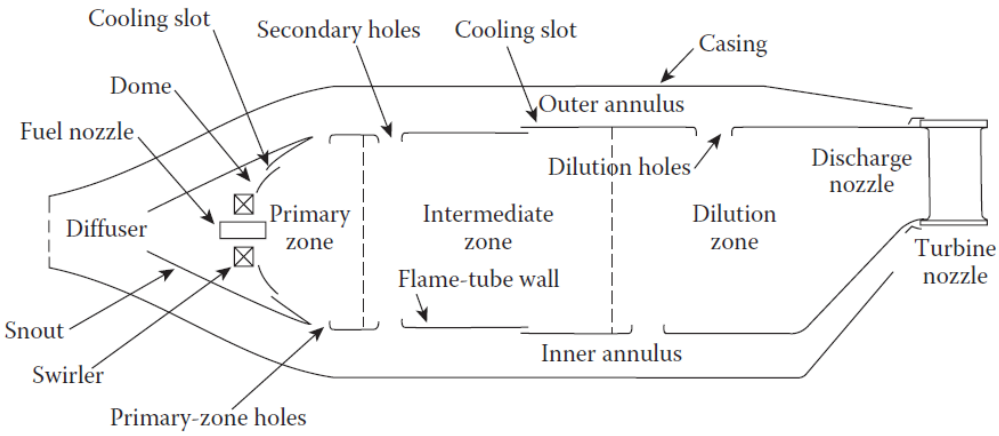

Figure 10 Components of a conventional combustor [21]

The velocity of the air entering into the combustion chamber needs to be reduced so that the pressure drop in the combustion is minimized. The diffuser serves the purpose of reducing the velocity. The main function of the primary zone is to initialize the flame and provide enough temperature and time for complete combustion. A small portion of the air flows into the primary zone and the remaining flows through the annulus. The temperatures attained in the primary zone are usually very high which results in the formation of carbon monoxide (CO) by dissociation. Secondly, some of the fuel remains un-oxidized causing the unburnt hydrocarbons (UHC) to appear. Finally, the material restrictions doesn't allow this high temperature gases to be passed to the turbine directly. This results in a need for an intermediate zone. Part of the air from the annulus enters into

the intermediate zone through the secondary holes. Any unburnt fuel left over (UHC) and CO is oxidized in this zone. Temperature reduces substantially in this zone.

The left-over air is then passed into the dilution zone. The amount of air that enters into dilution zone is usually 20% - 40%. This zone makes sure that the turbine sustainable temperature is attained by the combustion gases. Some of the CO is further oxidized depending on the temperature in this zone.

3.3.6 Heat exchangers design

Four heat exchangers namely, recuperator, water heater, intercooler, heat exchanger exists in the following analysis. ε-NTU method is employed in the thermal analysis of a heat exchanger.

In this method, the effectiveness (ε) of a heat exchanger is given as a function of number of transfer units (NTU) and ratio of specific heat capacity (C_r) which are defined as [82]

$$NTU = \frac{UA}{C_{min}}; \qquad C_r = \frac{C_{min}}{C_{max}}; \qquad C = \dot{m}C_p \tag{18}$$

U is the overall heat transfer coefficient and A is the heat exchanger surface area. These values are tabulated in Table 6 for the heat exchangers considered.

C is heat capacity of the two streams that flowing through the heat exchanger. The effectiveness of a heat exchanger which are a cross flow unmixed type is then given by [82,83]

$$\varepsilon = 1 - \exp\left[\left(\frac{1}{Cr}\right)(NTU)^{0.22}\{\exp[-C_r(NTU)^{0.78}] - 1\}\right] \tag{19}$$

3.3.7 Pressure evaluation

The pressure at the exit of each component is estimated by employing pressure drops given in Table 1. Mathematically, pressure at the exit of each component is given by [84]

$$(P_e = (1 - \theta)P_i)_{component} \quad (20)$$

Where P_e is the exit pressure out of the component, θ is the pressure drop from Table 1 and P_i is the inlet pressure into the component. For the components, such as compressor and turbines, pressure ratio dictates the exit pressure.

3.3.8 First Law Analysis of the proposed cycle

Conservation of mass and energy given in equation (1) and equation (2) are applied on every component of the system. This will result in the evaluation of pressure, temperature, humidity ratio and mass flow rate at all the state points. Some of the design parameters needed to evaluate the performance of the proposed gas turbine in tabulated in Table 6

Using the capacity of plant from Table 6, the mass flow rate of dry air was found out using the specific volume of that air at that temperature and pressure as

$$\dot{m}_8 = PC.v(T, P, \omega) \quad (21)$$

Then the detailed thermodynamic analysis for each component follows as

3.3.8.1 Mixing chamber (MC)

Conservation of mass across the mixing chamber gives

Table 6 Design and operating data of the proposed gas turbine power plant

Description		Value/Range
Power plant volumetric capacity at the exit of HPC (PC)		1 m^3/s
Ambient air temperature (T_0)		310 K (290 K – 320 K)
Ambient relative humidity (ϕ_0)		50% (20% - 80%)
Equivalence ratio (Φ)		0.85 (0.6 – 1.4)
Overall pressure ratio (r)		25 (10 – 40)
Extraction pressure ratio (x)		2.5 (1.5 – 4.5)
Extraction mass rate ratio (α)		0.1 – 0.4
Turbine inlet temperature (TIT)		1200 K (800 K – 1600 K)
Temperature rise of cooling fluid in the heat exchanger (ΔT)		10 K
Overall heat transfer coefficients [83]	Recuperator (Re)	0.05 kW/m^2-K
	Heat exchanger (HE)	0.1 kW/m^2-K
	Water heater (WH)	0.1 kW/m^2-K
	Intercooler (IC)	0.03 kW/m^2-K
Heat exchanger surface areas	Recuperator (Re)	1000 m^2
	Heat exchanger (HE)	200 m^2
	Water heater (WH)	50 m^2 (10 m^2 – 90 m^2)
	Intercooler (IC)	500 m^2
Residence time in combustor zones [21],[84],[85]	Primary zone	2 ms
	Intermediate zone	5 ms
	Dilution zone	10 ms

$$\dot{m}_1 = \dot{m}_0 + \dot{m}_5 \quad (22)$$

$$\omega_1 \dot{m}_1 = \omega_0 \dot{m}_0 + \omega_5 \dot{m}_5 \quad (23)$$

Energy balance across mixing chamber gives the temperature at state point 1

$$h_1 = \frac{\dot{m}_0 h_0 + \dot{m}_5 h_5}{\dot{m}_1} \quad (24)$$

3.3.8.2 Low pressure compressor (LPC)

Some of the mass is extracted from LPC at pressure P_2 while the remaining is sent to the gas turbine cycle at pressure P_6. The ratio of mass extracted to the total mass inlet to the compressor is defined as the extraction mass rate α, Mathematically, $\alpha = \frac{\dot{m}_2}{\dot{m}_1}$

Therefore, mass going to the refrigeration cycle $\dot{m}_2$and gas turbine cycle $\dot{m}_6$ is

$$\dot{m}_2 = \alpha \dot{m}_1; \qquad \dot{m}_6 = (1-\alpha)\dot{m}_1 \quad (25)$$

The humidity ratios in both the streams going to refrigeration cycle and gas turbine cycle remains the same. Hence,

$$\omega_2 = \omega_1; \qquad \omega_6 = \omega_1 \quad (26)$$

The overall pressure ratio is divided equally between the two compressors giving each pressure of each compressor as $r_{LPC} = r_{HPC} = \sqrt{r}$

The outlet temperatures of low pressure compressor can be calculated from the isentropic efficiency of the low pressure compressor (η_{LPC}) as

$$T_2 = T_1 + \frac{T_1}{\eta_{LPC,x}}\left(x^{\frac{k_{1-2}-1}{k_{1-2}}} - 1\right) \quad (27)$$

$$T_5 = T_1 + \frac{T_1}{\eta_{LPC,r}}\left(r_{LPC}^{\frac{k_{1-5}-1}{k_{1-5}}} - 1\right) \quad (28)$$

x is the extraction pressure ratio across the compressor and r_{LPC} is the overall pressure ratio of the low pressure compressor, η_{LPC} is the compressor efficiency, k is the polytropic index of compression, which is the ratio of specific heat at constant pressure to specific heat at constant volume

$$k = \frac{C_p}{C_v} \quad (29)$$

From the literature, the isentropic efficiency η_{LPC} is found to be a function of pressure ratio which can be given as,[86]

$$\eta_{LPC_y} = 1 - \left(0.04 + \frac{y-1}{150}\right) \quad (30)$$

Where y is either x or r.

The power input to the low pressure compressor needed for compression follows the energy balance as,

$$\dot{W}_{LPC} = \dot{m}_2 h_2 + \dot{m}_6 h_6 - \dot{m}_1 h_1 \quad (31)$$

3.3.8.3 Heat exchanger (HE)

There is no mass change across the heat exchanger, therefore mass flow rates and humidity content will remain the same.

$$\dot{m}_3 = \dot{m}_2; \qquad \dot{m}_3^1 = \dot{m}_0^{cfw}; \qquad \omega_3 = \omega_2 \quad (32)$$

The effectiveness of a HE was determined using the method defined in section3.3.6. Using the effectiveness, heat transfer through the heat exchanger can be determined [87]

$$q_{HE} = \varepsilon_{HE} C_{min,HE} (T_2 - T_0^{cfw}) \quad (33)$$

This amount of heat transfer is then used to find the output conditions of the heat exchanger using energy balance

$$h_3 = \frac{\dot{m}_2 h_2 - q_{HE}}{\dot{m}_3}; \qquad h_3^1 = \frac{q_{HE} - \dot{m}_0^{cfw} h_0^{cfw}}{\dot{m}_3^1} \quad (34)$$

3.3.8.4 Humidity Eliminator (HuE)

Humidity eliminator removes all the moisture giving mass flow rates as

$$\omega_4 = 0; \qquad \dot{m}_4^1 = \omega_3 \dot{m}_3; \qquad \dot{m}_4 = \dot{m}_3 \quad (35)$$

The outlet conditions of the humidity eliminator may be found using energy balance as

$$h_4 = \frac{\dot{m}_3 h_3 - \dot{m}_4^1 h_4^1}{\dot{m}_4} \quad (36)$$

3.3.8.5 Expander (Ex)

There is no mass change in the expander. Therefore,

$$\dot{m}_5 = \dot{m}_4; \qquad \omega_5 = \omega_4 \quad (37)$$

The outlet temperature of the expander can be found using the isentropic efficiency of the expander (η_{Ex}) from Table 2 as

$$T_5 = T_4 + \eta_{Ex} T_4 \left(\frac{1 - r_{Ex}^{\frac{k-1}{k}}}{r_{Ex}^{\frac{k-1}{k}}} \right) \quad (38)$$

Where k is the polytropic index for expansion process determined using the same equation (28) and r_{EX} is the expansion pressure ratio.

The power output from the expander is found out by conservation of energy across the expander as

$$\dot{W}_{Ex} = \dot{m}_4 h_4 - \dot{m}_5 h_5 \quad (39)$$

3.3.8.6 Air humidifier (AH)

This acts as an evaporative air cooler where water carries out the sensible enthalpy of air reducing its temperature. The air is fully saturated when it leaves the air humidifier. Using the equation (15), humidity ratio of the air ω_1^1 may be determined. Then, the mass balance across the air humidifier gives the outlet mass flow rate and water intake flow rate

$$\phi_1^1 = 100\ \%; \qquad \dot{m}_1^1 = m_0; \qquad \dot{m}_0^{ahw} = \dot{m}_1^1 \omega_1^1 - \dot{m}_0 \omega_0 \quad (40)$$

Applying energy balance gives the temperature at the exit of air humidifier,

$$h_1^1 = \frac{\dot{m}_0 h_0 + \dot{m}_0^{ahw} h_0^{ahw}}{\dot{m}_1^1} \quad (41)$$

3.3.8.7 Intercooler (IC)

There is change in the mass across the intercooler, hence mass flow rates and humidity content will remain the same.

$$\dot{m}_7 = \dot{m}_6; \qquad \dot{m}_1^{11} = \dot{m}_1^1; \qquad \omega_1^{11} = \omega_1^1 \tag{42}$$

Finding the effectiveness (ε_{IC}) of an intercooler follows the same procedure as for the heat exchanger where equations (17) through (18) are used. Using the effectiveness, the heat transfer rate followed by the outlet conditions of intercooler streams are determined as [87]

$$q_{IC} = \varepsilon_{IC} C_{min,IC}(T_6 - T_1^1) \tag{43}$$

$$h_7 = \frac{\dot{m}_6 h_6 - q_{HE}}{\dot{m}_7}; \qquad h_1^{11} = \frac{q_{HE} + \dot{m}_1^1 h_1^1}{\dot{m}_1^{11}} \tag{44}$$

3.3.8.8 High pressure compressor (HPC)

There is no mass or humidity deviation in the HPC giving the mass balance as

$$\dot{m}_8 = \dot{m}_7; \qquad \omega_8 = \omega_7 \tag{45}$$

Using the isentropic efficiency from equation (29) and the polytropic ratio from equation (28), the temperature at the exit of the HPC may be written as

$$T_8 = T_7 + \frac{T_7}{\eta_{LPC,r}}\left(r_{HPC}^{\frac{k_{7-8}-1}{k_{7-8}}} - 1\right) \tag{46}$$

Then, power needed to run the HPC is found using the energy balance,

$$\dot{W}_{HPC} = \dot{m}_8 h_8 - \dot{m}_7 h_7 \tag{47}$$

3.3.8.9 Water pump and Water heater (WH)

Water need to be heated to the saturation temperature of the inlet pressure of the after cooler and also water needs to be supplied at its inlet pressure before injecting into the after cooler for the complete evaporation.

$$T_{18} = T_{sat@P=P_8} \quad (48)$$

The pump serves the purpose to pressurize the water at that pressure. It increases the pressure of the water without any change in its temperature. The work needed for the pump then follows by using the efficiency of the pump from Table 2. Thus,

$$T_{17} = T_0^{whw}; \qquad \dot{W}_{pump} = \frac{\dot{m}_{17}h_{17} - \dot{m}_0^{whw}h_0^{whw}}{\eta_{pump}}; \qquad \dot{m}_{17} = \dot{m}_0^{whw} \quad (49)$$

The amount of heat exchange q_{WH} that needs to be carried out hence depends only on the mass flow rate but not on the temperatures

$$q_{WH} = \dot{m}_{18}h_{18} - \dot{m}_{17}h_{17} \quad (50)$$

Depending on the water heater surface area from Table 6, the effectiveness may be obtained using the equations (17) through (18). Using the effectiveness ε_{WH}, the heat transfer can also be written as [87]

$$q_{WH} = \varepsilon_{WH}C_{min,WH}(T_{15} - \mathrm{T}_{17}) \quad (51)$$

Combining the amount of heat transfer rate q_{WH} from equation (48) and equation (50), mass flow rate of the water $\dot{m}_{18}$ may be obtained.

The mass of water that could be injected depends on the water heater surface area. Larger surface area would be able to heat more amount of water increasing the amount of water that could be injected. But, there is an upper limit to the water injected. Any injection should not exceed the maximum amount of vapor that air can hold i.e., fully saturated air, at the exit of after cooler. This allows us to define water-to-air ratio (WAR) injected into the after cooler as

$$WAR = \frac{\dot{m}_{18}}{\dot{m}_8} \quad (52)$$

Also there is no change in the mass flow rates in the water heater,

$$\dot{m}_{17} = \dot{m}_{18}; \qquad \dot{m}_{16} = \dot{m}_{15} \quad (53)$$

The outlet condition of the gases follows from the energy balance of water heater,

$$h_{16} = \frac{\dot{m}_{15} h_{15} - q_{WH}}{\dot{m}_{16}} \quad (54)$$

3.3.8.10 After cooler (AC)

The mass balance for water vapor and air across the aftercooler gives the humidity ratio and mass flow rate of air at the exit of after cooler as

$$\omega_9 = \frac{\dot{m}_{18} + \dot{m}_8 \omega_8}{\dot{m}_9}; \qquad \dot{m}_9 = \dot{m}_8 \quad (55)$$

The energy balance for the after cooler then gives the outlet temperature as

$$h_9 = \frac{\dot{m}_8 h_8 + \dot{m}_{18} h_{18}}{\dot{m}_9} \quad (56)$$

3.3.8.11 Recuperator (Re)

Mass balance of air and water vapor through the recuperator gives

$$\dot{m}_{10} = \dot{m}_9; \qquad \omega_{10} = \omega_9; \qquad \dot{m}_{15} = \dot{m}_{14} \tag{57}$$

Same procedure as defined earlier in 3.3.6 is employed to find the effectiveness (ε_{Re}) using the equations (17) through (18) for which the area and overall heat transfer coefficient are given in Table 6.

The effectiveness is then used to find the heat transfer followed by output temperatures of recuperator [87]

$$q_{Re} = \varepsilon_{Re} C_{min,Re} (T_{14} - \mathrm{T}_9) \tag{58}$$

$$h_{10} = \frac{q_{Re} + \dot{m}_9 h_9}{\dot{m}_{10}}; \qquad h_{15} = \frac{\dot{m}_{14} h_{14} - q_{HE}}{\dot{m}_{15}} \tag{59}$$

3.3.8.12 Combustors (Combustion chamber CC and reheater RH)

The gas turbine plant under consideration uses natural gas as a fuel whose composition is defined in 3.3.4.3. The combustor model is explained in 3.3.5.

Molar humidity ratio $\bar{\omega}$ is more convenient to use in combustion reactions which is related to the humidity ratio ω as

$$\bar{\omega} = \frac{n_{vapor/H_2O}}{n_{air}} = 1.6075\omega \tag{60}$$

A general combustion equation for n moles of the fuel as natural gas and humid air including emissions as oxidizer with $\bar{\omega}$ as the molar humidity ratio is given as [51,72,88];

$$n_{fuel}(0.96CH_4 + 0.02C_2H_6 + 0.006C_3H_8 + 0.003C_4H_{10} + 0.011N_2) + n_{air}\bar{\omega}H_2O +$$

$$n_{air}\left(y_{CO_2}CO_2 + y_{O_2}O_2 + y_{N_2}N_2 + y_{Ar}Ar + y_{CO}CO + y_{NO}NO + y_{NO_2}NO_2\right) \rightarrow$$

$$n_{CO_2}CO_2 + n_{H_2O}H_2O + n_{O_2}O_2 + n_{N_2}N_2 + n_{Ar}Ar + n_{CO}CO + n_{NO}NO + n_{NO_2}NO_2 +$$

$$n_{UHC}(0.96CH_4 + 0.02C_4H_8 + 0.006C_3H_8 + 0.003C_4H_{10} + 0.011N_2) \quad (61)$$

Mass balance for the above reaction results in

$$1.03n_{fuel} + n_{air}\left(y_{CO_2} + y_{CO}\right) = n_{CO_2} + n_{CO} + 1.03n_{UHC} \text{ (Carbon balance)} \quad (62)$$

$$4.038n_{fuel} + 2n_{air}\bar{\omega} = 2n_{H_2O} + 4.038n_{UHC} \text{ (Hydrogen balance)} \quad (63)$$

$$0.022n_{fuel} + n_{air}\left(2y_{N_2} + y_{NO} + y_{NO_2}\right) = 2n_{N_2} + n_{NO} + n_{NO_2} + 0.022n_{UHC}$$

(Nitrogen balance) (64)

$$n_{air}\left(\bar{\omega} + 2y_{CO_2} + y_{H_2O} + 2y_{O_2} + y_{CO} + y_{NO} + 2y_{NO_2}\right) = 2n_{CO_2} + n_{H_2O} + 2n_{O_2} +$$

$$n_{CO} + n_{NO} + 2n_{NO_2} \text{ (Oxygen balance)} \quad (65)$$

$$n_{air}y_{Ar} = n\_Ar \text{ (Argon balance)} \quad (66)$$

The above reaction is applicable to all the zones of the combustors. However, some of the simplifications may be done based on the zone and combustor before using it.

1. Fuel term in the left hand side of the reaction will be zero for the dilution zones of both the combustion chamber and reheater.

2. The UHC term on the right hand side of the reaction will be zero for the intermediate and dilution zones for both the combustors.

3. The UHC term on the right hand side of the reaction from primary zone will act as a fuel for both the intermediate zones.

4. The mole fractions of CO, NO and NO_2 in the air will be zero for the primary zone of the combustion chamber, since clean air is supplied to it.

5. The exhaust composition of each zone is supplied as the air to the subsequent zone in both the combustors.

6. The exhaust composition of the combustion chamber dilution zone acts as an inlet air to the reheater.

3.3.8.12.1 Stoichiometric Fuel-Air ratio

The minimum amount of air needed for complete combustion of a fuel is called stoichiometric air and the corresponding ratio of the mass of fuel to the mass of air is known as stoichiometric fuel-air ratio. Different composition of air flow into the combustion chamber and reheater. Hence, different values of Stoichiometric fuel-air ratio are obtained. To find stoichiometric fuel-air ratio from the reaction (60), following sequence need to be followed.

a. Combustion chamber

   i. y_{CO}, y_{NO}, y_{NO_2} are zero.

   ii. $n_{O_2}, n_{CO}, n_{NO}, n_{NO_2}, n_{UHC}$ are zero.

   iii. $y_{CO_2}, y_{O_2}, y_{N_2}, y_{Ar}$ are taken from equation (12).

   iv. Find $\bar{\omega}$ from equation (59).

   v. Simultaneously solve equations (61) through (65) using $n_{fuel} = 1$.

   vi. $FA_{stoic} = \frac{n_{fuel} MW_{fuel}}{n_{air} MW_{air}}$ where MW is the molecular weight, that can be found using equation (10)

b. Reheater

i. $y_{CO_2}, y_{O_2}, y_{N_2}, y_{Ar}, y_{CO}, y_{NO}, y_{NO_2}$ are the same as in exhaust of combustion chamber from dilution zone

ii. n_{O_2}, n_{UHC} are zero.

iii. No more CO, NO, NO_2 are formed in the reheater during stoichiometric combustion. Hence, $n_{CO} = n_{air} y_{CO}; n_{NO} = n_{air} y_{NO}; n_{NO_2} = n_{air} y_{NO_2}$

iv. Find $\bar{\omega}$ from equation (59) using the exhaust of combustion chamber from dilution zone..

v. Simultaneously solve equations (61) through (65) using $n_{fuel} = 1$.

vi. $FA_{stoic} = \frac{n_{fuel} MW_{fuel}}{n_{air} MW_{air}}$ where MW is the molecular weight, that can be found for both fuel and air using equation (10)

3.3.8.12.2 Lower Heating Value of the fuel

The lower heating value (LHV) of the fuel is defined as the amount of heat released during an adiabatic complete or stoichiometric combustion after the combustion products are cooled down to the same temperature and pressure, i.e., ambient temperature and pressure at which the reactants enter [72]. Since, the composition of air entering the combustion chamber and reheater are different, LHVs obtained for them will be different. Mathematically, molar LHV is given by [72]

$$\overline{LHV} = \sum_{i=1}^{n_R} n_i \bar{h}_i - \sum_{j=1}^{n_P} n_j \bar{h}_j \qquad (67)$$

Where n_R is the number of reactants and n_P is the number of products of the reaction in the equation (60). n_i is the number of moles of the ith species in the reactants found using the steps shown in 3.3.8.12.1, and $\bar{h}_i$ is the molar specific enthalpy of that ith species at the ambient temperature. Similarly, n_j is the number of moles of the jth species in the products found using the steps shown in 3.3.8.12.1, and $\bar{h}_j$ is the molar specific enthalpy of that jth species at the ambient temperature.

3.3.8.12.3 Primary zone reaction

A small percentage of air δ_{PZ} flows into the primary zone of the combustors depending on the turbine inlet temperature needed. The ratio of actual fuel-air ratio to the stoichiometric fuel-air ratio is known as equivalence ratio. For a given mass fuel-air equivalence ratio Φ, amount of fuel is determined as [89]

$$\dot{m}_{fuel} = \frac{\delta_{PZ}\dot{m}_{in}FA_{stoic}}{\Phi} \quad (68)$$

Where $\dot{m}_{in}$ is the total mass flow rate of air into the combustors, $\dot{m}_{10}$ for combustion chamber, $\dot{m}_{12}$ for the reheater. This amount of air and fuel into the primary zone is then converted to number of moles (n_{fuel}, n_{air}) using equation (11). Following sequence should be followed to find the temperature and exhaust composition in the primary zone,

a. Combustion chamber

   i. y_{CO}, y_{NO}, y_{NO_2} are zero.

   ii. $n_{CO}, n_{NO}, n_{NO_2}, n_{UHC}$ are estimated from the environmental analysis discussed in 3.3.11.

iii. $y_{CO_2}, y_{O_2}, y_{N_2}, y_{Ar}$ are taken from equation (12).

iv. Find $\bar{\omega}$ from equation (59).

v. Simultaneously solve equations (61) through (65) using n_{fuel}, n_{air} found earlier in this section. This will result in the composition of exhaust determination.

vi. Apply energy balance to find the temperature as, [90]

$$\sum_{j=1}^{n_P} n_j \bar{h}_j = \eta_{CC} \left[\sum_{i=1}^{n_R} n_i \bar{h}_i) \right] \qquad (69)$$

b. Reheater

i. $y_{CO_2}, y_{O_2}, y_{N_2}, y_{Ar}, y_{CO}, y_{NO}, y_{NO_2}$ are the same as in exhaust of combustion chamber from dilution zone.

ii. $n_{CO}, n_{NO}, n_{NO_2}, n_{UHC}$ are estimated from the environmental analysis discussed in 3.3.11 and added cumulatively only for his zone.

iii. Find $\bar{\omega}$ from equation (59) using the exhaust of combustion chamber from dilution zone..

iv. Simultaneously solve equations (61) through (65) using n_{fuel}, n_{air} found earlier in this section. This will result in the evaluation of composition of exhaust.

v. Apply energy balance to find the temperature as, [90]

$$\sum_{j=1}^{n_P} n_j \bar{h}_j = \eta_{RH} \left[\sum_{i=1}^{n_R} n_i \bar{h}_i) \right] \qquad (70)$$

In equations (68) and (69), n_R is the number of reactants and n_P is the number of products of the reaction in the equation (60). n_i is the number of moles of the ith species in the reactants already found, and $\bar{h}_i$ is the molar specific enthalpy of that ith species at the inlet temperature i.e., air temperature T_{10} for combustion chamber, air temperature T_{12} for reheater and fuel temperature T_0. Similarly, n_j is the number of moles of the jth species in the products already found and $\bar{h}_j$ is the molar specific enthalpy of that jth species at the primary zone temperature which will be found using this algorithm.

3.3.8.12.4 Intermediate zone reaction

Remaining air is divided between the intermediate zone and dilution zone. It is assumed that percentage of air through dilution zone δ_{DZ} is twice that of intermediate zone δ_{IZ}. The amount of air into this zone will thus be $\delta_{IZ,CC}\dot{m}_{10}$ for combustion chamber and $\delta_{IZ,RH}\dot{m}_{12}$ for reheater. This corresponding number of moles (n_{CO_2}, n_{N_2}, etc) from the air coming in and exhaust of primary zone are added giving total number of moles of air for this zone (n_{air}). The moisture content in the air and n_{H_2O} from the previous zone is also added to give the n_{H_2O} as an inlet to this zone. n_{UHC} formed in the primary zone is taken as the fuel (n_{fuel}) to this zone supplied at the primary zone temperature.

Following sequence should be followed to find the temperature and exhaust composition in the primary zone for both combustion chamber and reheater as,

i. $y_{CO_2}, y_{O_2}, y_{N_2}, y_{Ar}, y_{CO}, y_{NO}, y_{NO_2}$ are calculated after adding corresponding number of moles from the exhaust of primary

zone and air coming in i.e., $\delta_{IZ,CC}\dot{m}_{10}$ for combustion chamber and $\delta_{IZ,RH}\dot{m}_{12}$ for reheater.

ii. n_{CO}, n_{NO}, n_{NO_2} are estimated from the environmental analysis discussed in 3.3.11. No more UHC will be left $n_{UHC} = 0$.

iii. Find $\bar{\omega}$ from equation (59) using the n_{H_2O} inlet to this zone as discussed above in this section.

iv. Simultaneously solve equations (61) through (65) using n_{fuel}, n_{air} found earlier in this section. This will give the composition at the end of reheater.

v. Apply energy balance to find the temperature as, [90]

$$\sum_{j=1}^{n_P} n_j \bar{h}_j = \eta_{CC/RH} \left[\sum_{i=1}^{n_R} n_i \bar{h}_i) \right] \qquad (71)$$

In equation (70), n_R is the number of reactants and n_P is the number of products of the reaction in the equation (60). n_i is the number of moles of the ith species in the reactants already found, and $\bar{h}_i$ is the enthalpy of that ith species at the inlet temperature i.e., primary zone temperature. Similarly, n_j is the number of moles of the jth species in the products already found and $\bar{h}_j$ is the enthalpy of that jth species at the intermediate zone temperature which will be found using this algorithm.

3.3.8.12.5 Dilution zone reaction

The amount of air and fuel into this zone is, $\delta_{DZ,CC}\dot{m}_{10}$ for combustion chamber and $\delta_{DZ,RH}\dot{m}_{12}$ for reheater. This corresponding number of moles (n_{CO_2}, n_{N_2}, etc) from the

air coming in and exhaust of intermediate zone are added giving total number of moles of air for this zone (n_{air}). The moisture content in the air and n_{H_2O} from the previous zone is also added to give the n_{H_2O} as an inlet to this zone. There will be no fuel supplied to this zone. Only suppression of the temperature will be carried out in this zone that is dictated by material considerations.

Following sequence should be followed to find the temperature and exhaust composition in the primary zone for both combustion chamber and reheater as,

i. $y_{CO_2}, y_{O_2}, y_{N_2}, y_{Ar}, y_{CO}, y_{NO}, y_{NO_2}$ are calculated after adding corresponding number of moles from the exhaust of intermediate zone and air coming in i.e., $\delta_{DZ,CC}\dot{m}_{10}$ for combustion chamber and $\delta_{DZ,RH}\dot{m}_{12}$ for reheater.

ii. n_{CO}, n_{NO}, n_{NO_2} are estimated from the environmental analysis discussed in 3.3.11. No more UHC will be formed $n_{UHC} = 0$.

iii. Find $\bar{\omega}$ from equation (59) using the n_{H_2O} inlet to this zone as discussed above in this section.

iv. Simultaneously solve equations (61) through (65) using n_{air} found earlier in this section. This will give the composition at the end of reheater.

v. Apply energy balance to this zone as, [90]

$$\sum_{j=1}^{n_P} n_j \bar{h}_j = \eta_{CC/RH} \left[\sum_{i=1}^{n_R} n_i \bar{h}_i \right] \qquad (72)$$

In the above equation, temperature of the products is known, which is turbine inlet temperature. The percentage of air into this zone is found using the energy balance. In equation (71), n_R is the number of reactants and n_P is the number of products of the reaction in the equation (60). n_i is the number of moles of the ith species in the reactants already found, and $\bar{h}_i$ is the molar specific enthalpy of that ith species at the inlet temperature i.e., intermediate zone temperature. Similarly, n_j is the number of moles of the jth species in the products already found and $\bar{h}_j$ is the enthalpy of that jth species at the dilution zone temperature which is turbine inlet temperature.

The mass flow rate out of the combustion chamber and reheater.

$$\dot{m}_{11} = \dot{m}_{10} + \dot{m}_{fuel,CC}; \qquad \dot{m}_{13} = \dot{m}_{12} + \dot{m}_{fuel,RH} \tag{73}$$

3.3.8.13 High pressure gas turbine (HPGT)

Mass flow rate remain the same across HPGT

$$\dot{m}_{12} = \dot{m}_{11} \tag{74}$$

The pressure ratio is divided equally among the two pressure turbines giving, $r_{HPGT} = r_{LPGT}$. Using the isentropic efficiency of turbine (η_t) from Table 2, the outlet temperature of high pressure gas turbine is then found out by

$$T_{12} = T_{11} + \eta_t T_{11} \left(\frac{1 - r_{HPGT}^{\frac{k-1}{k}}}{r_{HPGT}^{\frac{k-1}{k}}} \right) \tag{75}$$

Where k is the polytropic index for this expansion process determined using the same equation (28). The power produced by the HPGT may be written by considering the balance of energy as

$$\dot{W}_{HPGT} = \dot{m}_{11}h_{11} - \dot{m}_{12}h_{12} \quad (76)$$

3.3.8.14 Low pressure gas turbine (LPGT)

Mass balance in LPGT gives,

$$\dot{m}_{14} = \dot{m}_{13} \quad (77)$$

Using the isentropic efficiency of turbine (η_t) from Table 2, the outlet temperature of low pressure gas turbine is then found out by

$$T_{14} = T_{13} + \eta_t T_{13}\left(\frac{1-r_{LPGT}^{\frac{k-1}{k}}}{r_{LPGT}^{\frac{k-1}{k}}}\right) \quad (78)$$

Where k is the polytropic index for this expansion process determined using the same equation (28). Therefore, power developed by this turbine is

$$\dot{W}_{LPGT} = \dot{m}_{13}h_{13} - \dot{m}_{14}h_{14} \quad (79)$$

3.3.9 Exergy formulation of different species

Not all the energy in the stream or component is capable of doing work. The capacity of doing work through that energy has been accepted as a measure of the quality of energy. Therefore, exergy is the shaft or electrical work necessary to produce a material in its specified state from materials common in the environment in a reversible way. The chief

aim of exergy analysis is to detect and to evaluate quantitatively the causes of the thermodynamic imperfections of the process. The thermal exergy is the major concern when evaluating the steady flow process which can be written as the sum of physical and chemical exergy [29]. Therefore,

$$\dot{X}_{th} = \dot{X}_{ph} + \dot{X}_{ch} \quad (80)$$

Physical exergy $\dot{X}_{ph}$ is the work which can be obtained reversibly from its initial temperature T, pressure P, to the dead state, which is determined by temperature T_0 and the pressure P_0. Chemical exergy $\dot{X}_{ch}$ is the work that can be obtained when the substance at the dead state initially is taken to the datum level of components of the environment. Now, employing this basic concept of exergy to formulate specific exergy of different species involved in the study is presented.

3.3.9.1 Specific exergy of humid air

Humid air contains three functions through which work could be produced, through temperature, pressure and its moisture content. The specific exergy e_x of a humid air at any given temperature T, pressure P, relative humidity ϕ, and humidity ratio ω with the environment of temperature T_0, pressure P_0, relative humidity ϕ_0 is given by [29], [91]

$$e_x(kJ/kg\ of\ dry\ air) = C_{p,a}(T - T_0) - T_0\left[C_{p,a}\ln\left(\frac{T}{T_0}\right) - R_a \ln\frac{P - \phi P_{sat@T=T}}{P_0 - \phi_0 P_{sat@T=T_0}}\right] +$$

$$\omega[h_{v@T=T} - h_{v@T=T_0} - T_0(s_{v@T=T} - s_{v@T=T_0})] \quad (81)$$

Where $C_{p,a}$ is the specific heat of air at temperature T, which can be found by using equations (10), (12) and (11). R_a is the gas constant for air that can be evaluated using equation (11).

3.3.9.2 Specific exergy of water

The specific exergy of water at a temperature T and pressure P with ambient conditions of temperature T_0, relative humidity ϕ_0 is given by [91]

$$e_x = h_{f@T=T} - h_{v@T=T_0} - T_0(s_{f@T=T} - s_{v@T=T_0}) + [P - P_{sat@T=T}]v_{f@T=T} - R_v T_0 ln\phi_0 \quad (82)$$

where f and g denotes the liquid and gaseous states of water; v is the specific volume of water; $R_v$is the gas constant for water vapor.

3.3.9.3 Specific exergy of combustion gases

Thermal exergy of the combustion gases consists of three components. Firstly, due to its elevated temperature, second, due to its pressure and third, due to its composition. It can be written mathematically as [29]

$$e_x = e_x(T) + e_x(P) + e_x(y) \quad (83)$$

In the composition dependent exergy, work that could be developed from combustible and non-combustible matters such as CO, CO_2, etc need to be accounted for. Therefore, molar specific exergy of combustion gases is given by [29]

$$\bar{e}_x = \left[(\bar{h} - \bar{h}_0) - T_0(\bar{s} - \bar{s}_0)\right] + \left[\bar{R}T_0 \ln\left(\frac{P}{P_0}\right)\right] + \Bigg[\bar{R}T_0 (y_{N_2} \ln\left(\frac{y_{N_2}}{y_{N_{2air}}}\right) +$$

$$y_{O_2} \ln\left(\frac{y_{O_2}}{y_{O_{2air}}}\right) + y_{CO_2} \ln\left(\frac{y_{CO_2}}{y_{CO_{2air}}}\right) + y_{Ar} \ln\left(\frac{y_{Ar}}{y_{Ar_{air}}}\right) + \bar{\omega} \ln\left(\frac{\bar{\omega}}{\bar{\omega}_0}\right) + (1 + \bar{\omega}) \ln\left(\frac{1+\bar{\omega}_0}{1+\bar{\omega}}\right) +$$

$$y_{CO}\left(\overline{e^0_{x\,CO}} + \bar{R}T_0 \ln\left(\frac{y_{CO}P_0}{P_n}\right)\right) + y_{NO}\left(\overline{e^0_{x\,NO}} + \bar{R}T_0 \ln\left(\frac{y_{NO}P_0}{P_n}\right)\right) + y_{NO_2}\left(\overline{e^0_{x\,NO_2}} +$$

$$\bar{R}T_0 \ln\left(\frac{y_{NO_2}P_0}{P_n}\right)\Bigg)\Bigg] \qquad (84)$$

Where $\bar{h}, \bar{s}$, are evaluated at the gases temperature T and P. h_0, s_0 are evaluated at the reference temperature T_0, P_0. $\bar{R}$ is the universal gas constant. $\bar{\omega}$ is the molar humidity ratio of the gases where as $\bar{\omega}_0$ is the molar humidity ratio in the environment. y_i is the mole fraction of the ith species in a given mixture and $y_{i,air}$ is the mole fraction of the same species in the environment. $y_{N_2}, y_{O_2}, y_{CO_2}, y_{Ar}, y_{CO}, y_{NO}, y_{NO_2}$ are the mole fractions of combustible and non-combustible species. $\overline{e^0_{x\,CO}}, \overline{e^0_{x\,NO}}, \overline{e^0_{x\,NO_2}}$ are the standard chemical exergy tabulated in Table 5 and P_n is 101.325 kPa. This molar specific exergy of gases can then be converted into specific exergy per mass using (10) and (11).

3.3.9.4 Specific exergy of fuel

Since, the fuel is supplied at the ambient temperature. The specific exergy of the fuel contains only two parts. Exergy due to its elevated pressure and due to its chemical content. For a substance such as fuel, which does not exist in the reference environment, the chemical exergy is divided into two reversible reactions.

1. A reference chemical reaction act T_0 and P_0 where the substance reacts with substances from the environment and generating substances that exist in the environment.

2. Change in concentrations of these products so that they are in equilibrium with the reference environment. [72], [92]

$$\overline{e_{x}}_{fuel,ch} = -\Delta\overline{G_0} - \left[\sum_{i=1}^{n_R} n_i \overline{e_{x_i}^0}\right]_{co-reactants} + \left[\sum_{j=1}^{n_P} n_j \overline{e_{x_j}^0}\right]_{products} \quad (85)$$

Where n_R is the number of reactants except fuel and n_P is the number of products of the reaction in the equation (60). n_i is the number of moles of the ith species in the co-reactants found using the steps shown in 3.3.8.12.1, and $\overline{e_{x_i}^0}$ is the molar standard exergy of that ith species at the ambient temperature. Similarly, n_j is the number of moles of the jth species in the products found using the steps shown in 3.3.8.12.1, and $\overline{e_{x_j}^0}$ is the standard chemical exergy of that jth species at the ambient temperature. Standard chemical exergies are tabulated in Table 5. $\Delta\overline{G_0}$ is the molar gibbs function for the reaction in the equation (60). It is given by [72], [92]

$$\Delta\overline{G_0} = \sum_{j=1}^{n_P} n_j \bar{g}_j - \sum_{i=1}^{n_R} n_i \bar{g}_i \quad (86)$$

For which n_R is number of reactants including fuel, n_P, number of products of the reaction in the equation (60). Use the same procedure as in 3.3.8.12.1 to find n_i, n_j. $\bar{g}_i$ is the molar free gibbs energy for the ith reactant and $\bar{g}_j$ is the molar free gibbs energy for

the ith product at the reference temperature T_0 and pressure P_0. Gibbs free energy $\bar{g}$ can be found from the corresponding enthalpy and entropy at any temperature T and pressure P as [88]

$$\bar{g}_{(T,P)} = \bar{h}_{(T)} - T_0 \bar{s}_{(T,P)} \quad (87)$$

The exergy of the fuel due to its pressure is therefore, [72]

$$e_{x_{fuel},ph} = \bar{R} T_0 \ln\left(\frac{P_{fuel}}{P_0}\right) \quad (88)$$

Now the thermal exergy or total exergy of the fuel can be written as

$$e_{x_{fuel}} = \bar{R} T_0 \ln\left(\frac{P_{fuel}}{P_0}\right) - \left[\sum_{j=1}^{n_P} n_j \bar{g}_j - \sum_{i=1}^{n_R} n_i \bar{g}_i\right] - \left[\sum_{i=1}^{n_R} n_i \overline{e_{x_i}^0}\right]_{co-reactants} + \left[\sum_{j=1}^{n_P} n_j \overline{e_{x_j}^0}\right]_{products} \quad (89)$$

3.3.10 Second Law Analysis of the proposed cycle

Once, the temperature, pressure, humidity ratio, mass flow rates at all the states points are known, a general exergy balance (equation (3) through (5)) on each component of the cycle was performed. If the process would have been reversible, all the exergy input to the component would have been converted into the output. Due to irreversibility in all the components, some of the input exergy is destructed. The exergy content of each stream at each state is found using the method shown in 3.3.9. Then, the exergy destruction formulation in each component of the cycle is found which is tabulated in Table 7.

Table 7 Component-wise exergy destruction formulation [93]

Component	Exergy Destruction ($\dot{I}_{comp}$)
Mixing chamber (MC)	$\dot{m}_0 e_{x_0} + \dot{m}_5 e_{x_5} - \dot{m}_1 e_{x_1}$
Low pressure compressor (LPC)	$\dot{W}_{LPC} + \dot{m}_1 e_{x_1} - \dot{m}_2 e_{x_2} - \dot{m}_6 e_{x_6}$
Heat exchanger (HE)	$\dot{m}_2 e_{x_2} - \dot{m}_3 e_{x_3} + \dot{m}_0^{cfw} e_{x_0}^{cfw} - \dot{m}_3^1 e_{x_3}^{\ 1}$
Humidity eliminator (HuE)	$\dot{m}_3 e_{x_3} - \dot{m}_4 e_{x_4} - \dot{m}_4^1 e_{x_4}^1$
Expander (Ex)	$\dot{m}_4 e_{x_4} - \dot{W}_{ex} - \dot{m}_5 e_{x_5}$
Air humidifier (AH)	$\dot{m}_0^{aha} e_{x_0}^{aha} + \dot{m}_0^{ahw} e_{x_0}^{ahw} - \dot{m}_1^1 e_{x_1}^1$
Intercooler (IC)	$\dot{m}_6 e_{x_6} - \dot{m}_7 e_{x_7} + \dot{m}_1^1 e_{x_1}^1 - \dot{m}_1^{11} e_{x_1}^{11}$
High pressure compressor (HPC)	$\dot{W}_{HPC} + \dot{m}_7 e_{x_7} - \dot{m}_8 e_{x_8}$
After cooler (AC)	$\dot{m}_8 e_{x_8} + \dot{m}_{18} e_{x_{18}} - \dot{m}_9 e_{x_9}$
Recuperator (Re)	$\dot{m}_9 e_{x_9} - \dot{m}_{10} e_{x_{10}} + \dot{m}_{14} e_{x_{14}} - \dot{m}_{15} e_{x_{15}}$
Combustion chamber (CC)	$\dot{m}_{10} e_{x_{10}} + \dot{m}_{f,CC} e_{x_{f,CC}} - \dot{m}_{11} e_{x_{11}}$
High pressure gas turbine (HPGT)	$\dot{m}_{11} e_{x_{11}} - \dot{m}_{12} e_{x_{12}} - \dot{W}_{HPGT}$
Reheater (RH)	$\dot{m}_{12} e_{x_{12}} + \dot{m}_{f,RH} e_{x_{f,RH}} - \dot{m}_{13} e_{x_{13}}$
Low pressure gas turbine (LPGT)	$\dot{m}_{13} e_{x_{13}} - \dot{m}_{14} e_{x_{14}} - \dot{W}_{LPGT}$
Water heater (WH)	$\dot{m}_{14} e_{x_{14}} - \dot{m}_{15} e_{x_{15}} + \dot{m}_{17} e_{x_{17}} - \dot{m}_{18} e_{x_{18}}$
Pump	$\dot{m}_0^{whw} e_{x_0}^{whw} + \dot{W}_{pump} - \dot{m}_{17} e_{x_{17}}$

3.3.11 Environmental Analysis

One of the main objective of present research was also to predict the amount of emissions found in the exhaust of the gas turbine. It was also to highlight the emissions reducing potential of after cooling or water injection. To predict the emissions from the turbine, many researchers were able to relate the emissions produced to the temperature, pressure and the residence time of fuel air mixture in the combustors from experimental and numerical results [21], [64], [94]. The amount of oxides of nitrogen (NOx), carbon monoxide (CO) and unburnt hydrocarbons (UHC) are estimated in this study. The correlations used in the study are discussed in the subsequent subsections

3.3.11.1 Oxides of Nitrogen

Since, the combustor modelled consist of three zones, i.e., primary zone, intermediate zone and dilution zone. A proper model was needed which can predict NOx from a conventional combustor. Since, the temperature changes considerably in each zone, a separate semi-analytical relation is used in each zone

3.3.11.1.1 Primary zone (PZ)

The NOx formation in the primary zone has been found to be dependent on the inlet pressure P_{in}, temperature T_{pz}, residence time in the zone τ and the fuel-air equivalence ratio Φ. This may be found as [64]

If $\Phi < 1.08$

$$m_{NOx}\left(\frac{g}{kg} of\ fuel\right) = 1e13\left(\frac{P_{in}}{1.4e6}\right)^{aa} \exp\left(-\frac{71442}{T_{pz}}\right)(7.56\Phi^{-7.2} - 1.6)\tau^{0.64} \quad (90)$$

If $\Phi > 1.08$

$$m_{NOx}\left(\frac{g}{kg} of\ fuel\right) = 1e13\left(\frac{P_{in}}{1.4e6}\right)^{aa} \exp\left(-\frac{71442}{T_{pz}}\right)(5.21\Phi^{-2.99} - 1.6)\tau^{0.64} \quad (91)$$

Where aa exponent is,

$$aa = 11.949 \exp\left(-\frac{\Phi}{5.76}\right) - 10 \quad (92)$$

3.3.11.1.2 Intermediate zone (IZ)

Temperatures are still high enough in the intermediate zone for the formation of NOx. Based, on the results, the following equation was proposed, [64]

$$m_{NOx}\left(\frac{g}{kg} of\ fuel\right) = 1e14\left(\frac{P_{in}}{1.4e6}\right)^{aa} \exp\left(-\frac{71442}{T_{iz}}\right)(1.172\Phi^{-4.56} - 0.6)\tau^{0.876} \quad (93)$$

3.3.11.1.3 Dilution zone (DZ)

If the temperature in the dilution zone prevails high too, such as in high turbine inlet temperature conditions, the following equation may be used to estimate the amount of NOx formed. [64]

$$m_{NOx}\left(\frac{g}{kg} of\ fuel\right) = 1e14\left(\frac{P_{in}}{1.4e6}\right)^{aa} \exp\left(-\frac{71442}{T_{dz}}\right)(1.172\Phi^{-4.56} - 0.6)\tau^{0.876} \quad (94)$$

3.3.11.1.4 Oxides of nitrogen ratio

It has been found that initially formed NO eventually gets converted to NO_2 with time. Based on some results in the literature, ratio between the amounts of NO_2 to the total amount of NO_2 is derived [95]–[98]. The behavior of primary zone is much different than

the other two zones, hence, two different relations were found based on the research carried out.

a. Primary Zone

The ratio of the mass of NO_2 to the total amount of NOx in primary zone was found to be dependent on the equivalence ratio which may be expressed as [95]

$$\frac{m_{NO_2}}{m_{NOx}} = 1 - \exp(-4.038749e-4\Phi^{26.5238}) \quad (95)$$

b. Intermediate and Dilution zone

When sufficient concentration of NO has been formed in a zone, it starts converting into NO_2. Realizing this, the ratio was found to be [97]

$$\frac{m_{NO_2}}{m_{NOx}} = 1.393\left(1 - \frac{31.594e-9}{m_{NOx}}\right) \quad (96)$$

3.3.11.1.5 Molar basis for oxides of nitrogen

The amount of NOx estimated by the equations (89) through (93) gives the amount formed per kilogram of the fuel supplied. To complete the mass and energy balance in the section 3.3.8.12, number of moles in each zone is needed. Further, the number of moles of each NO_2 and NO is needed. Therefore, the amount of NOx is divided into amount of each NO_2 and NO using equation (94) and (95) then converted into number of moles by [51]

$$n_{NO_2} = \frac{m_{NO_2}\dot{m}_{f,CC/RH}*10^3}{MW}; \qquad n_{NO} = \frac{m_{NO}\dot{m}_{f,CC/RH}*10^3}{MW} \quad (97)$$

Where MW is the molar mass of NO and NO_2 respectively, $\dot{m}_{f,CC/RH}$ is either mass if the fuel supplied to combustion chamber or reheater depending on whose zone is been studied. The total NOx out of the combustors is the sum of all the NOx from each zone.

3.3.11.2 Carbon monoxide (CO)

The sequence of events in a combustor has been found to follow the following sequence [6], [81].

1. The available oxygen firstly burns all the hydrogen in the fuel to water vapor
2. Carbon from the fuel then burns to carbon monoxide.
3. If any oxygen is left, then it oxidized formed carbon monoxide into carbon dioxide.

A similar approach as oxides of nitrogen has been carried out to estimate the amount of CO in each zone. They are given as follows

3.3.11.2.1 Primary zone (PZ)

In the primary zone, the initial CO is formed is found to be dependent on the inlet pressure P_{in}, temperature T_{pz},, residence time τ and equivalence ratio Φ as follows [64]

If $T_{pz} > 1370\ K$

$$m_{CO}(g/kg\ offuel) = \exp\left(-\frac{CE}{T_{pz}}\right) Cph \left(\frac{P_3}{1.4e6}\right)^{a1} \left(\frac{\tau}{0.5}\right)^{a2} \quad (98)$$

If $T_{pz} < 1370\ K$

$$m_{CO}(g/kg\ of fuel) = \left(7e - 15\exp\left(\frac{T_{pz}\tau^{0.057}}{36.1}\right) + 140\right)\left(\frac{P_{in}}{4.34e5}\right)^{-0.62} \quad (99)$$

For which variables $a1, a2, Cph, CE$ are

$$a1 = -0.447\Phi^{-1.87} + 0.2; \qquad a2 = -0.362\Phi^{-1.9} + 0.2;$$

$$Cph = 4.54e3\Phi^{4}\exp\left(-\frac{\Phi}{1.02}\right)^{2.23}; \qquad CE = 6.23e4\Phi^{3.8}\exp\left(-\frac{\Phi}{0.56}\right)^{1.75} \quad (100)$$

3.3.11.2.2 Intermediate zone (IZ)

The concentrations of CO formed in the downstream zones depend on the inlet concentration to those zones. In these zones, some amount of carbon monoxide is oxidized in the presence of extra oxygen. Hence, the concentration of CO at the exit of this zone depends on the inlet concentration of CO denoted as $COIN$ will be given by [64]

If $T_{iz} > 2000\ K$

$$m_{CO}(g/kg\ of\ fuel) = 2.52\exp\left(-\frac{5000}{T_{iz}}\right)\left(1.7e - 4\exp\left(\frac{\Phi}{0.126}\right) + 0.05\right)COIN\left(\frac{P_{in}}{1.4e6}\right)^{a3}\tau^{a4} \quad (101)$$

If $T_{iz} < 2000\ K$

$$m_{CO}(g/kg\ of\ fuel) = 0.122T_{iz}^{-0.2}\Phi^{-2.45}COIN\left(\frac{P_{in}}{4.34e5}\right)^{a3}\tau^{a4} \quad (102)$$

Where variables $a3, a4$ are

$$a3 = 3.79\exp\left(-\frac{1.56}{\Phi}\right) - 0.8; \qquad a4 = 0.875\Phi^{0.94} - 1 \quad (103)$$

3.3.11.2.3 Dilution zone (DZ)

A further reduction in CO concentration will occur in the dilution zone due to the excess air and it depends on the amount of CO entering into the dilution zone $CIND$. The amount of CO then has been found to be [64]

$$m_{CO}(g/kg\ offuel) = 0.122T_{dz}^{-0.2}\Phi^{-2.45}CIND\left(\frac{P_3}{4.34e5}\right)^{-0.16}\tau^{a4} \quad (104)$$

3.3.11.2.4 Molar basis for carbon monoxide

The amount of CO estimated by the equations (97) through (103) gives the amount formed per kilogram of the fuel supplied. To complete the mass and energy balance in the section 3.3.8.12, number of moles in each zone is needed. Therefore, the amount of CO is converted into number of moles by using [51]

$$n_{CO} = \frac{m_{CO}\dot{m}_{f,CC/RH}*10^3}{MW} \quad (105)$$

Where MW is the molar mass of CO, $\dot{m}_{f,CC/RH}$ is either mass if the fuel supplied to combustion chamber or reheater depending on whose zone is been studied. The total CO out of the combustors is the amount of CO from the dilution zone.

3.3.11.3 Unburnt hydrocarbons (UHC)

The contributor to the UHC are the primary zones of the combustors. In the intermediate and dilution zone, sufficient amount of air is present to burn the fuel completely. The amount of UHC formed in the primary zone is eventually burned in the intermediate zone. The amount of UHC formed is given as a function of primary zone temperature T_{pz},

inlet pressure P_{in}, pressure drop θ and residence time τ. It is found to be given by [64], [94]

$$m_{UHC}(g/kg\ of\ fuel) = \frac{0.755e11 \exp\left(\frac{9756}{T_{pz}}\right)}{P_{in}^{2.3}\tau^{0.1}\theta^{0.6}} \quad (106)$$

This amount of UHC is needed to convert into number of moles for the mass and energy balance of section 3.3.8.12 which is done by [51]

$$n_{UHC} = \frac{m_{UHC}\dot{m}_{f,CC/RH} * 10^3}{MW}$$

Where MW is molar mass of the fuel found using equation (11), $\dot{m}_{f,CC/RH}$ is either mass if the fuel supplied to combustion chamber or reheater depending on the combustor.

3.3.12 Performance indicating parameters

The following parameters are used to assess the whole performance of the proposed gas turbine cycle which will be discussed in the subsequent chapters.

3.3.12.1 Net power output of the proposed cycle

Net power developed from the proposed cycle would be equal to the power produced by the turbines and expander minus the power needed to run the compressors and pump.

$$\dot{W}_{net} = \left(\dot{W}_{HPGT} + \dot{W}_{LPGT} + \dot{W}_{Ex} - \dot{W}_{LPC} - \dot{W}_{HPC} - \dot{W}_{pump}\right)\eta_{gen} \quad (107)$$

3.3.12.2 First law efficiency of the proposed cycle

Overall first law efficiency of the cycle, which gives the measure of how well the system is operating thermodynamically from the energy point of view, may be found as, [46], [48]

$$\eta_I = \frac{\dot{W}_{net}}{\dot{m}_{fuel,CC}.LHV_{CC}+\dot{m}_{fuel,RH}.LHV_{RH}} \quad (108)$$

3.3.12.3 Second law efficiency of each component of the proposed cycle

This is a measure that indicates, how well a component is utilizing the energy quality. One of the major attraction towards the second law analysis is its component wise efficiency which the first law is not able to provide. This will help pin point the components which have higher irreversibility and which needs to be improved and optimized. The second law efficiency of a component is given by [56]

$$\eta_{II,component} = 1 - \frac{\dot{I}_{component}}{\dot{X}_{in,component}} \quad (109)$$

Where $\dot{I}_{component}$ is the exergy destruction in a component, and $\dot{X}_{in,component}$ is the exergy input to that component which can be taken from Table 7.

3.3.12.4 Second law efficiency of the proposed cycle

This parameter gives hints the performance of the overall system from the second law point of view, i.e., how effectively the quality of the fuel is the used to run the system. Overall second law efficiency is given as, [48]

$$\eta_{II} = \frac{\dot{W}_{net}}{\dot{m}_{fuel,CC} \cdot e_{x,fuel,CC} + \dot{m}_{fuel,RH} \cdot e_{x,fuel,RH}} \quad (110)$$

3.3.12.5 Emission Parameters

The amount of emissions in the most general form are expressed in parts per million in the exhaust volume of the power plant. This unit is used in accordance to the regulations. Therefore to compare the emissions from the proposed turbine to the regulations and other build turbines, the CO and NOx emitted by the turbine are found in ppm as follows [21]

$$NOx(ppm) = \left(y_{NO_2} + y_{NO}\right) * 10^6; \qquad CO(ppm) = y_{CO} * 10^6 \quad (111)$$

Where y_{CO}, y_{NO_2}, y_{NO} are the mole fractions that are leaving the gas turbine power plant at state 16.

CHAPTER 4

RESULTS AND DISCUSSION

4.1 Results overview

The natural gas fueled intercooled reheat regenerative combustion gas turbine subjected to inlet air cooling using reverse Brayton refrigeration cycle and evaporative after cooling of the compressed air was analyzed from exergo-enivronment point of view using the mathematical model developed and presented in the previous chapter. The effects of changing the equivalence ratio, extraction pressure ratio, extraction mass rate, overall pressure ratio, ambient relative humidity, ambient temperature, water-to-air ratio and turbine inlet temperature were examined on the cycle performance parameters. The range of these parameters could be found from Table 6. The increase in power output obtained by the proposed cycle, overall first law efficiency and second law efficiency of the cycle were calculated. Component wise exergy destruction was also computed to determine the degree of thermodynamic imperfection followed by second law efficiency of each component to visualize the irreversibilities in each component. Furtherance to this, the CO and NOx emissions associated with the turbine exhaust were predicted. Also, the proposed cycle performance was compared with the thermodynamic performance of the basic gas turbine plant. The basic gas turbine plant has all the major components except the inlet cooling and evaporative after cooling components. Therefore, it serves as a base while evaluating the performance of the proposed cycle. Lastly, an attempt was made to locate the optimum regions of affecting parameters where the cycle could perform

thermodynamically efficient and environment friendly. The conditions prevailed at each state point when the proposed cycle works at the mean operating conditions are tabulated in Table 8 for the reference sake.

Table 8 Thermodynamic properties at all the state points including temperature and pressure of the proposed cycle at TIT=1200 K, r=25, x=2.5, ϕ_0=50%, Φ=0.85, α=0.2, T_0=305 K, water heater surface area = 50 m^2

Point	Stream	T (K)	P (kPa)	ω (kg/kg (of dry air))	$\dot{m}$ (kg/s)	h (kJ/kg)	ex (kJ/kg)
0	Air	305	101.3	0.01483	13.78	69.95	0
1	Air	294.1	100.8	0.01236	16.54	52.43	0.09696
2	Air	386	252	0.01236	2.756	147.2	91.21
3	Air	305.3	250.7	0.01236	2.756	63.93	81.25
4	Air	305.3	248.2	0	2.756	32.31	80.52
5	Air	238.1	101.3	0	2.756	-35.15	10.64
6	Air	474.9	504	0.01236	13.78	239.8	180.2
7	Air	391.5	498.9	0.01236	13.78	152.8	153.4
8	Air	626	2495	0.01236	13.78	400.5	396.2
9	Air	482	2470	0.09158	13.78	476.7	355.9
10	Air	748.8	2420	0.09158	13.78	807.7	503.6
11	Gases	1200	2323	-	15.24	-752.9	1185
12	Gases	852.6	502.7	-	15.24	-1199	588.4
13	Gases	1200	482.6	-	15.44	-1375	930
14	Gases	858.4	104.4	-	15.44	-1826	326.9
15	Gases	618.6	102.3	-	15.44	-2121	150.6

16	Gases	569.4	101.3	-	15.44	-2180	120.3
0^{cfw}	Cooling water	305	101.3	-	5.487	133.5	97.68
3^{1}	Cooling water	315	101.3	-	5.487	175.3	98.35
4^{1}	Humidity eliminator moisture	305	101.3	-	0.03406	2559	3.316
0^{aha}	Air humidifier air	305	150	0.01483	13.78	69.95	35.86
0^{ahw}	Air humidifier water	305	101.3	-	0.02173	133.5	97.68
1^{1}	Air humidifier air	301.3	148.5	0.01641	13.78	70.16	34.17
1^{11}	Air humidifier air	385	147	0.01641	13.78	157.1	42.62
0^{whw}	Evaporating water	305	101.5	-	1.092	133.5	97.68
17	Evaporating water	305	2520	-	1.092	135.7	100.1
18	Evaporating water	497	2495	-	1.092	961.4	287.8
F,CC	Fuel	305	2420	-	0.2087	48908	50741
F,RH	Fuel	305	502.7	-	0.1948	48908	50743

To model the combustors realistically, three zones were considered and the reaction determination was explained in 3.3.8.12. For reference, actual combustion reaction at mean operating conditions in three zones in combustor and reheater is presented in appendix A.3

4.2 Model Validation

The performance predicted by the proposed model must be able to accurately correspond to the represented or actual system. To verify the credibility of the model developed, some of the results obtained using the model is compared with the results in the literature. These results are discussed in the following sections.

4.2.1 Flame Temperature in Combustor

The temperature of the flame obtained in the combustor depends on the inlet conditions of the oxidizer, pressure, equivalence ratio and the type of the fuel. Gulder [99] presented an approximate formula after developing a detailed equilibrium code and fitting the results as a function of input parameters. The Gulder's approximate formula could be found from Appendix A.4. The temperature obtained using Gulder's formula is compared with the temperature predicted by the proposed model and is shown in the Figure 11.

Maximum difference in the temperature obtained and the temperature from Gulder's formula was found to be 10 K. At higher equivalence ratio, a larger difference was obtained. This was observed due to the fact that, in the proposed model, all the emissions including CO and UHC are considered, where Gulder neglected the formation of UHC. From Figure 11 (a), It is also observed that peak temperatures are obtained at the stoichiometric equivalence ratio when the complete combustion occurs. From Figure 11 (b), it can be seen that increasing pressure ratio reduces the combustion temperature. Increasing pressure ratio increases inlet pressure to the combustor, which increases the velocity in the combustor resulting in a slight reduction in temperature.

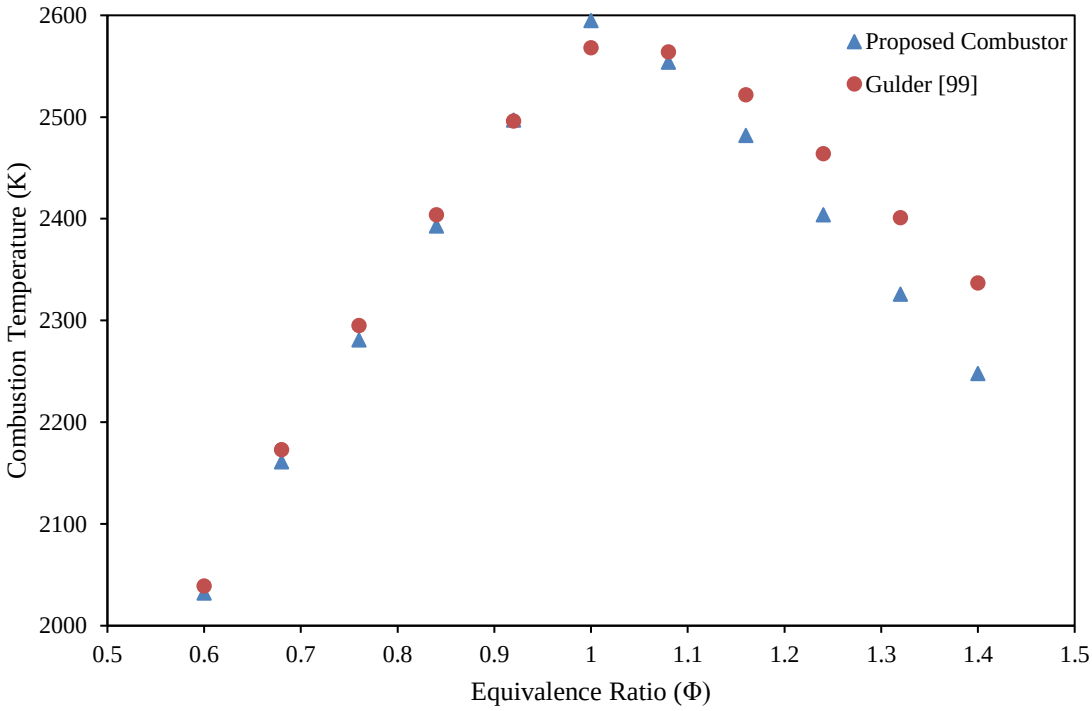
Proposed Combustor
Gulder [99]
Combustion Temperature (K)
Equivalence Ratio (Φ)
2600
2500
2400
2300
2200
2100
2000
0.5
0.6
0.7
0.8
0.9
1
1.1
1.2
1.3
1.4
1.5

(a)

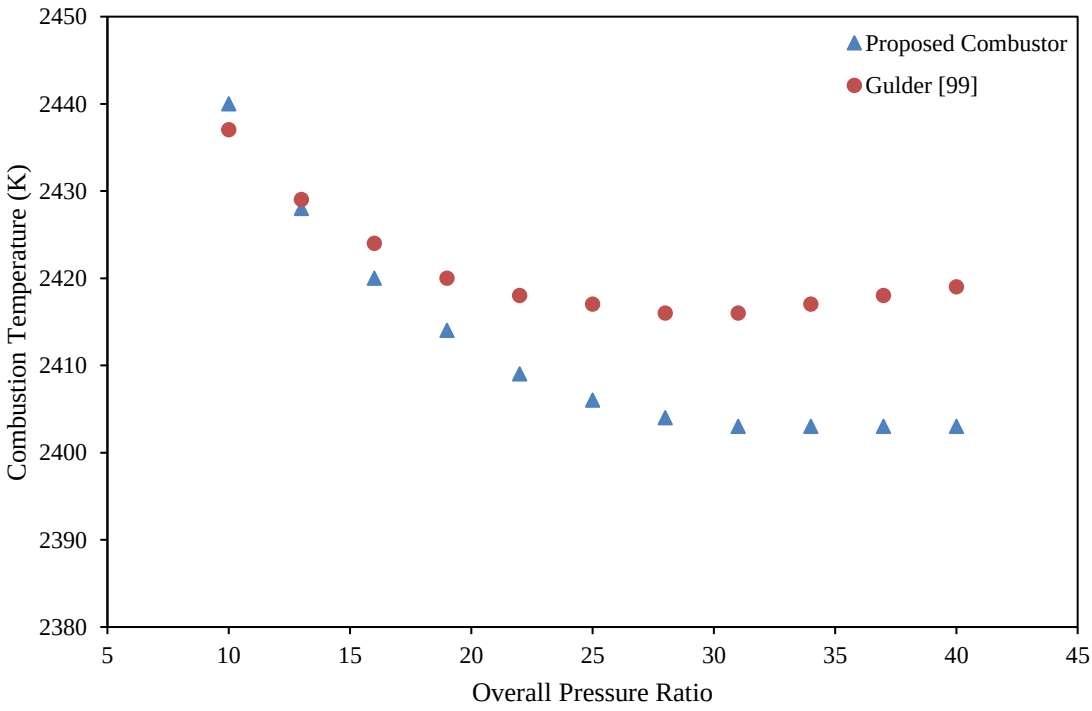
Proposed Combustor
Gulder [99]
Combustion Temperature (K)
Overall Pressure Ratio
2450
2440
2430
2420
2410
2400
2390
2380
5
10
15
20
25
30
35
40
45

(b)

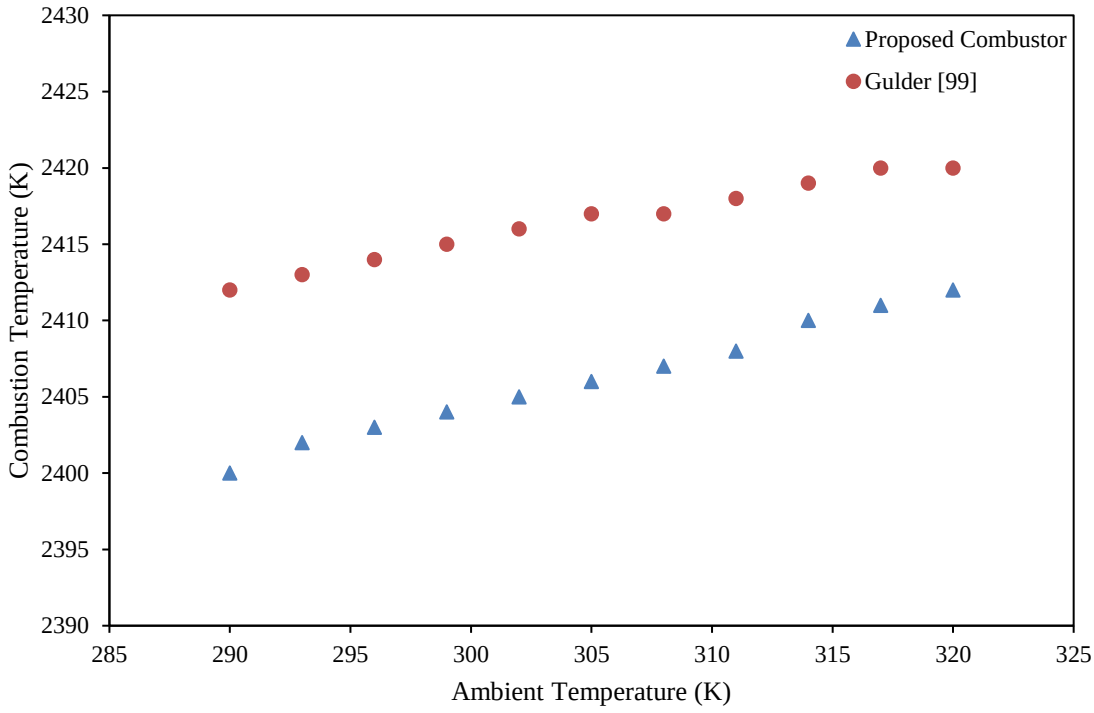

(c)

Figure 11 Comparison of Combustion Temperature with the temperature obtained using Gulder [99] **(a) Comparison with variation of Equivalence Ratio (b) Variation with Overall Pressure Ratio (c) Variation with Ambient Temperature**

Effect of ambient temperature can be seen from Figure 11 (c). It shows that increasing ambient temperature results in a nominal increase in combustion temperature. This occurs due to increase in inlet temperature to combustor when ambient temperature is increased.

4.2.2 Emission Model Validation

The amount of NOx formed using the model described above was compared with the experimental results compiled by Correa [57]. Similar trends were obtained for NOx when its variation with water to fuel ratio and equivalence ratio. It is seen from Figure Figure 12 (a) that, increase in water to fuel ratio reduces the amount of NOx formed. This happens because more amount of water injected reduces the combustion temperature.

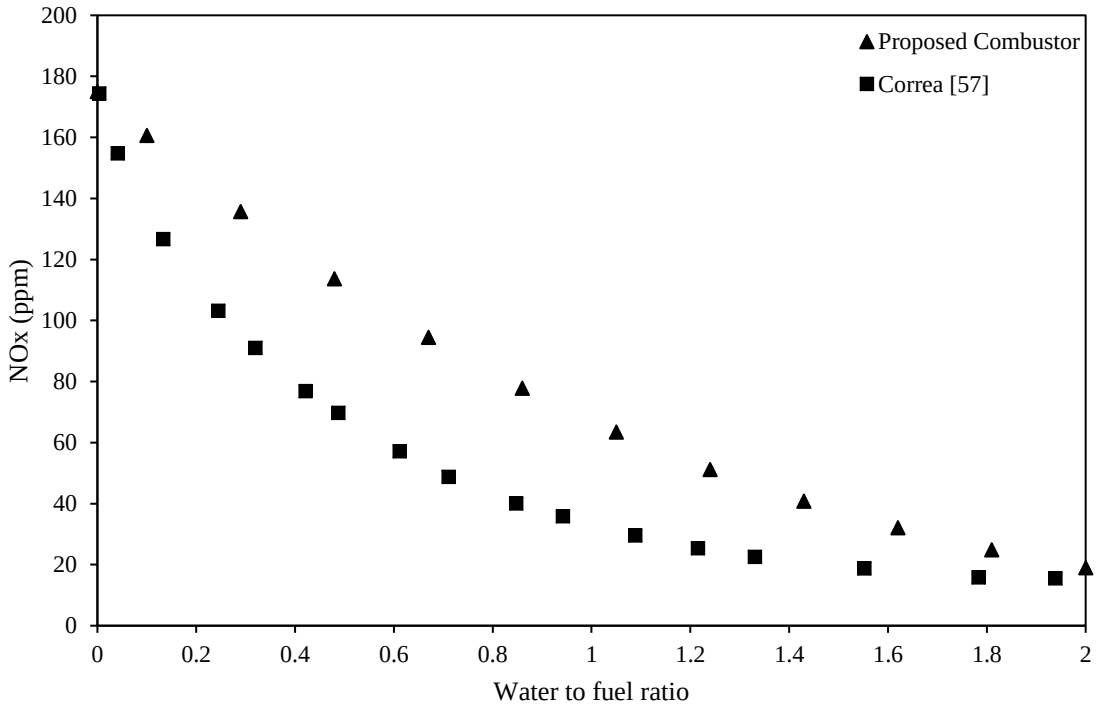

(a)

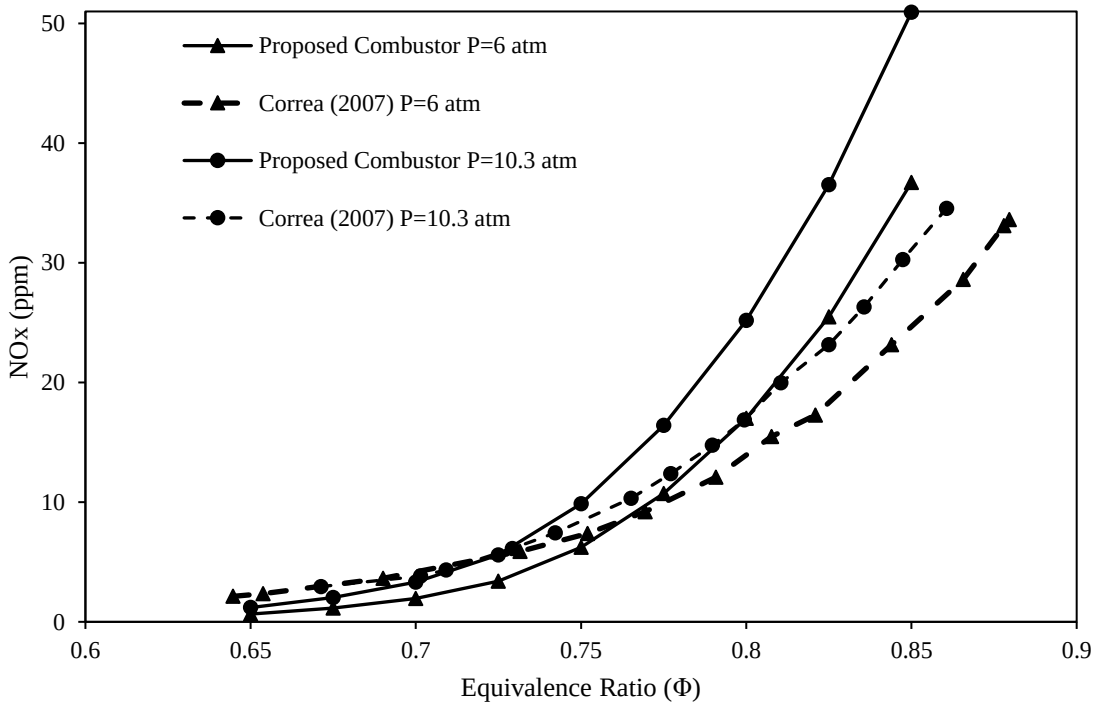

(b)

Figure 12 Comparison of NOx formed with the experimental results compiled by Correa [57] (a) Variation of NOx with water to fuel ratio (b) Variation of NOx with Equivalence Ratio

It is also seen that increasing equivalence ratio up to stoichiometric increases the amount of NOx due to higher temperature attained in the combustors. Also from Figure 12 (b), it is seen that inlet pressure to the combustor aids in the production of NOx.

4.3 Effect on power output

The proposed gas turbine cycle is expected to enhance the power output in addition to considerable reduction in the emissions. No variation in power output was observed when the equivalence ratio of the primary zone was varied. This is because, changing the equivalence ratio in the primary zone, will actually control the percentages of air in the three zones, viz., primary zone, intermediate zone, and dilution zone which will affect the mean temperature obtained in the combustors resulting in the same turbine inlet temperature at all the values of equivalence ratio. Also, same pressure ratio is available for expansion at all the equivalence ratios, which causes the same power output. The degree of power augmentation attained by changing remaining design parameters are presented in the following section.

4.3.1 Extraction mass rate

Employment of reverse Brayton refrigeration cycle for inlet air cooling in gas turbines requires the splitting of compressed air as a refrigerant and as an oxidizer. In this regard, a portion of compressed air goes to the reverse Brayton refrigeration cycle and rest enters the combustion chamber as an oxidizer. Extraction mass rate (α) which is ratio of mass of air utilized as a refrigerant to the total mass of compressed air could be considered as one of the operating parameter for the performance analysis of gas turbine subjected to inlet air cooling. In this context, the effect of change in extraction mass rate on the power

augmentation in gas turbines was observed and shown in Figure 13. The result show that increase in extraction mass rate causes a steadily rise in power output of gas turbine. This is because increase in extraction mass rate leads to the reduction of compressor inlet air temperature which increases the air density means, mass flow rate of combustion gases and hence the turbine output. It is further seen that increase in extraction mass rate from 0.1 to 0.4 results in the decrease of compressor inlet temperature from 299 K to 287 K which gives a corresponding rise in power output from 7454 kW to 7617 kW. It is further interesting to see that without the application of evaporative after cooling and inlet air cooling, means $\alpha = 0$, the power output of gas turbine was 5809 kW which shows a remarkable improvement in power output of 31.1 % in gas turbines when the extraction mass rate increases from 0 to 0.4 along with the application of evaporative after cooling.

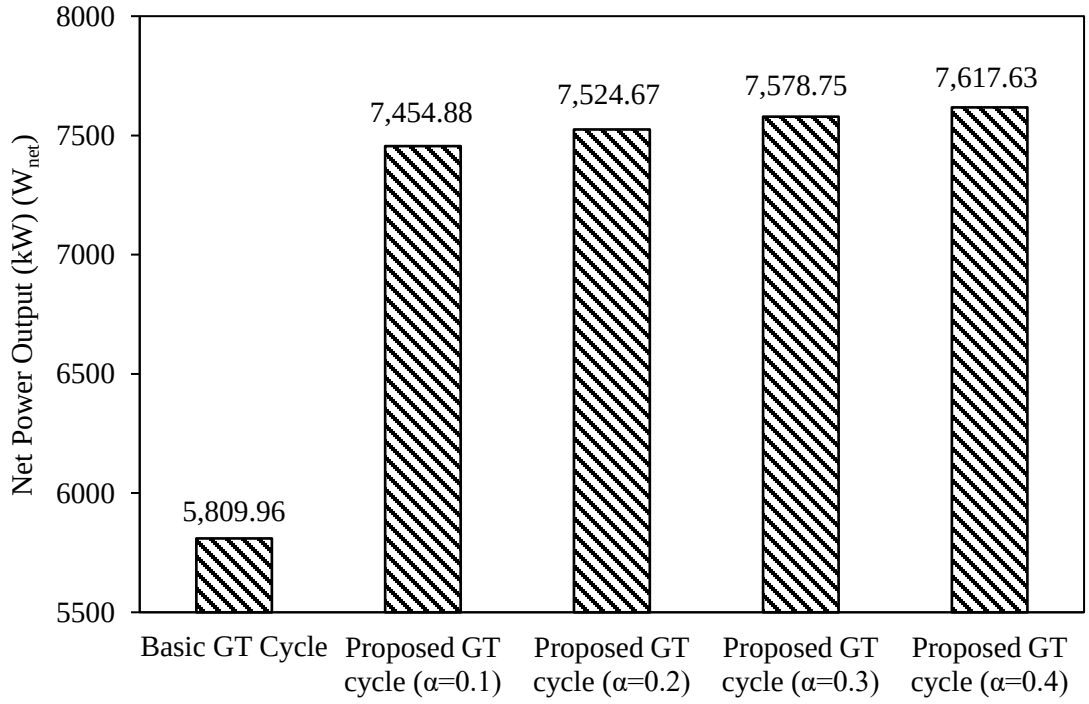

Figure 13 Effect of extraction mass rate (α) on power output

4.3.2 Extraction pressure ratio

Since, the compressor inlet air temperature depends on the extraction mass rate and extraction pressure ratio, therefore, the effect of increase in extraction pressure ratio was also observed on the power output of gas turbine cycle subjected to evaporative after cooling and inlet air cooling shown in Figure 14.

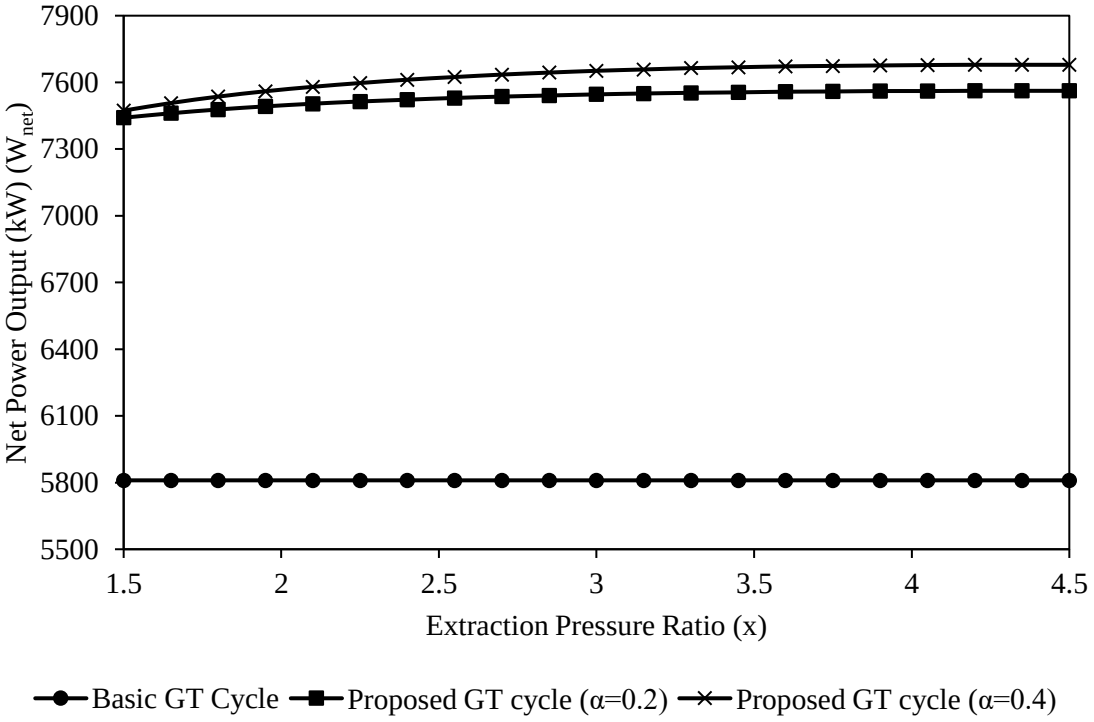

Figure 14 Effect of extraction pressure ratio (x) on the power output

From Figure 14, it is observed that, with the increase of extraction pressure ratio a small rise in the power output was obtained which is due to the fact that, compressor inlet air temperature is majorly affected with the variation of extraction mass rate rather than the extraction pressure ratio. It is further seen that the effect of extraction pressure ratio on power output is more pronounced at lower values and becomes insignificant in the range

of higher values. This is because, at higher values of extraction pressure the amount of power required by the compressor will dominate over the amount of power gained due to inlet air cooling.

4.3.3 Overall pressure ratio

The effect of overall pressure ratio on the power output of gas turbine cycle was examined and the trends obtained are shown in Figure 15.

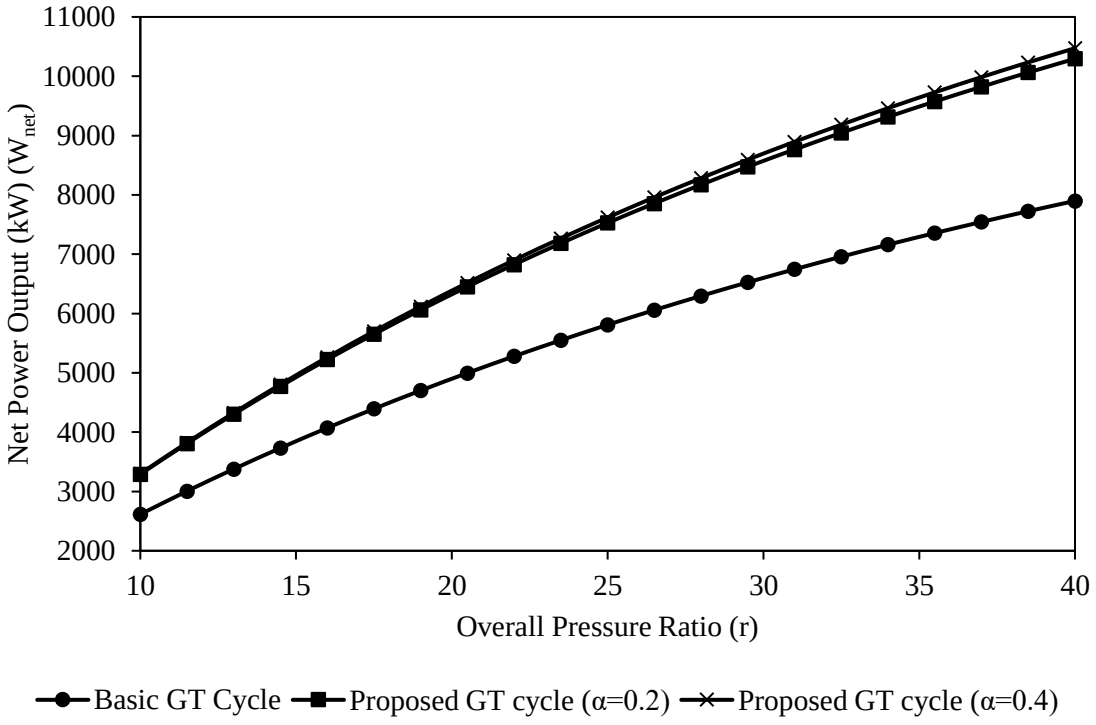

Figure 15 Effect of overall pressure ratio (r) on the power output

It is seen that, power output increases considerably as the overall pressure ratio increases significantly which is due to the reason overall pressure ratio contributes towards the power output in two ways: Firstly, the power output increases due to reduction in compressor inlet air temperature due to simultaneous increase of extraction pressure ratio.

Secondly, increase in overall pressure ratio means higher combustion pressure which increases the enthalpy of combustion gases which in turn increases the turbine power output due to higher difference of thermal energy across the turbine. Therefore, increase in overall pressure ratio increases the mass flow rate of combustion gases and their enthalpy by virtue of employing the inlet air cooling. A significant enhancement in the power output is observed due to the employment of evaporative cooling along with the inlet air cooling and it is seen that, the power output increases approximately from 3000 kW to 10000 kW when the overall pressure ratio rises from 10 to 40. Effect of employing the evaporative cooling along with the inlet air cooling is more pronounced at higher values of overall pressure ratio which is due to the fact that, at higher values of overall pressure ratio the effect of extraction pressure ratio prevails which enhances the power output in addition to enhancement due to the higher expansion ratio across the turbine.

4.3.4 Ambient relative humidity

The effect of change in the ambient relative humidity on the power output of gas turbine was observed and shown in Figure 16. It is seen that the power output decreases slightly after a large increase in the ambient relative humidity. This decrease is observed due to the reason that, the increase in relative humidity increases the compressor inlet air temperature which reduces the mass flow rate of air and hence the power output. Secondly, it decreases due to the reason, higher ambient relative humidity means more water vapor in the air which act as a ballast to absorb heat from the flame, lowering the temperature and hence the power output. It is seen that the increase in ambient relative from 20% to 80% reduces the turbine output by a percent. It is further seen that increase

in extraction mass rate increases the power output slightly and the difference between the two is almost same at all values of ambient relative humidity.

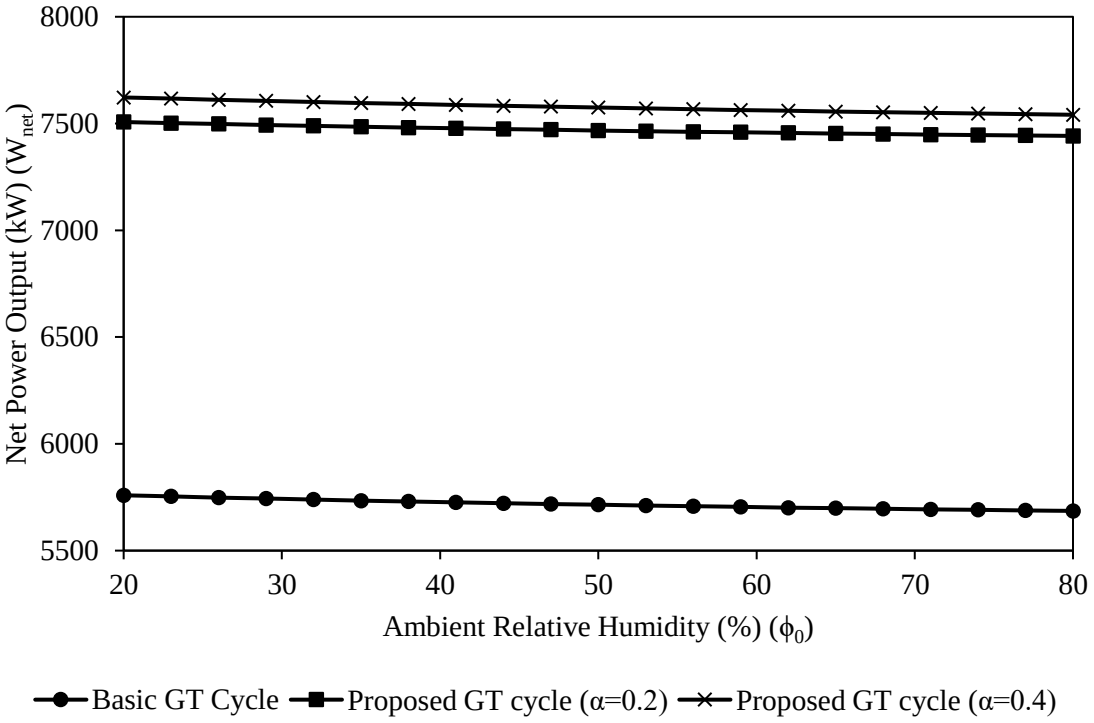

Figure 16 Effect of ambient relative humidity (ϕ_0) on power output

4.3.5 Ambient temperature

As obvious, the gas turbine output decreases with the increase of ambient temperature. Therefore, in order to compensate the power reduced due to the operation of gas turbines at peak ambient conditions, the concept of reduction in inlet air temperature was introduced and its effect is shown in Figure 17. It is shown that, the turbine output decreases considerably as the ambient temperature increases. This is because a lower mass flow rate of air enters the compressor due to reduced density as a result of higher ambient temperature. Hence, lower power output from turbine obtained for a given

turbine inlet temperature and overall pressure ratio. In the proposed gas turbine arrangement, due to increased mass flow rate while lowering the ambient air temperature from 320 K to 290 K, power output of gas turbine increases by around 10%. Since the ambient air temperature related to compressor inlet air temperature which governs with the extraction mass rate, therefore, increase in extraction mass rate from 0.2 to 0.4 shows a clear enhancement in the power output of the gas turbine from 7500 kW to 7650 kW at the ambient temperature of 305 K

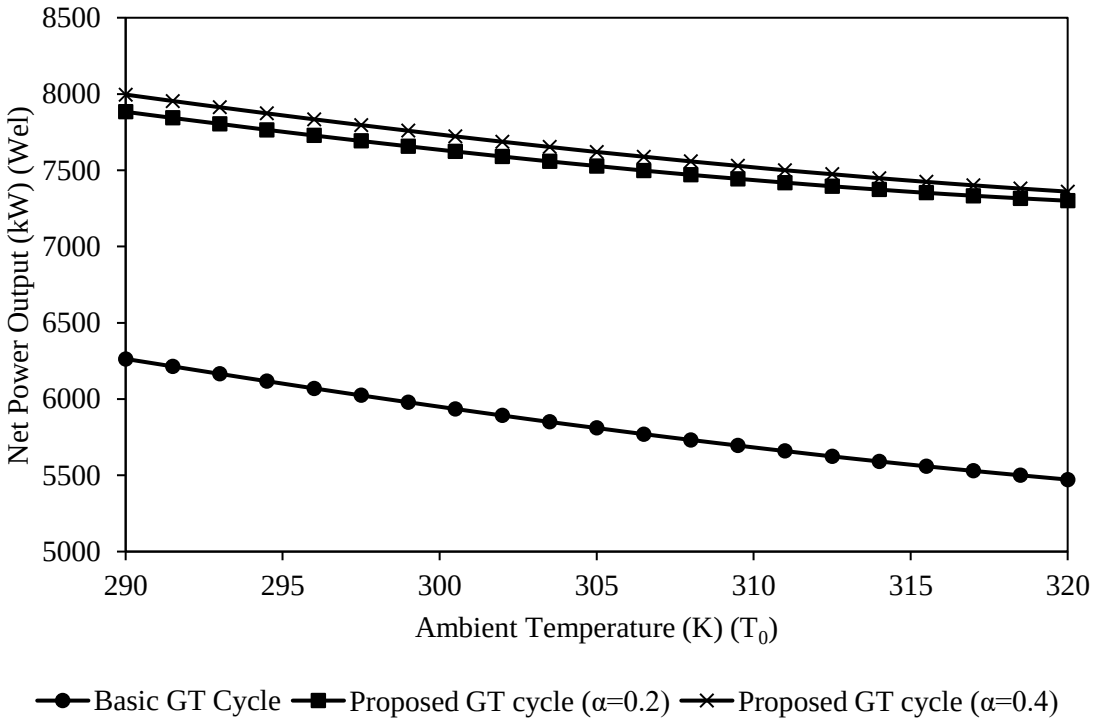

Figure 17 Effect of ambient temperature (T_0) on power output

4.3.6 Water-to-air ratio

The effect of water-to-air ratio on power augmentation of gas turbine is shown in Figure 18. It is seen that the turbine power increases considerably with the increase of water-to-

air ratio which is due to the increase of mass flow rate of air goes to combustion chamber due to the addition of water injection. Increase in water-to-air ratio means increase in the amount of injection water and decrease in the amount of dry air which contributes towards the power enhancement greatly due to the increase in mass flow rate and increase in temperature of combustion gases. Power augmentation due to increase in water injection dominates over the power augmentation due to reduction in compressor inlet air temperature. That is why, while changing α from 0.2 to 0.4 the increase in power is marginal. It should be noted that there is an upper limit in the water injection which is due to the maximum limit of water that could be injected into the air at a certain temperature and pressure which will create an upper limit to power augmentation using after cooling.

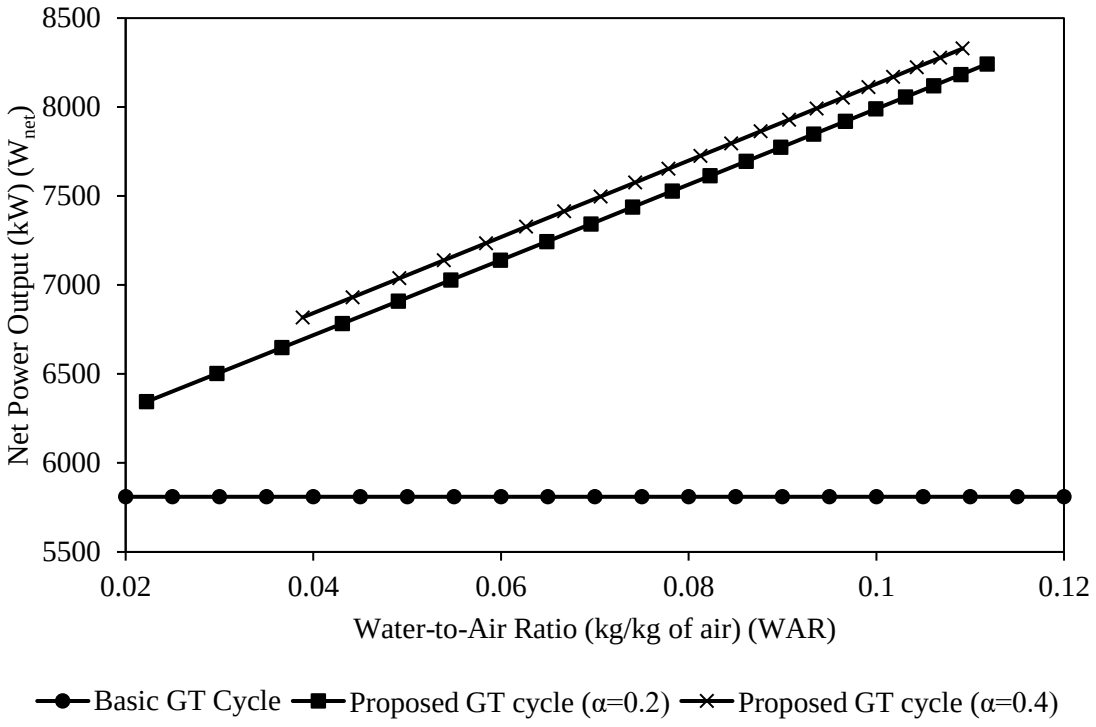

Figure 18 Effect of water-to-air ratio (WAR) on power output

4.3.7 Turbine inlet temperature

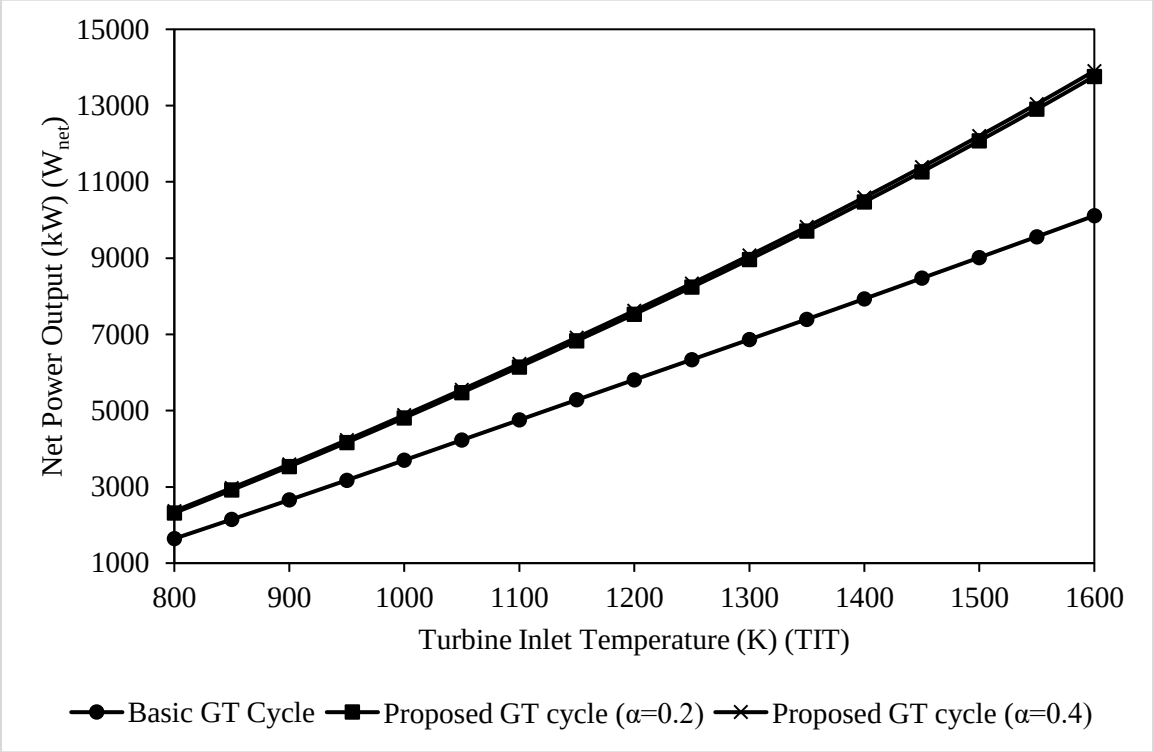

Figure 19 Effect of turbine inlet temperature (TIT) on power output

Figure 19 depicts the variation of turbine power output with the change of turbine inlet temperature and it is sown that the turbine power increases significantly with the increase of temperature as the turbine power output dominates the rising of fuel requirement to increase the turbine inlet temperature due to combined effect of evaporative after cooling and inlet air cooling. Evaporative after cooling considerably increases the mass flow rate of combustion gases expanded over the turbine which in turn increases the power output along with the power enhancement due to the decrease of compressor inlet air temperature. The results clearly shows a greater enhancement in the power output of gas turbines subjected to evaporative after cooling and inlet air cooling than the enhancement of power output in basic gas turbines with the increase of turbine inlet temperature In

basic gas turbines, the effect of increase in fuel addition to achieve the higher turbine inlet temperature dominates over the power enhancement. Therefore, increase in power output is more in the proposed gas turbines at higher turbine inlet temperature.

4.4 Effect on overall first and second law efficiency of the cycle

Overall first law efficiency is used to assess the performance of the whole cycle which would display the percentage of work developed for the amount of the fuel energy supplied. Whereas overall second law efficiency provides clear picture about the quality of the fuel which is utilized to produce the work output. By the recent researchers, the overall second law efficiency has been considered as more accurate measure than first law efficiency as it considers the quality of energy rather than its quantity. In all the cases studied, the second-law efficiency of the cycle was observed lower than the first-law efficiency. This is because the quality of fuel i.e. the exergy associated with the heat addition is more than the heating value or energy of fuel because the exergy of fuel would also include the expansion of the products in the combustion to a condition that is in equilibrium with the reference environment. This shows the reason of popularity of the second law analysis over the first law analysis, which takes into the consideration the quality of the energy rather than just energy content and it gives a clear picture of the performance of the system from utilization of the resources point of view.

4.4.1 Equivalence ratio

As discussed earlier, the equivalence ratio doesn’t significantly affect the power output from the gas turbine due to the same pressure ratio and turbine inlet temperature at all the values of equivalence ratio. However, it was interesting to observe the first and second

law efficiency of the system against the equivalence ratio as shown in the Figure 20. For the basic gas turbine, the expected independency of the equivalence ratio on the first and second law efficiency was observed, as the equivalence ratio didn't change the amount of fuel supplied in the primary zone, but controlled the amount of primary air been supplied to it making it lean or rich combustion. However, for proposed gas turbine cycle, efficiency slightly increased as the equivalence ratio was increasing. The reason for this was found out to be that, the exhaust from the turbine at higher equivalence ratio had a reduced temperature due to the presence of excess CO than NOx. This exhaust gases when exchanged heat with the water in water heater was able to produce less water for evaporation at higher equivalence ratio than at the lower equivalence ratio. This caused lesser vapor content to be present when the water entered the combustor. The lesser amount of temperature suppressor resulted in a reduced mass flow rate of fuel resulting in a net increase in the efficiency.

Figure 20 also compares the efficiency of the basic gas turbine cycle with the proposed gas turbine cycle. It may be observed that, the efficiency of the basic gas turbine cycle is higher than that of the proposed gas turbine cycle. The major concern in the future gas turbine systems are said to be their environmental impact which is huge for a basic gas turbine cycle even though the efficiency sounds attractive as would be seen in the upcoming sections. A reduction in efficiency in the proposed gas turbine cycle is because of the water injection that will suppress the temperature in the combustor and that will be used to restrict the emissions to the regulatory limits. The difference between them is reduced at higher equivalence ratio due to the lesser water injection as already explained. From the Figure 20, it is also observed that increasing the extraction mass rate or the

capacity of the refrigeration cycle can enhance the efficiency of the system by 0.5 % compensating for the effect of reduction in efficiency due to water injection. This trend increases the attraction towards the proposed gas turbine cycle which can compensate for the decrease in efficiency occurring in the power plant due to water injection by inlet air cooling. However, this increased mass flow rate will cause an increase the capital cost of the gas turbine plant. The second law efficiency shows the same trend and has a value lesser than first law efficiency as explained earlier.

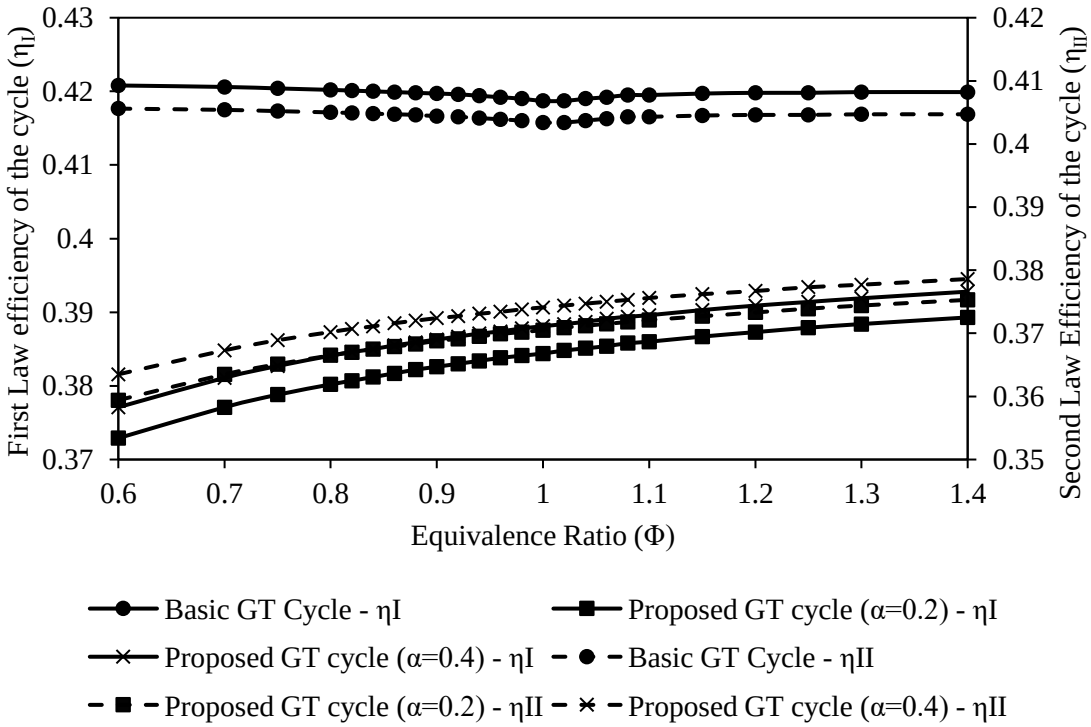

Figure 20 Effect of equivalence ratio (Φ) on the first and second law efficiency of the cycle

4.4.2 Extraction pressure ratio

Figure 21 shows the variation of first and second-law efficiencies of gas turbine cycle subjected to inlet air-cooling and evaporative after cooling with respect to extraction

pressure ratio. It is seen that first law efficiency increases initially with an increase in extraction pressure ratio which is due to the enhanced chilling effect of the inlet air to the compressor. This results in the mass of air flowing into the gas turbine cycle which will allow more power to be developed. Further increase in extraction pressure ratio leads to more consumption of fuel than the equivalent power augmentation causing to causing the efficiency to decrease.

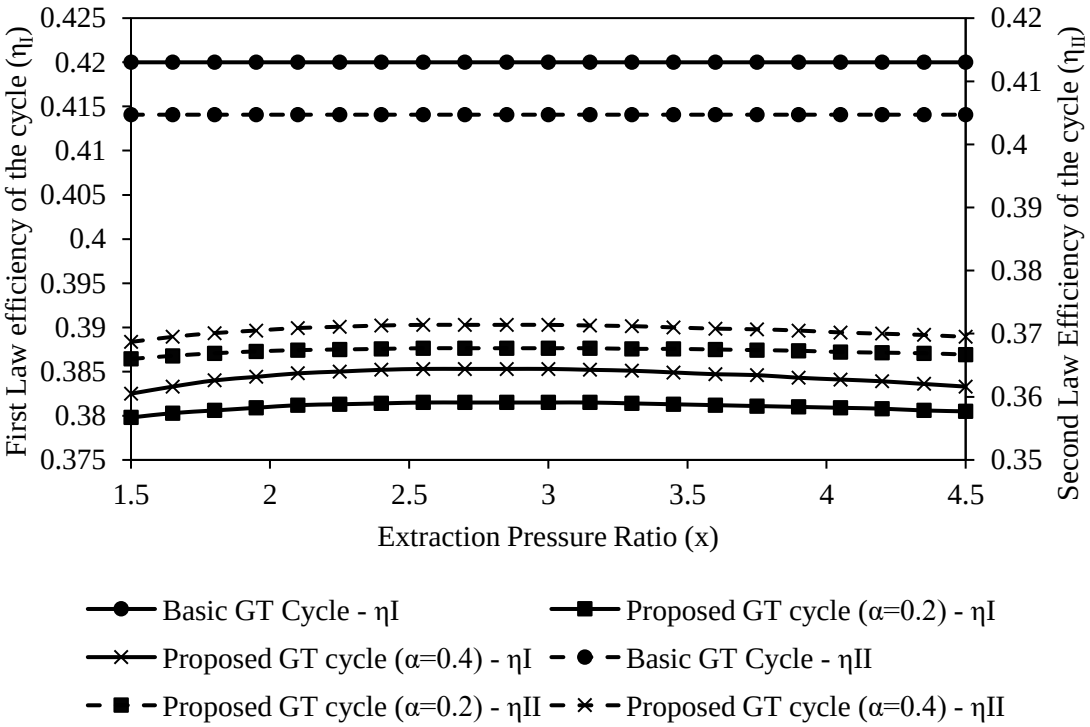

Figure 21 Effect of extraction pressure ratio (x) on the first and second law efficiency of the cycle

The variation of the second-law efficiency of proposed gas turbine cycle with the extraction pressure ratio is also shown in Figure 21. The same increasing-decreasing trend is observed with a lesser value of second law efficiency at each value of extraction pressure ratio. It can also be observed that combined effect of evaporative after cooling and inlet air cooling provides a reduction of around 4% in the efficiency of gas turbine

cycle as it is evident from the comparison of results shown in Figure 21. This reduction is due to the suppression of temperature due to the water injection in after cooler. A significant improvement in power output and reduction in the amount of emissions was obtained at the expense of increased fuel supply or reduction in thermal efficiency. From the above result, it was found that the optimum extraction ratio is around 2.5, which is the half of the pressure ratio of that compressor (square root of 25). Therefore, for the remaining case studies, air for the refrigeration cycle is extracted at the midpoint of the compressor.

Figure 21 also depicts the effect of extracted mass rate from the compressor on the first and second-law efficiency of the cycle. As seen from the figure, both first and second law efficiencies improved with the higher values of the extracted mass rate. The figure indicates that increases the air through reverse Brayton refrigerator from 20% to 40% of the total intake air at 2.5 bar pressure the efficiency of the turbine by 0.2%. This is because increase in the extracted mass rate passing through the refrigeration cycle enhances the chilling effect increasing the mass flow rate that goes to the gas turbine cycle. This increases the power output causing the efficiency to rise.

4.4.3 Overall pressure ratio

The effect of overall pressure ratio of the compressor is also a major influencing parameter in gas turbines. The power output needed for operation is usually dictated by the volumetric capacity of plant and overall pressure ratio. As shown in the preceding sections, power output was found to considerably increase with an increase in overall pressure ratio. However, a decrease in efficiency is usually observed due to an increase in

the pressure ratio for a normal gas turbine plant as can be seen from the Figure 22. In a normal gas turbine plant, for a fixed turbine inlet temperature, higher overall pressure ratio results in higher expansion in the turbine cause of the increased power output. It also results in a higher temperature going into the recuperator. In addition, it will also reduce the temperature leaving the turbine, resulting in a lesser heat transfer occurring in a recuperator that will bring down the efficiency.

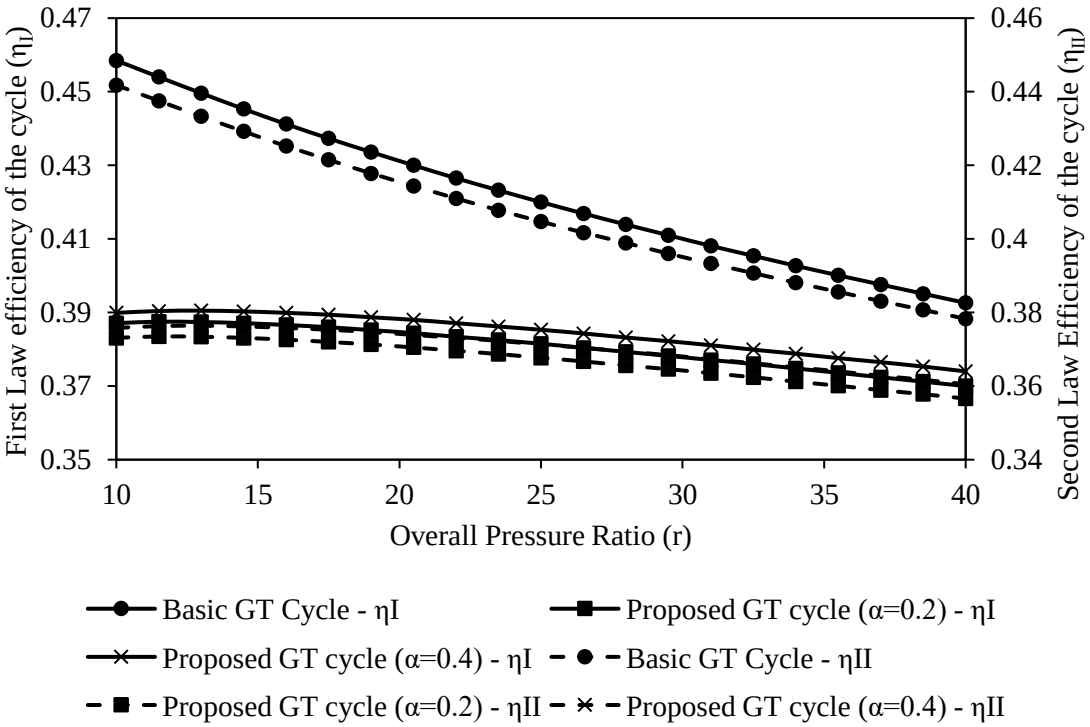

Figure 22 Effect of overall pressure ratio (r) on the first and second law efficiency of the gas turbine cycle

In contrast, an interesting result was found for the proposed gas turbine system in which, the efficiency tend to reduce very less than the basic gas turbine. For the proposed gas turbine cycle, an increased temperature at the outlet of the compressor will result in higher absorption of water in the air stream, as the capacity of air to absorb water increases with increasing temperature. This will result in an increase in power output

which will be compensated for the reduced heat transfer in the recuperator causing the efficiency to remain almost constant. This helped to reduce the loss in the efficiency between the basic and proposed gas turbine, hence making the proposed gas turbine much more thermodynamically effective in the higher pressure ratio ranges, which can not only produce enhancement in power but also reduced emissions. Further, the effect of extraction pressure ratio on the first and second law efficiency of the cycle is also shown the Figure 22, an increase of 0.2% in efficiency is obtained as explained earlier.

4.4.4 Ambient relative humidity

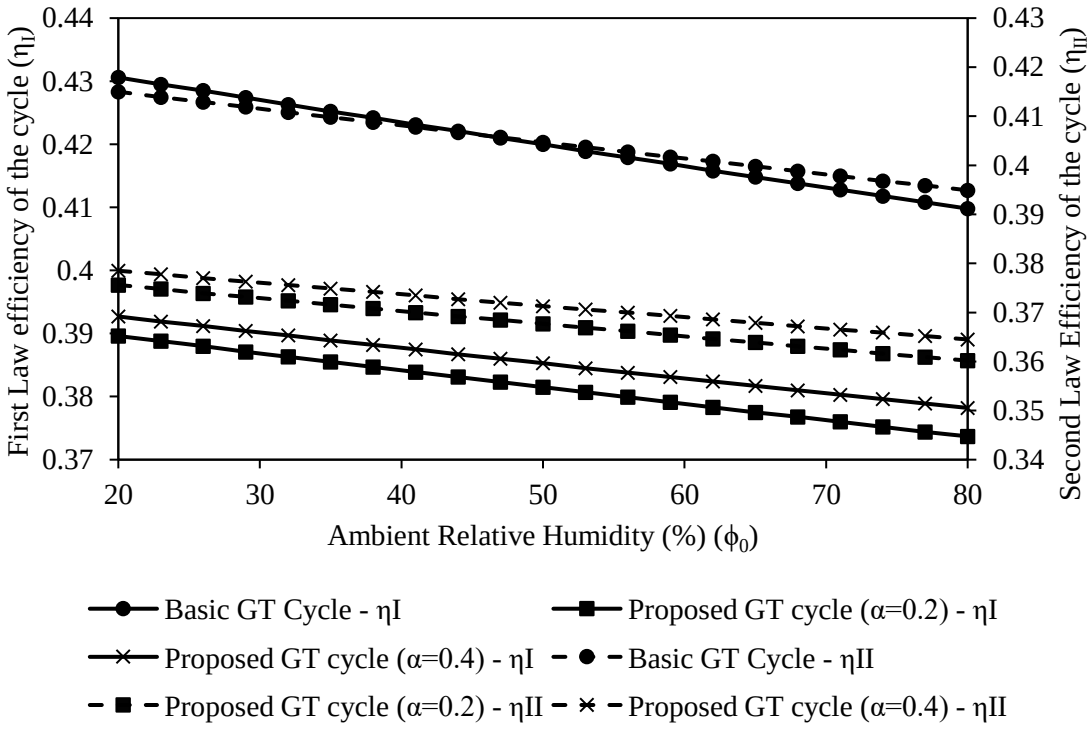

Figure 23 Effect of ambient relative humidity (ϕ_0) on the first and second law efficiency of the cycle

Figure 23 depicts the variation of cycle first and second-law efficiency with the elevation of ambient relative humidity. At a given compressor inlet air temperature, a linear

reduction in the cycle efficiency is observed at elevated ambient relative humidity due to density reduction with increasing relative humidity which resulted in a decrease in the power output as already shown in the previous results. In addition, increased humidity content in the ambient air will be responsible in suppressing the temperature in the combustors resulting in an increased mass flow rate of fuel that will bring down the efficiency. It can also be seen that, there is a constant difference in the efficiencies of basic and proposed gas turbine cycle. Therefore, for the basic and proposed gas turbine cycle there is a continuous decrease in the efficiency as the relative humidity increases. Further, a difference of around 2% in the first and second law efficiency of both basic gas turbine and the gas turbine subjected to evaporative after cooling and inlet air cooling may be noted for all the values of ambient relative humidity concerned and the reason is well explained earlier in this chapter.

4.4.5 Ambient temperature

It was earlier shown that the power output of a gas turbine cycle reduces with an increase in ambient temperature. To assess it from the efficiency point of view, the effect of ambient temperature was also investigated on the overall first and second law efficiency of the gas turbine and shown in the Figure 24. Results show a drastic decrease in the efficiency of gas turbine. Firstly, the power output of the gas turbine reduces at elevated temperature. Secondly, increase in ambient temperature results in higher water absorption capacity of air. Therefore, larger amount of water vapor is observed in the after cooler. When this air with high concentrations of moisture enters the combustors, the combustion temperatures are reduces which are attributed to the presence of higher water molecules. Therefore, fuel requirements rise resulting in a decrease of overall first and second law

efficiency. It is further observed that a constant difference exist between the proposed gas turbine and basic gas turbine efficiencies which indicate the similar influence of both the gas turbine cycle studied. From the basic gas turbine cycle results, it can also be stated that, reducing the ambient temperature from 320 K to 290 K can increase the efficiency by 12.8 %. Therefore, highlights the importance of inlet air cooling in hot and humid climates. The efficiency of the current proposed cycle is lower due to presence of evaporative after cooling rather than inlet air cooling as can be seen from the increasing the extraction mass rate. An increase in extraction mass rate from 0.2 to 0.4 which produced the enhanced chilling effect in the refrigeration cycle by reducing the compressor inlet temperature from 308 K to 301 K when the ambient temperature was 320 K, was found to increase the first law efficiency from 35.5% to 36%

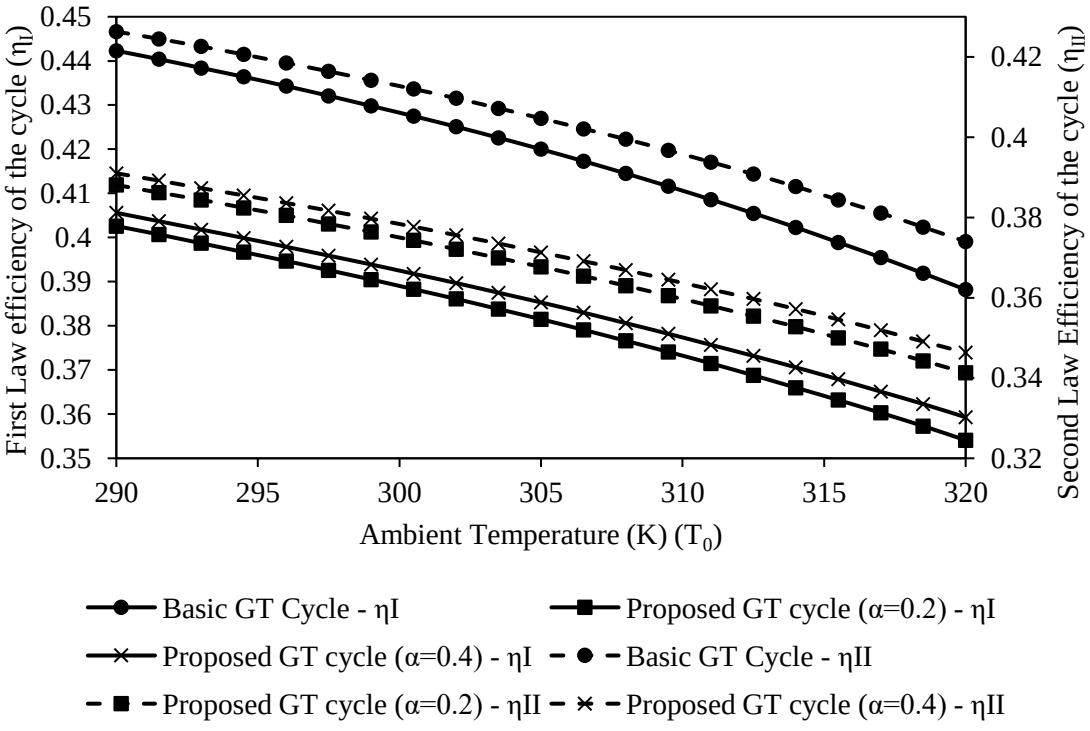

Figure 24 Effect of ambient temperature (T_0) on the first and second law efficiency of the cycle

4.4.6 Water-to-air ratio

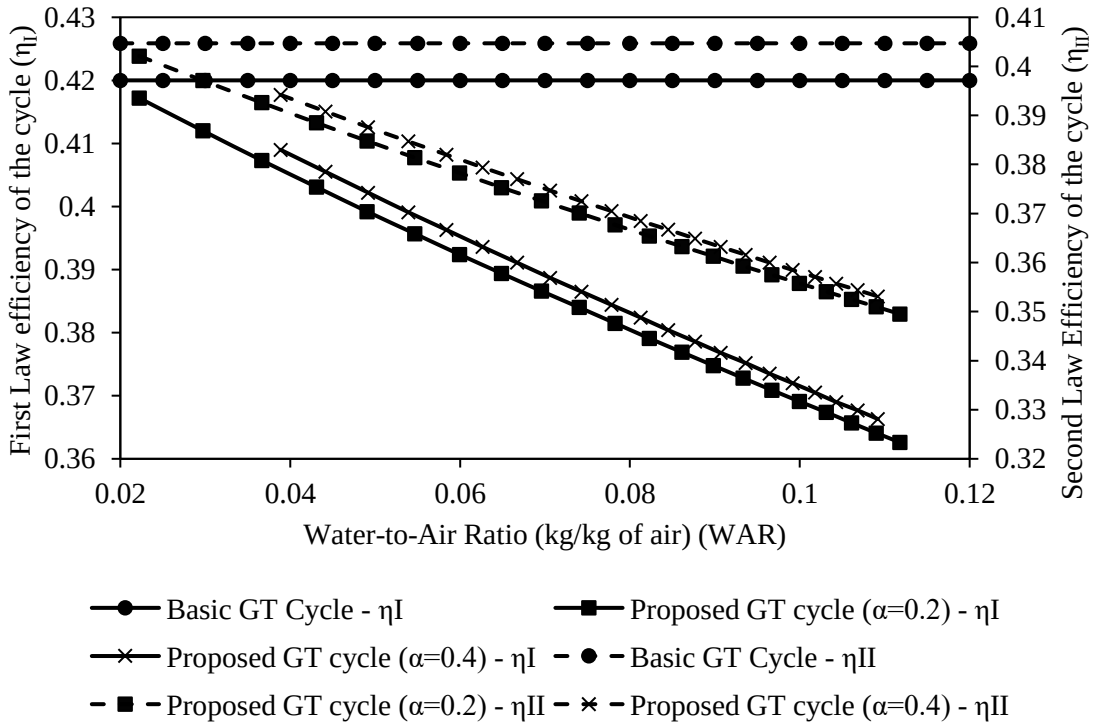

Figure 25 Effect of water-to-air ratio (WAR) on the first and second law efficiency of the cycle

Figure 25 shows the variation of cycle efficiency with different amount of water injected to the compressed air. It is seen that as the amount of water injected to the air in the evaporative after cooler increases cycle efficiency decrease. This is due to the fact that increase of mass flow rate of water reduces the temperature attained in the combustors. This will increase the amount of fuel needed for combustion. Therefore, increase in the amount of fuel dominates over the increase in power output causing a drop in overall first and second law efficiency of the cycle when compared with basic gas turbine cycle. This reduction should not be worried for, since, this reduction will result in a decrease of emissions to practical limits with an advantage of increase of power output. The amount of water-to-air ratio should depend on the power augmentation needed keeping the

emissions under control. It is observed that a rise in water-air ratio from 0.02 to 0.12 results in the decrease of first law efficiency from 42% to 36% and second law efficiency from 40% to 35%.

4.4.7 Turbine inlet temperature

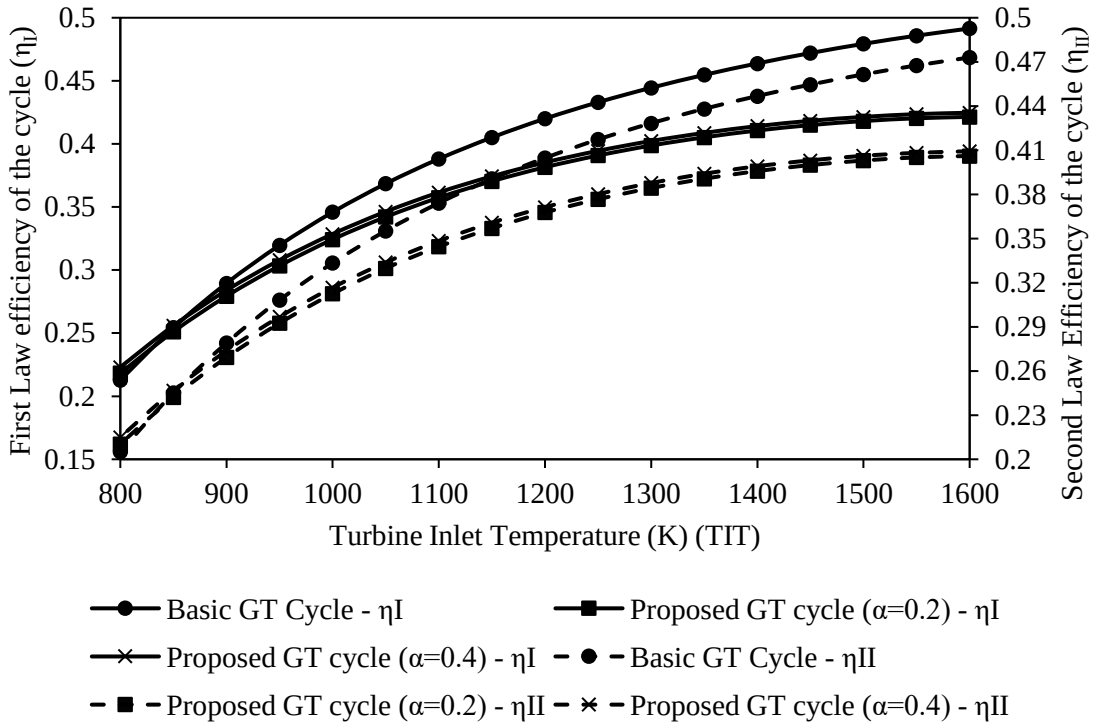

Figure 26 Effect of turbine inlet temperature (TIT) on the first and second law efficiency of the cycle

Figure 26 shows the effect of variation of turbine inlet temperature (TIT) on the cycle first and second-law efficiencies. Results show that both first and second law efficiencies of the cycle increases as TIT increases. This is because for the given values (mid values) of extraction pressure, extracted mass rate, ambient relative humidity, and equivalence ratio, the application of evaporative aftercooling causes the warm water coming out from the water heater to evaporate after coming in contact with air causing the air temperature

inlet to the heat exchanger to decrease. This will further enhance the heat transfer rate by absorbing greater heat from the turbine exhaust in the heat exchanger and hence the temperature of air inlet to the combustion chamber would increase, which in turn would increase the mean temperature of heat addition that leads to reduction of the magnitude of heat supplied to the cycle. Therefore, increase in TIT causes a significant increase in the cycle efficiency. Combined effect of inlet air cooling and evaporative cooling is more pronounced at lower values of TIT from the efficiency point of view. This is because at lower values of TIT, the increase in power output dominates over the rising fuel requirement of the cycle. Further, it may be observed that the second law efficiency of the gas turbine is lower than its first-law efficiency. A loss of 6 % in the first law efficiency is observed at the turbine inlet temperature of 1600 K.

4.5 Effect on the exergy distribution

The distribution of the exergy of fuel in terms of the exergetic output, exergy destroyed, and exergy lost for both basic gas turbine cycle and the gas turbine subjected to evaporative after cooling and inlet air cooling is depicted in Figure 27 and Figure 28 respectively. For a basic gas turbine cycle, it is seen that out of 100% fuel exergy 40% is produced as the exergetic output, 42% is destroyed due to entropy generation among various components of the basic gas turbine cycle and rest of the 18% is lost to the ambient via exhaust gases, air from the intercooler and cooling fluid.

Total exergy input by the fuel = 14849 kW

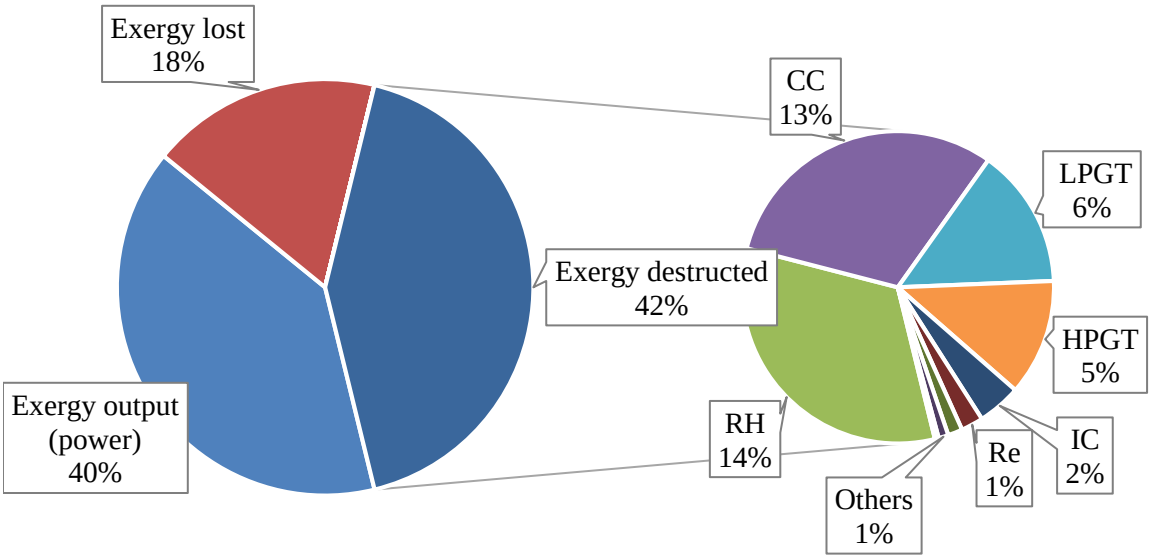

Figure 27 Exergy balance of a basic gas turbine cycle

Total exergy input by the fuel = 21619 kW

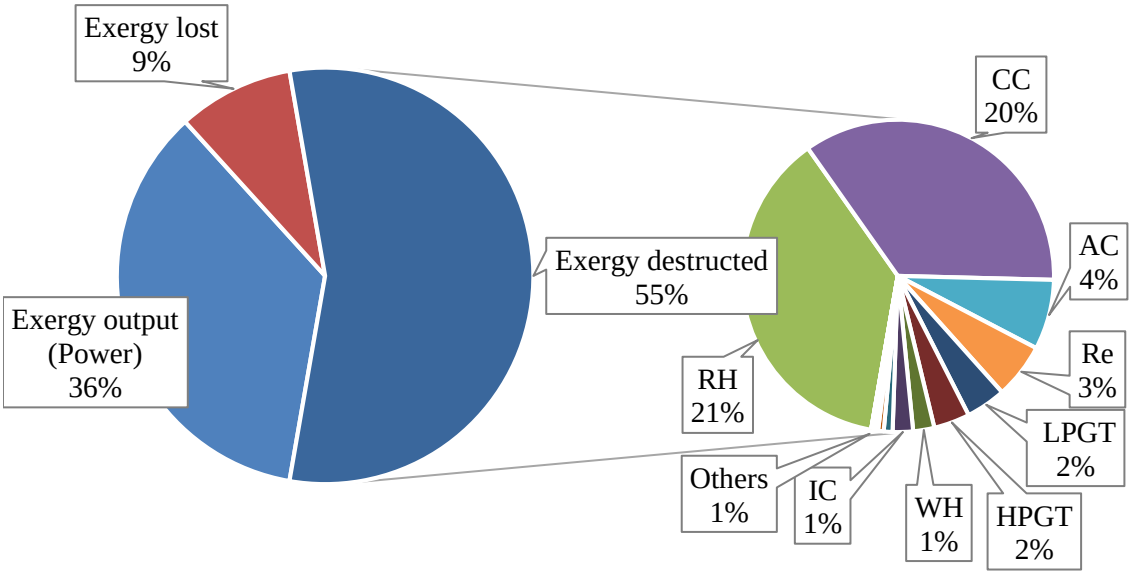

Figure 28 Exergy balance of the proposed gas turbine cycle (α=0.2)

It is interesting to note that application of evaporative after cooling and inlet air cooling at $\alpha=2$ change these figures of fuel exergy distribution and takes the form; 36% of the fuel exergy is produces as the exergetic output, 55% is destroyed due to entropy generation among various components of the cycle, and only 9% is lost via exhaust gases, moisture from humidity eliminator, cooling air from the intercooler and cooling water as shown in Figure 28. Another important revelation is the exergy input to the gas turbine cycles. A significantly larger exergy is supplied to the proposed gas turbine than the basic gas turbine cycle for same volumetric capacity plants. Therefore, even though the percentage of work output sounds less, a net increase in the exergetic output is obtained.

Comparison of the results plotted in above figures also reveals the percentages of exergy destruction in the individual components of the cycle when it is operated in the basic gas turbine cycle mode and in the evaporative after cooling and inlet air cooling mode. It is seen that major contribution to exergy destruction comes from the reheater and combustion chamber in both the cases. The reason for having the high exergy destruction in the reheater and combustion chamber is that due to high combustion zone temperature, a significant amount of exergy of the combustion gases is lost due to heat transfer from the combustion zone to the combustor wall. The exergy destruction in the reheater and combustor are 14% and 13% respectively for basic gas turbine cycle. The exergy destruction in both reheater and combustion chamber are 21% and 20% respectively for the case of proposed gas turbine cycle. The second largest exergy destruction occurs in the after cooler which is around 4%. The exergy destruction in the after cooler is large due to the reason of high entropy generation via heater transfer mixing of compressed air and injected water in the after cooler. Third largest exergy destruction is found in the

recuperator which is due to the reason of a significant entropy generation via heat transfer from the turbine exhaust to the water injected air. Since there is no mixing of two fluids in the recuperator, therefore, the exergy destruction is 3% as compared to 4% in the aftercooler where the heat transfer followed by mixing. The exergy destruction in rest of the cycle components is much smaller than the exergy destruction in the reheater, combustion chamber, after cooler and recuperator. It is also interesting to note a reduction in the percentage of exergy destruction in the turbines for the proposed gas turbine cycle to basic gas turbine cycle. The quantified values of component wise exergy destruction for the proposed cycle are reported in Table 9.

Table 9 Exergy distribution in the proposed cycle at its mean operating conditions.

	kW	Percent ratio (%)
Fuel exergy input	21619	100
Net power output of proposed cycle	7681	35.53
Exergy destruction in reheater	4497	20.80
Exergy destruction in combustion chamber	4210	19.47
Exergy destruction in after cooler	869.5	4.02
Exergy destruction in recuperator	685.6	3.17
Exergy destruction in low pressure gas turbine	496.5	2.30
Exergy destruction in high pressure gas turbine	447.5	2.07
Exergy destruction in water heater	262.6	1.21
Exergy destruction in intercooler	252.9	1.17
Exergy destruction in low pressure compressor	109.5	0.51

Exergy destruction in high pressure compressor	69	0.31
Exergy destruction in mixing chamber	27.72	0.14
Exergy destruction in air humidifier	25.53	0.13
Exergy destruction in heat exchanger	23.78	0.12
Exergy destruction in expander	6.646	0.04
Exergy destruction in humidity eliminator and pump	2.0703	0.02
Exergy lost to the surroundings	1944	8.99

4.6 Effect on second law efficiency of major components

The second-law efficiency that provides a better assessment of the energy conversion device than its first-law efficiency has been depicted in Figure 29 for individual components of the cycle. For the proposed gas turbine cycle, it is seen that the second law efficiency of the combustion chamber and reheater are lowest 81% and 75% respectively followed by the gas turbines which are 84% for LPGT 86% for HPGT. The low second law efficiencies in turbines is due to reason of considerable exergy destruction due to entropy generation via heat transfer at a finite temperature difference across the turbine. Therefore, the second law analysis pinpoints the components where a room for the improvement is available. From the results shown, it reveals that, combustors and turbines need to be improved for the better performance of the cycle which can improve the overall first law and second law efficiencies of the cycle.

It is further interesting to note that the second law efficiency of the combustion chamber and reheater reduced by a little amount due to the simultaneous effect of exergy destruction and exergy input after the application of evaporative after cooling and inlet

air cooling while the second law efficiency of the recuperator reduces from 97% to 93%. This is because, a higher temperature difference exists when after cooling and inlet cooling is employed increasing the irreversibility resulting in lower second law efficiency. As a summary of Figure 29, it can be said that, improving the design for combustion chamber, reheater, after cooler, water heater and gas turbines is expected to improve the thermodynamic performance of the proposed system.

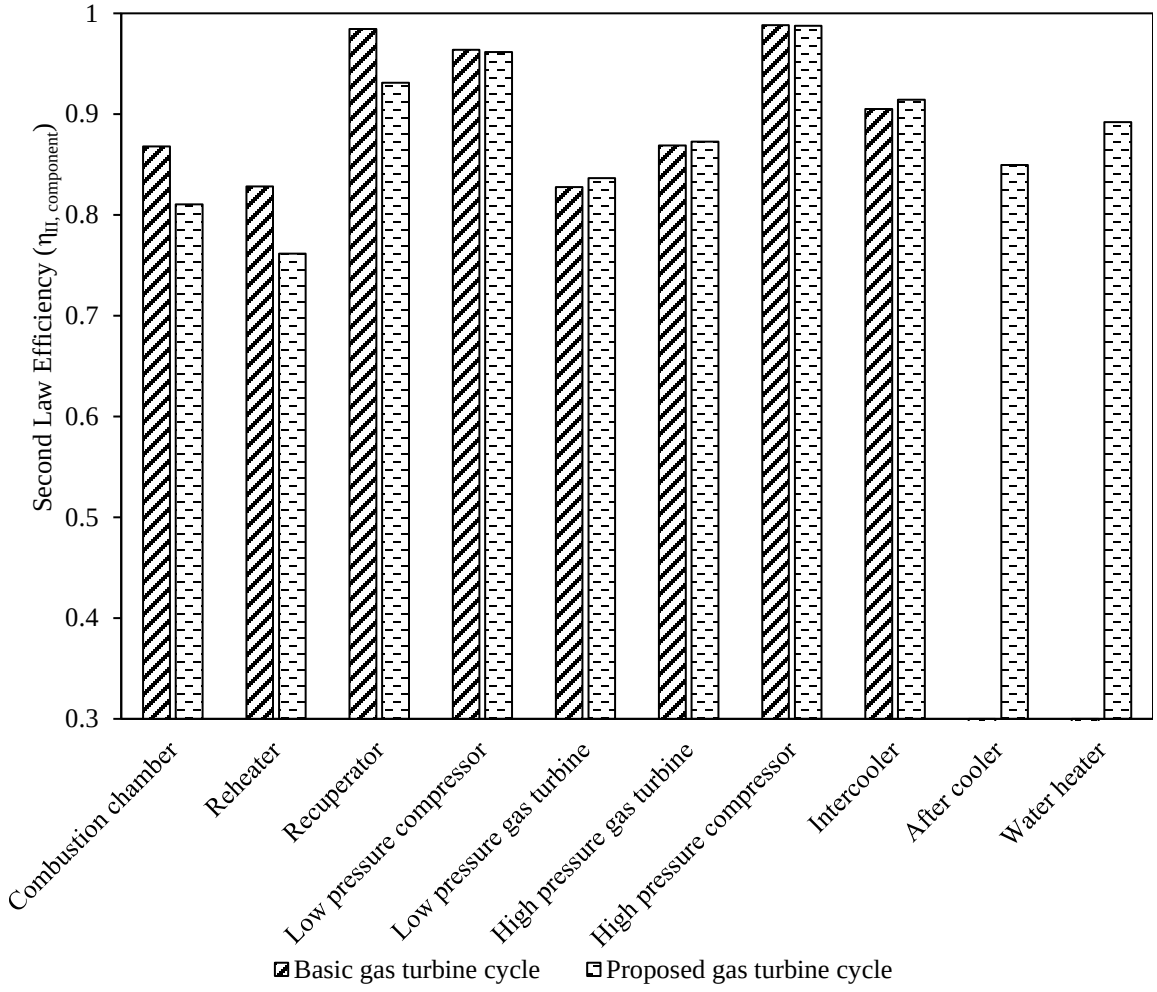

Figure 29 Effect on second law efficiency of the major components in the cycle

4.7 Effect on emissions

Many researchers have tried to suppress the combustion temperature to reduce the amount of NOx using many techniques, but very few results are reported which are able to quantify the amount of emissions produced. The potential of water injection to reduce the emissions is assessed in this section. Further, the effect of inlet air cooling observed as counteractive to emissions is also observed. Lastly, the emissions in the gas turbine proposed and the gas turbine operating without inlet air cooling and after cooling is also observed.

4.7.1 Equivalence ratio

Figure 30 shows the concentration of the NOx emissions formed in the gas turbine with the variation of fuel-air equivalence ratio. It is shown that the amount of NOx formed increases as the value of equivalence ratio approaches to stoichiometric. A constant increase in the NOx emissions was found due to increase in temperature as a result of higher equivalence ratio. For the convenience of the reader, the variation of temperature in combustion chamber and reheater across the length of the combustor for various values of equivalence ratios is shown in Figure 31. These results, clearly shows the dependence of NOx on the equivalence ratio. The peak of NOx formation is found on fuel-lean side of stoichiometric. This is due to the result of competition between fuel and nitrogen for available oxygen. It is further observed that the NOx emission is slightly higher on fuel rich side of stoichiometric and then the amount of NOx emissions decreases drastically as the equivalence ratio increases beyond stoichiometric which shows the exponential dependence of thermal NOx on flame temperature. The combined effect of using

evaporative after cooling and inlet air cooling on the amount of NOx formed is also shown in the Figure 30. It is found that the amount of NOx increases significantly as the equivalence ratio approaches to unity. It is further seen that the amount of NOx reduced drastically from 1000 ppm to 100 ppm after the employment of inlet air cooling after cooling at stoichiometric combustion conditions. The trend shown in the Figure 30 reveals that change in the extraction mass rate from 0.2 to 0.4 causes an insignificant increase in the NOx emissions. This is due to the reason that, increase in extraction mass rate slightly reduces the amount of oxidizer going to combustion chamber which in turn results in slight increase of NOx.

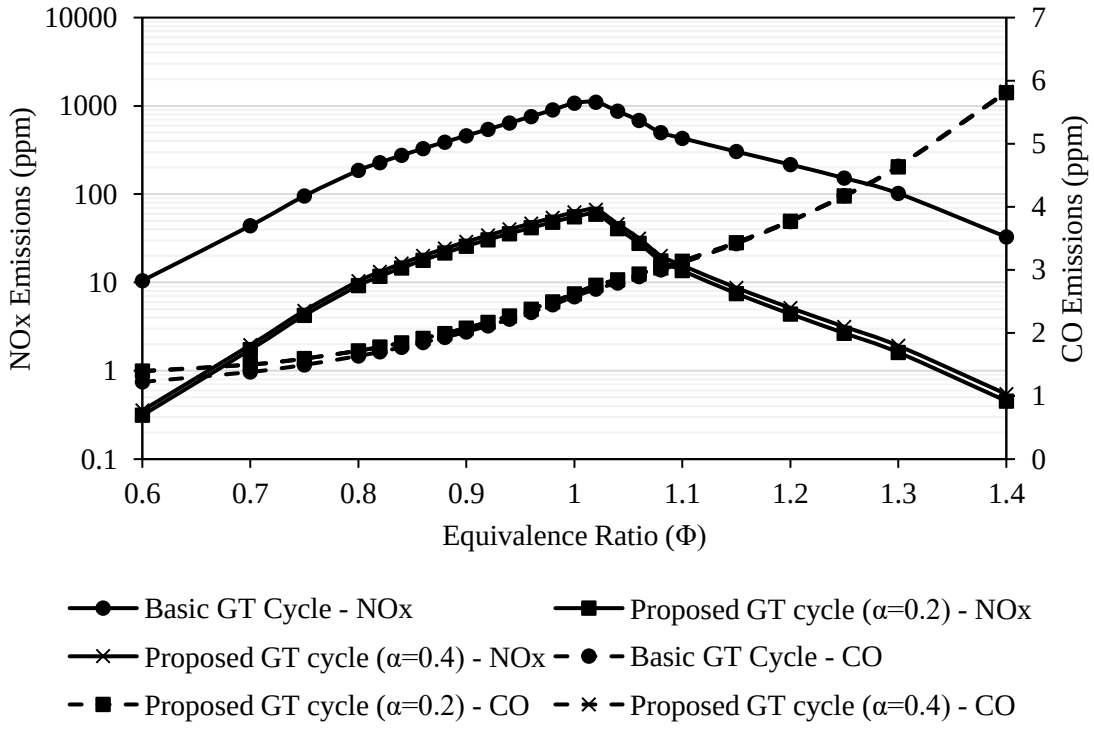

Figure 30 Effect of equivalence ratio (Φ) on the amount of NOx and CO formed

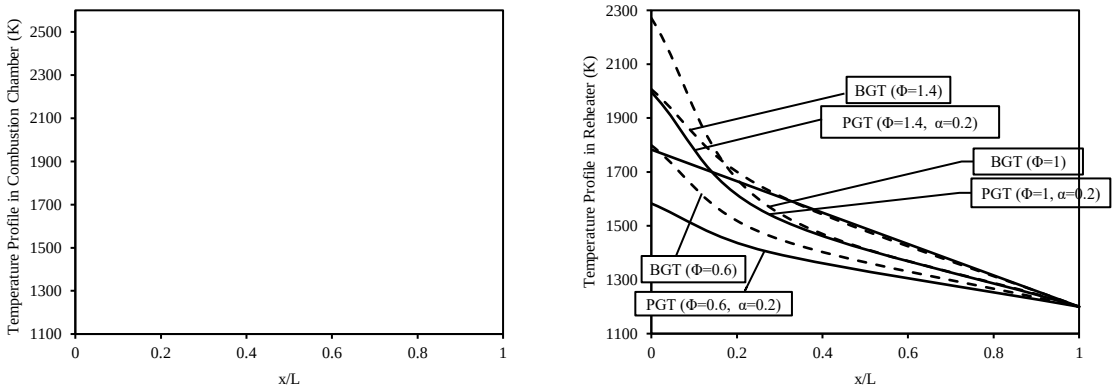

(a) **(b)**

Figure 31 Temperature profiles in combustion chamber and reheater as a function of equivalence ratio (Φ)

(BGT – Basic gas turbine cycle; PGT – Proposed gas turbine cycle)

Figure 30 also shows a trend for the formation of CO in the combustion chamber and reheater with the variation of equivalence ratio. A continuous increase in the emission of CO is observed while increasing the equivalence ratio. This is due to the fact that decreasing the amount of leads to the possibility of incomplete combustion which in turn increases the CO. It is further shown that the concentration of CO would increase due to the employment of evaporative after cooling and inlet air cooling in gas turbines. This is due to the fact that water injection into the combustor and reheater suppress the flame temperature which leads to increase in CO to some extent. An increase in the extraction mass rate doesn't alter the concentration of CO since it results in a very small increase in primary zone temperature which is insignificant in altering the values of CO. Application of evaporative after cooling at a given equivalence ratio affects the NOx emission more than the CO emission and it is seen that, for all the values of equivalence ratio considered the reduction in amount of NOx formed is more pronounced that the enhancement in CO formed. Therefore, evaporative after cooling could be considered as of the promising

options for reducing the NOx emissions while maintaining a higher thermal efficiency of gas turbine plants.

4.7.2 Extraction pressure ratio

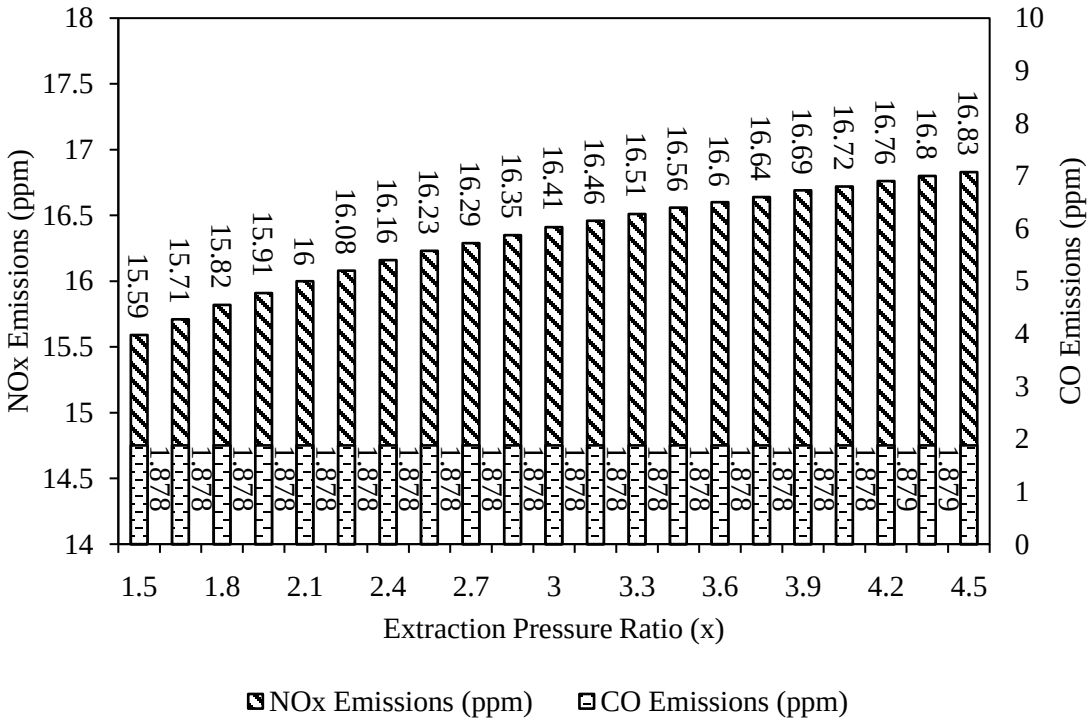

Figure 32 Effect of extraction pressure ratio (x) on the amount of NOx and CO formation

The effect of change in extraction pressure on the NOx emissions is shown in the Figure 32 where it is seen that increase in extraction pressure ratio causes a moderate increase in the NOx emission. This is in accordance with the trend, higher extraction pressure through the reduction of compressor inlet air temperature provides a significant cooling of incoming air which further results in the reduction of the air at the inlet of evaporative aftercooler. This reduces the capacity of air to absorb water from the injector which leads a gain in the primary combustion zone temperature and hence an increase in the NOx

emissions. The variation of primary combustion zone temperature with the change of extraction pressure ratio was minimal and was not worth presenting which shows a light dependence of inlet air cooling on NOx emissions which shows it is employed mainly for power augmentation in gas turbines. For this reason, the evaporative after cooling is employed along with the inlet air cooling which makes the gas turbine operation thermodynamically efficient and environment friendly. The reduction in the NOx emission for this arrangement is quite significant as shown in the Figure 33. The effect of extraction pressure ratio on CO emission was also investigated and it was found to be almost constant at a given extraction mass rate.

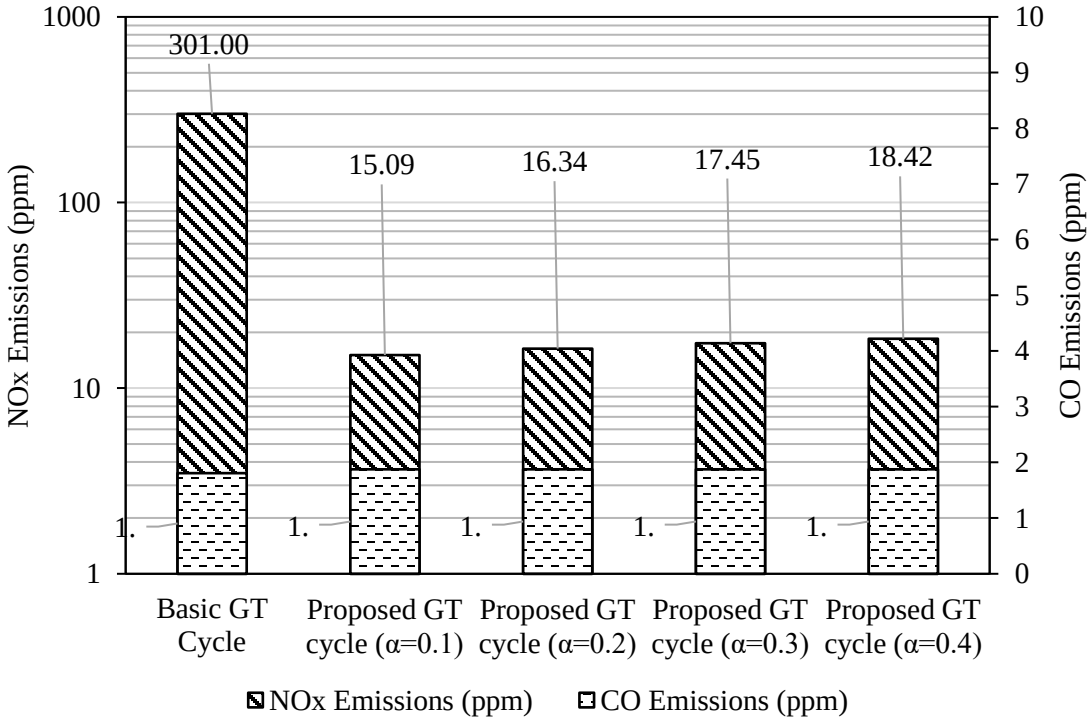

Figure 33 Effect of extraction mass rate (α) on the amount of NOx and CO formed

4.7.3 Overall pressure ratio

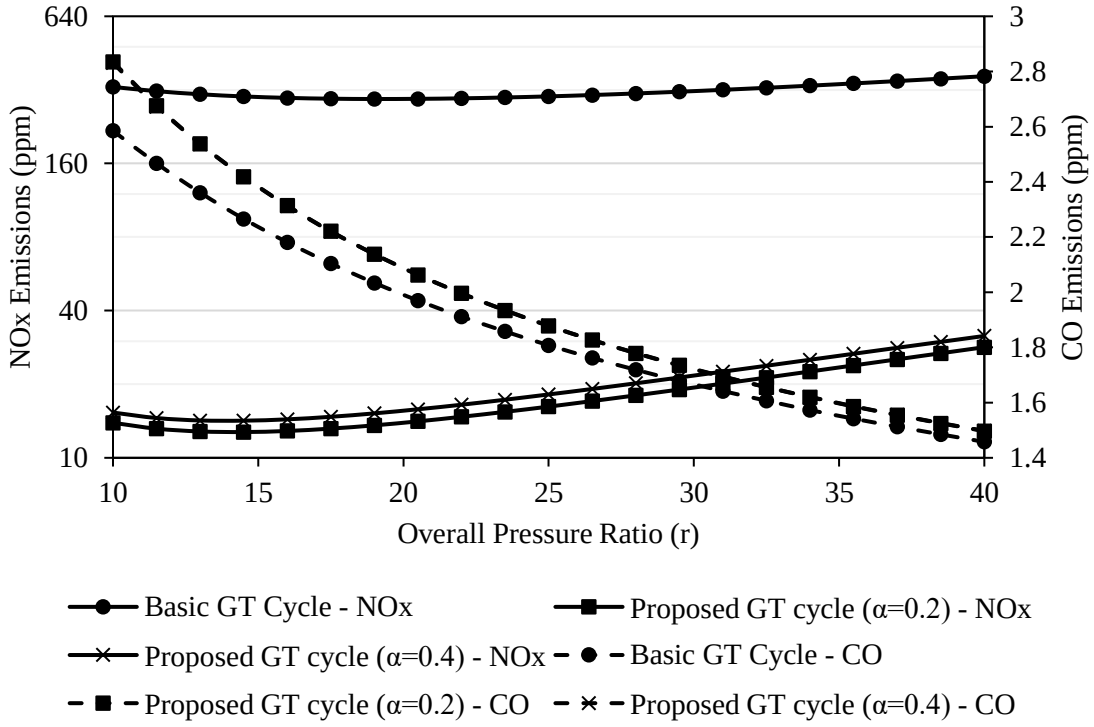

Figure 34 Effect of overall pressure ratio (r) on the amount of NOx and CO formed

The effect of change in cycle's overall pressure ratio on NOx emissions and CO emission is shown in Figure 34. It is seen that the amount of NOx formed increases as the overall pressure ratio increases. This is due to the reason that, increasing the overall pressure ratio means the higher combustion pressure which leads to the more formation of NOx via thermal route as the thermal NOx is the square-root dependence of combustion pressure. The effect of change in the extraction mass rate from α=0.2 to α=0.4 is also plotted at a given overall pressure ratio. It is also seen that, increase in the extraction mass from 0.2 to 0.4 raises the amount of NOx from 20.9 ppm to 23.7 ppm. Its reason is well explained in the previous graphs. Effect on the temperature profiles due to change in the overall pressure was found to be non-significant since, the turbine inlet temperature remains the same allowing the air to enter at almost the same temperature for all the

overall pressure ratio. Hence, the temperature profiles are not presented. The only parameter affecting NOx formation is the change in inlet pressure into the combustors. The emission CO decreases considerably as the overall pressure ratio increases. This decrease in the CO at higher values of overall pressure ratio is observed due to the suppression of chemical dissociation. Similar to the reasons, explained above, the amount of CO emissions increases slightly after the employment of evaporative after cooling and inlet air cooling in gas turbines.

4.7.4 Ambient relative humidity

The ambient relative humidity which has also been considered as one of the effective parameters relative to gas turbine cycle performance was also investigated and its effect on the emissions of NOx and CO was examined and shown in Figure 35. It is observed that the amount of NOx decreases as the ambient relative humidity increases. This is because increase in ambient relative humidity means the increase of moisture in the air where it will act as ballast to absorb heat from the flame which will result in the suppression of flame temperature, resulting in the lower NOx emission. It is further seen that, the amount of NOx reduces drastically from 500 ppm to 30 ppm when the gas turbine is subjected to evaporative after cooling and inlet air cooling at the ambient relative humidity of 30%. Carbon Monoxide (CO) is produced by incomplete combustion of fuel containing carbon and this can be easily converted into CO_2 in the event of complete combustion. Presence of water vapor in the air due to the absorption of the heat from the flame results in the reduction of flame temperature which increases the possibility of higher CO formation. The trend for the formation of CO with the change of

ambient relative humidity is very much shown in the Figure 33 and its reason is as explained.

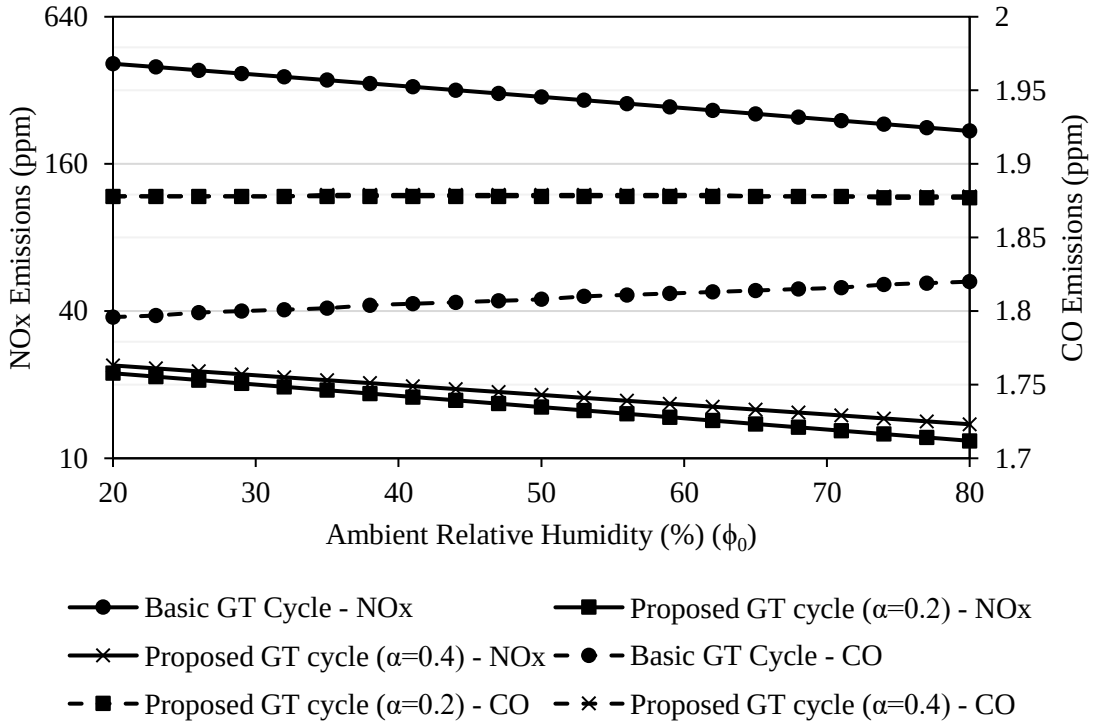

Figure 35 Effect of ambient relative humidity (ϕ_0) on the amount of NOx and CO formed

4.7.5 Ambient temperature

In view of observing the effects of key ambient conditions, the effect of change in the ambient temperature was also ascertained on the amount of NOx and CO formed in gas turbines. In case of conventional burners where the dry air is utilized as an oxidizer, the amount of NOx increases with the rise of ambient air temperature. In the current study where compressor discharge air is cooled down through the use of water injector show that increase in ambient air temperature which increases the compressor discharge temperature enhances the capacity of air to absorb more water which in turn when enters

the combustors suppress the flame temperature and hence reduces the NOx emissions as can be seen from Figure 36. To illustrate further the reduction of temperatures in the combustors, temperature profiles in the combustion chamber and reheater are presented in the Figure 37. It is clearly seen that the gas turbine subjected to evaporative after cooling and inlet air cooling leads to a drastic decrease of NOx emissions. The effect of ambient temperature on emission of CO was also investigated and it shows almost independency for the proposed gas turbine.

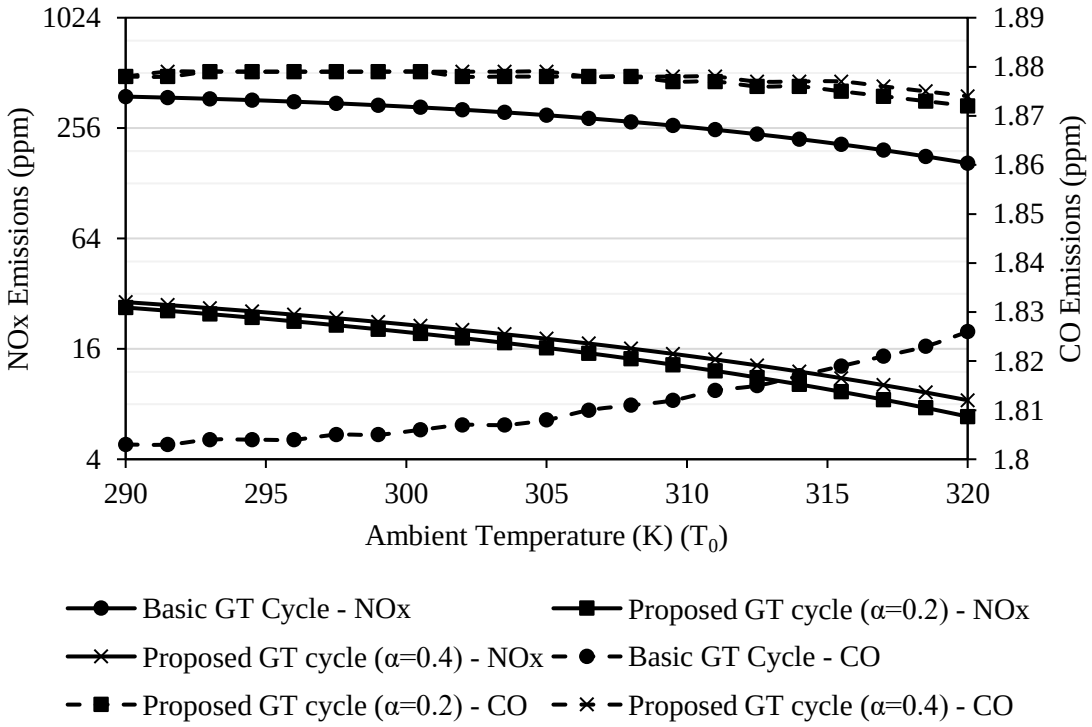

Figure 36 Effect of ambient temperature (T_0) on the amount of NOx and CO formed

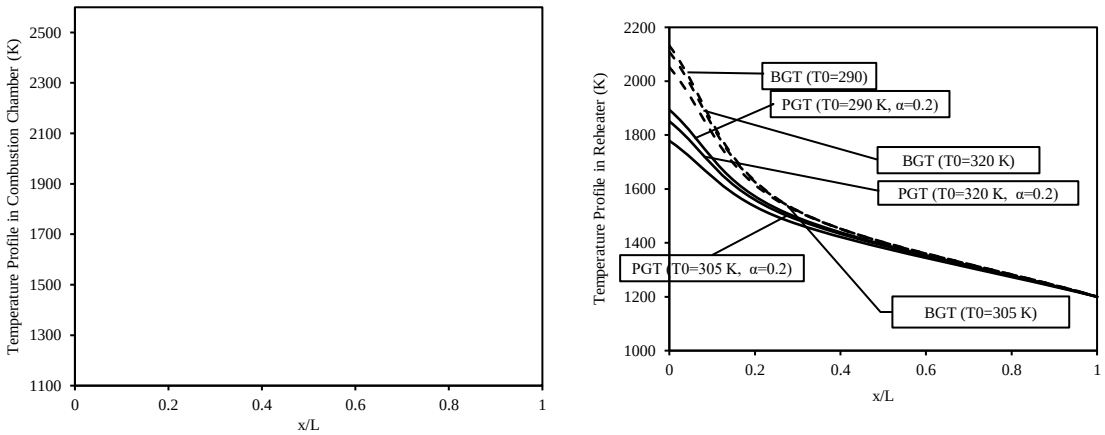

(a) **(b)**

Figure 37 Temperature profiles in combustion chamber and reheater as a function of ambient temperature (BGT – Basic gas turbine cycle; PGT – Proposed gas turbine cycle)

4.7.6 Water-to-air ratio

One of the key aspects of the current study was the application of the evaporative after cooling which is a water injector supplied at the compressor exit to absorb heat in view of making the gas turbines environment friendly. In this regard, the effect of change in the water-to-air ratio was observed on the amount of NOx and CO formed during combustion. From the Figure 38, it is seen that, the amount of NOx reduces drastically as the water-to-air ratio increases. This is due to the reason, increase in water injection absorbs a greater amount of heat from the flame which results in the reduction of flame temperature and hence in the decrease of NOx emissions. Further decrease in the NOx is due to the decrease in the amount of dry air which makes the combustion richer because water-to-air ratio is amount of water injected to the amount of air supplied. Therefore, increase in water-to-air ratio means increase in the amount of water and decrease in the amount of air. This will affect the amount of NOx emissions in two ways as discussed above. The deviation in the amount of NOx formed between the proposed gas turbine and

basic gas turbine is more pronounced at higher values of water-to-air ratio and at extremely lower values, this deviation becomes minimum. The temperature profiles in the combustion chamber and reheater with the variation of water heater surface area is also shown in the Figure 39. The more surface area available on the water heater, more amount of water could be heated that could be injected into the after cooler which in turn increases the water-to-air ratio. Temperature profiles clearly shows the temperature reducing potential with an increase in mass flow rate in the combustors.

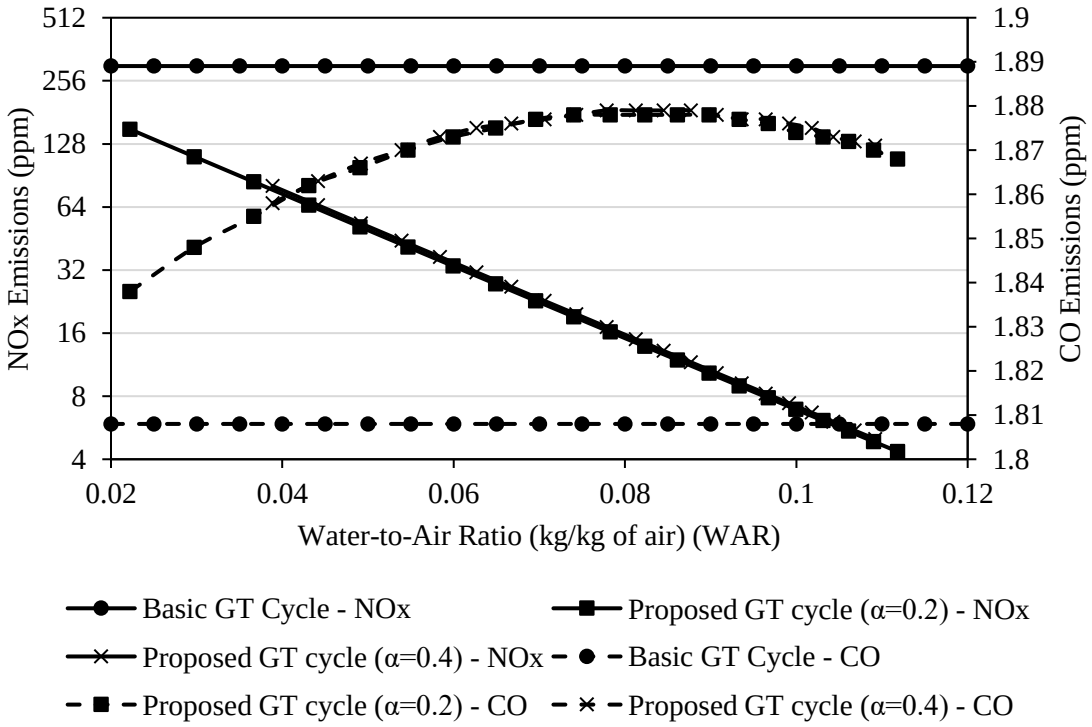

Figure 38 Effect of water-to-air ratio (WAR) on the amount of NOx and CO formed

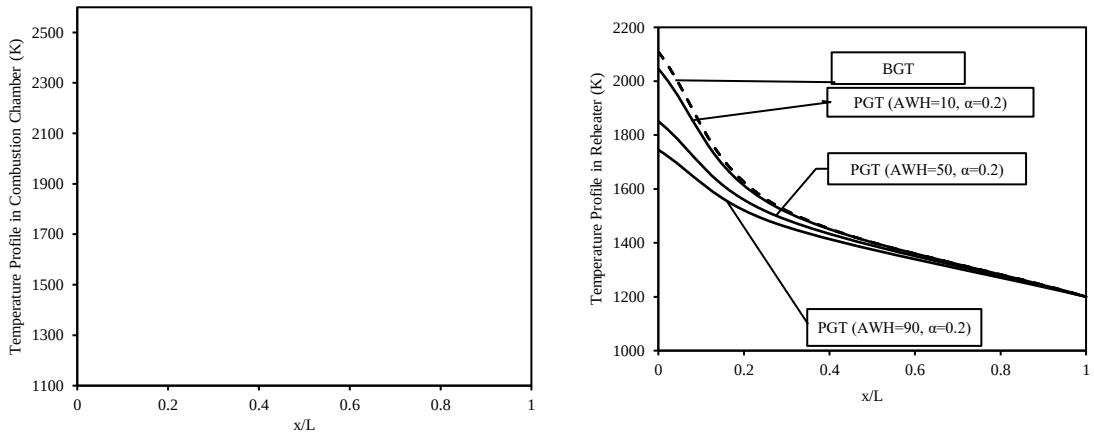

Figure 39 Temperature profiles in combustion chamber and reheater as a function of ambient temperature (T_0)

(BGT – Basic gas turbine cycle; PGT – Proposed gas turbine cycle)

The carbon monoxide which is considered as one of the most dangerous pollutant from the fossil fuel combustion is also taken in the current study and its variation with the change of water-to-air ratio is investigated and shown in Figure 36. An exponential increase in the amount of CO formation is observed as the water-to-air ratio rises from 0.02 to 0.08. This is due to the fact that, increase in water-to-air ratio will suppress the combustion temperature in two ways: through water injection and lean combustion which increases the possibility of incomplete combustion and hence, increases the CO formation. It is interesting to see that the amount of CO starts decreasing after attaining the water-to-air ratio of 0.08. This is due to the fact that further increase in water-to-air ratio results in the increase of the number of moles of water species and CO species but increase in the number of moles of water is greater than increase in the number of moles of CO which results in the decrease of CO (ppm) as shown in figure. It may further be mentioned that the water-to-air ratio more that 0.08 is quite favorable from environment point of view as it reduces both NOx and CO emissions.

4.7.7 Turbine inlet temperature

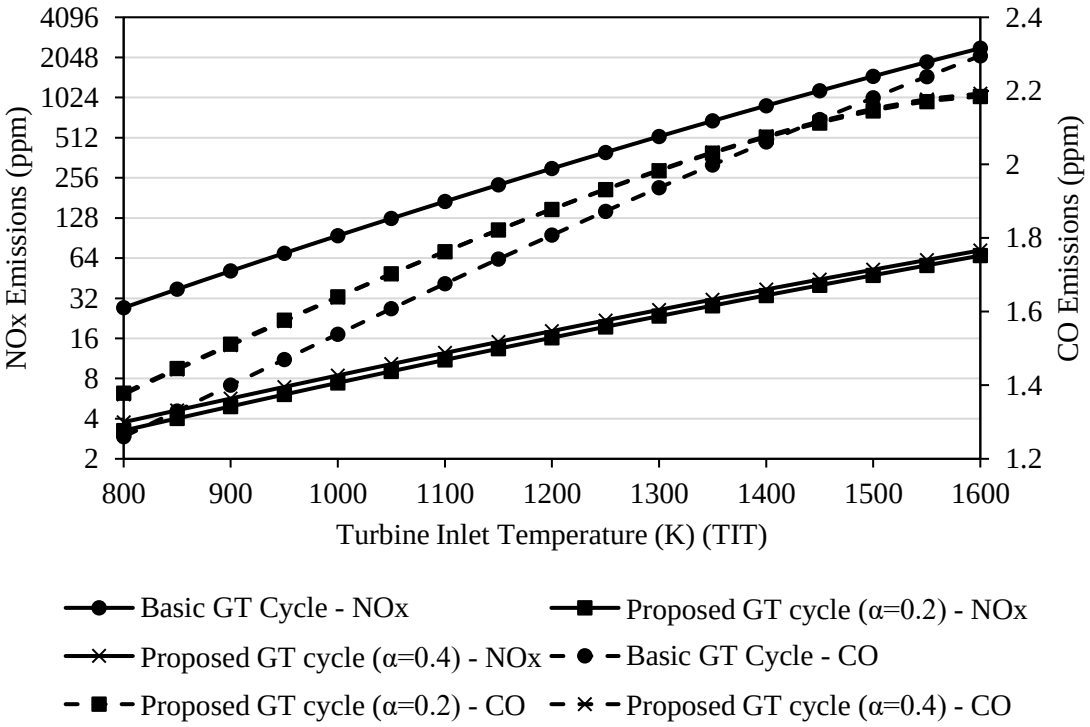

Figure 40 Effect of turbine inlet temperature (TIT) on the amount of NOx and CO formed

Turbine Inlet Temperature (TIT) is usually considered as one of the most important parameter from emissions point of view in gas turbines. The variation of NOx and CO emissions with the change of turbine inlet temperature was examined and shown in Figure 40. It is found that with the increase of turbine inlet temperature the NOx emission increases significantly which is mainly the thermal NO. Usually in gas turbines, NOx formation start beyond the combustion temperature of 1400 K. In order to make the gas turbine operation environment friendly while maintaining a higher thermal efficiency in the hot and humid climatic regions, use of evaporative after cooling and inlet air cooling is required. To this effect, current study results shown in Figure 40 reveals that even at higher turbine inlet temperatures the NOx emissions may be reduced significantly when

the gas turbine is subjected to evaporative after cooling along with inlet air cooling. A drastic reduction in the amount of NOx formed was observed and it is seen that the NOx was reduced from 2400 ppm to 70 ppm at the gas turbine inlet temperature of 1600 K when the method of evaporative after cooling and inlet air cooling were applied to basic gas turbine cycle. Further, for the convenience a temperature profile across the combustor length was plotted as shown in Figure 41, which shows a steep falling in the temperature at a given length especially for a reheater when evaporative after cooling was applied along with inlet air cooling.

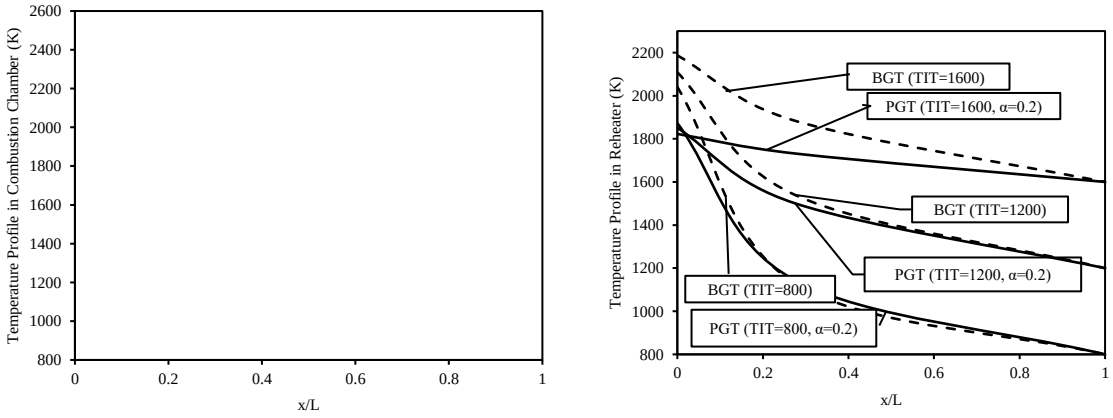

(a) **(b)**

Figure 41 Temperature profiles in combustion chamber and reheater as a function of turbine inlet temperature (TIT) (BGT – Basic gas turbine cycle; PGT – Proposed gas turbine cycle)

The emission of CO formed in gas turbines was also investigated with the increase of turbine inlet temperature and it is shown that the amount of CO also increases with the increase of turbine inlet temperature though its increase is much less than the increase of NOx. It is noticed that the amount of NOx increases from 4 ppm to 70 ppm and amount of CO increases from 1.4 ppm to 2.2 ppm when the gas turbine inlet temperature from 800 K to 1600 K as the trend shown in Figure 40. The increase in amount of CO along

with the increase of NOx is due to the fact that, at a given turbine speed increase in turbine inlet temperature requires more amount of fuel to be supplied which results in the process of inadequate burning rate and inadequate mixing of fuel and air which are considered to be as one of the major causes of CO formation. Therefore, the amount of CO also increases as the turbine inlet temperature increases, but its increase is significantly less than the increase of NOx formation. At very high values of turbine inlet temperatures, increase in CO in basic gas turbines dominates over the proposed gas turbine due to the process dissociation where the CO_2 transforms into CO and O_2 while in the gas turbine subjected to evaporative after cooling and inlet air cooling the increase is steadily as the application of evaporative after cooling prevents the process of dissociation due to the suppression of flame temperature.

CHAPTER 5

CONCLUSIONS AND FUTURE RECOMMENDATIONS

5.1 Conclusions

Gas turbines are playing a major role in power generation of today. The performance of gas turbines suffers while operation in the hot and humid climatic regions of the world. It has been greatly observed that the performance of gas turbines heavily depend on ambient conditions like ambient air temperature and ambient relative humidity. Rise in ambient temperature reduces the power output of gas turbines due to decrease in mass flow rate. It is estimated that 30% increase in power output could be obtained if the gas turbine temperature is reduced from 35^{o}C to -6.6^{O}C. In view of the above trend, a novel method of compressor inlet air cooling and evaporative after cooling of the compressor discharge was employed in gas turbine power plant in order to compensate the power output reduced due to elevated ambient conditions and to reduce the emissions. In this context, a comprehensive thermodynamic analysis using the cascaded energy and exergy theory was carried out to ascertain the effects of some influencing operating variables like equivalence ratio, extraction mass rate, extraction pressure ratio, overall pressure ratio, ambient relative humidity, ambient temperature, water-to-air ratio and turbine inlet temperature on the energetic, exergetic and environmental performance on the gas turbine engine where Brayton refrigeration cycle was employed along with the evaporative after cooling of the compressed air to reduce a compressor inlet temperature and increase the mass flow rate of gas turbine working fluid. A detailed thermo-environmental study using

the EES software was conducted on the proposed gas turbine cycle configuration which leads to the following conclusions:

1. Increase in extraction mass rate from 0.1 to 0.4 resulted in the reduction of compressor inlet air temperature from 299 K to 287 K which in turn enhances the power output from 7454 kW to 7617 kW.
2. Increase in overall pressure ratio considerably enhanced the power output and it was noticed that increase in overall pressure ratio from 10 to 40 shows an exponential rise in power output from 3 MW to 10 MW in the gas turbines which are subjected to evaporative after cooling along with the inlet air cooling.
3. Ambient relative humidity was found another environment parameter but the gas turbine performance affects marginally with the increase of ambient relative humidity. It is shown that increase in ambient relative humidity from 20 % to 80 %, reduces the turbine output just by 1 %.
4. Water-to-air ratio was found much in favor of gas turbine operation as it enhances the power output and reduces emissions significantly.
5. Power enhancement due to increase in turbine inlet temperature for the proposed gas turbine cycle configuration was found much greater than the power enhancement achieved with the increase in turbine inlet temperature in basic gas turbine cycle.
6. The change in equivalence ratio shows a marginal effect on both energy and exergy efficiency of the proposed gas turbine cycle.
7. Both extraction mass rate and extraction pressure ratio affects the first and second law efficiency of the proposed gas turbine cycle

8. The first law efficiency of the gas turbine cycle decreases considerably with the increase in overall pressure ratio and ambient relative humidity.
9. Increase in water-to-air ratio showed a high impact on both first and second law efficiency of the gas turbine cycle.
10. Comprehensive exergy analysis carried out for the basic gas turbine cycle reveals that, out of 100% fuel exergy, only 40% could be produced as the exergetic output and 42% is destroyed due to irreversibility in the components and rest 18% is lost to the environment. On the other hand, exergy analysis of the proposed cycle shows a 36% of exergetic output, 55% is the exergy destroyed due to irreversibility and 9% is lost to the environment.
11. Component wise irreversibility analysis shows that combustion chamber and reheater are the major exergy destructive components of the proposed cycle.
12. Recuperator and turbine were found to be the components of highest second law efficiency while combustion chamber and reheater were of lowest second law efficiency among all the cycle components.
13. The amount of NOx was found to increase as the equivalence ratio approaches to stoichiometric while the same was found to decrease drastically as the equivalence ratio increase beyond stoichiometric.
14. When the basic gas turbine cycle was subjected to inlet air cooling and evaporative after cooling, the amount of NOx was reduced drastically from 1000 ppm 100 ppm at stoichiometric combustion conditions.

15. Increase in equivalence ratio showed a continuous increase in the emission of CO. Effect of employing an evaporative after cooling reduces the NOx in greater amount than the rise in the emission of CO.
16. Increase in extraction mass rate from 0.2 to 0.4 raises the amount of NOx from 20.9 ppm to 23.7 ppm.
17. Increase in ambient relative humidity shows a drastic reduction in NOx emissions and it is shown that when the gas turbine cycle subjected to inlet air cooling along with evaporative after cooling operated at ambient relative humidity of 30%, the NOx reduces drastically from 500 ppm 30 ppm.
18. Increase in water-to-air ratio causes a drastic reduction in NOx emission and a significant rise in CO emission. It is shown a little rise in water-to-air ratio causes an exponential rise in the amount of CO formation. The most interesting point was to see that increasing the water-to-air ratio beyond 0.08 could result in the reduction of both NOx and CO emissions.
19. In the proposed gas turbine cycle arrangement, it was noticed that increase in turbine inlet temperature from 800 K to 1600 K shows a rise in NOx emission from 4 ppm to 70 ppm and in CO emission from 1.4 ppm to 2.2 ppm. This trend of greater rise in NOx emission than CO emission reverses when turbine inlet temperature becomes extremely high.

The overall conclusion drawn from the current study was that, theoretically, the thermo-environmental performance of gas turbine cycle can be measured when it is subjected to inlet air cooling along with evaporative after cooling. The range of operating parameters at which the proposed gas turbine provides a considerable reduction in the emissions

while maintaining a higher performance could be determined. Further, it can be stated that the results obtained from the study could be utilized as a source of data by the gas turbine manufacturers for the design and development of gas turbine plants required to be operated in hot and humid climatic regions.

5.2 Future Recommendations

Advanced thermodynamics applied to assess the performance of power plants reveals that, along with the energy, exergy must be applied to measure a true thermodynamic performance. This calls thermodynamics as a science of energy and entropy (first and second law). Environmental degradation caused due to the combustion of fossil fuels plants creates a need of carrying out a thermo-environmental analysis which makes thermodynamics a science of energy, entropy and environment. The results reported in the current thesis adopted this methodology of energy, exergy and environment in order to predict the thermo-environmental performance of gas turbine plant subjected to inlet air cooling along with evaporative after cooling. Incorporation of the heat exchangers to provide inlet air cooling and evaporative after cooling put a financial burden on the power plant engineer as the heat exchangers are quite expensive. Therefore, in order to confirm the economic viability of employing these heat exchangers in the gas turbine plant, thermo-environmental-economic analysis of the proposed gas turbine cycle need to be carried out. This future study will open the door for making the gas turbine plants efficient environment friendly and cost effective.

Appendix A

A.1 Vapor Compression Refrigeration Cycle

An ideal vapor-compression refrigeration cycle consists of four components namely compressor, condenser, expansion valve and evaporator. Its schematic is as shown in the Figure A.1 (a) and T-s diagram in the Figure A.1 (b). It consists of four processes:

1-2 Isentropic compression in a compressor

2-3 Constant-pressure heat rejection in a condenser

3-4 Isenthalpic throttling in an expansion device

4-1 Constant-pressure heat absorption in an evaporator

The refrigerant enters as the saturated vapor into the compressor where it is compressed isentropically (1-2) to the condenser pressure. During the isentropic compression, the temperature of the refrigerant increases as a result of increase in pressure. The superheated vapor condition refrigerant condenses in a condenser (2-3) and leaves as the saturated liquid at constant pressure. This temperature is still more than the ambient temperature. This high temperature liquid is throttled in an expansion valve to the evaporator pressure. The expansion process is assumed to occur at constant enthalpy. This expansion causes the temperature to fall below the refrigerated space allowing the heat exchange to occur between the refrigerant and space to cool. The refrigerant leaves the evaporator as a saturated vapor and cycle repeats thereafter [51]. In the mechanical chillers as discussed in 1.4.3 the refrigerant in the evaporator reduces the temperature of water that comes in after absorbing the sensible heat from the air.

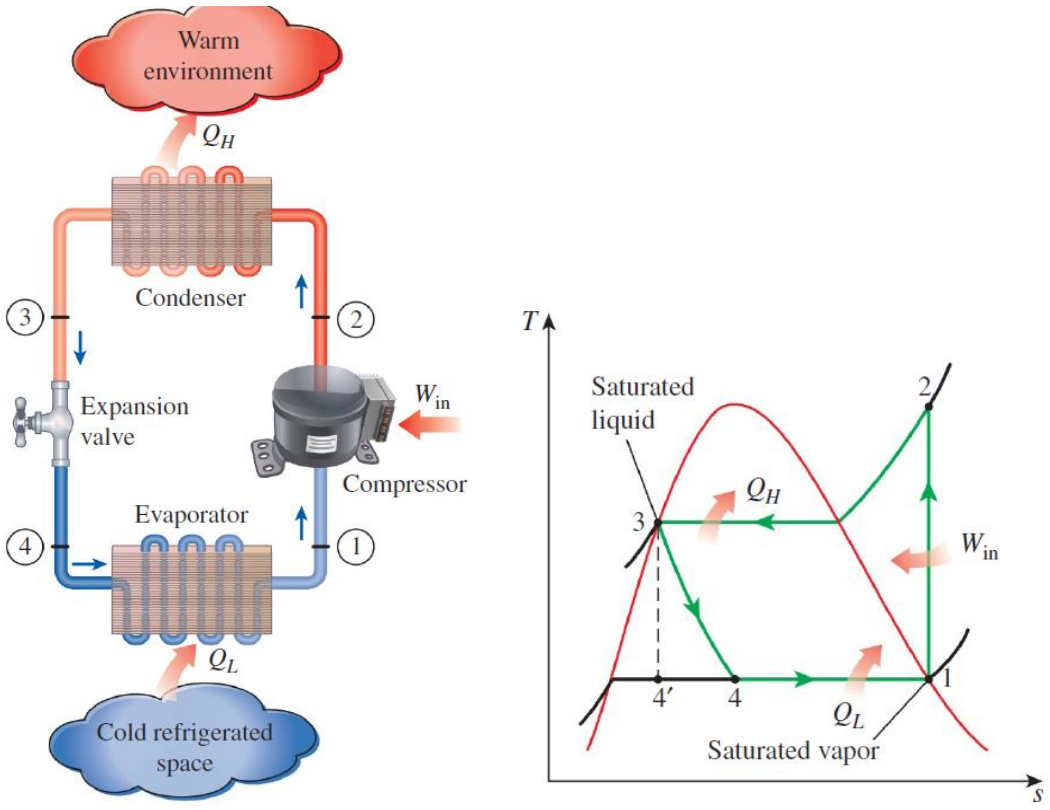

(a) **(b)**

Figure A.1 Ideal Vapor Compression Refrigeration Cycle (a) Schematic (b) T-s diagram [51]

A.2 Vapor Absorption Refrigeration Cycle

The most widely used vapor absorption refrigeration cycle is shown in the Figure A.2 Ammonia Vapor Absorption Refrigeration CycleFigure A.1 which uses ammonia (NH_3) and water (H_2O). Ammonia serves as a refrigerant whereas water as a transport medium. Other configurations such as Li-Br and water solution are possible too [100]. The system is similar to the vapor compression except the compressor is replaced with a complex absorption mechanism hence the name absorption. In the evaporator, ammonia leaves as a vapor and enters the absorber where NH_3-H_2O solution is formed after reacting with water. The water needs to be cooled down so that sufficient vapor could be absorbed.

This solution, known as the rich solution (high concentration of NH_3 – refrigerant) is pumped into the generator where energy is supplied in the form of thermal energy. This causes the ammonia to evaporate. Some of the water evaporates with ammonia. A rectifier separates the water from ammonia and returns it to the generator. The solution in the generator, known as the weak solution (low concentration of NH_3 – refrigerant) is sent to the absorber through a regenerator.

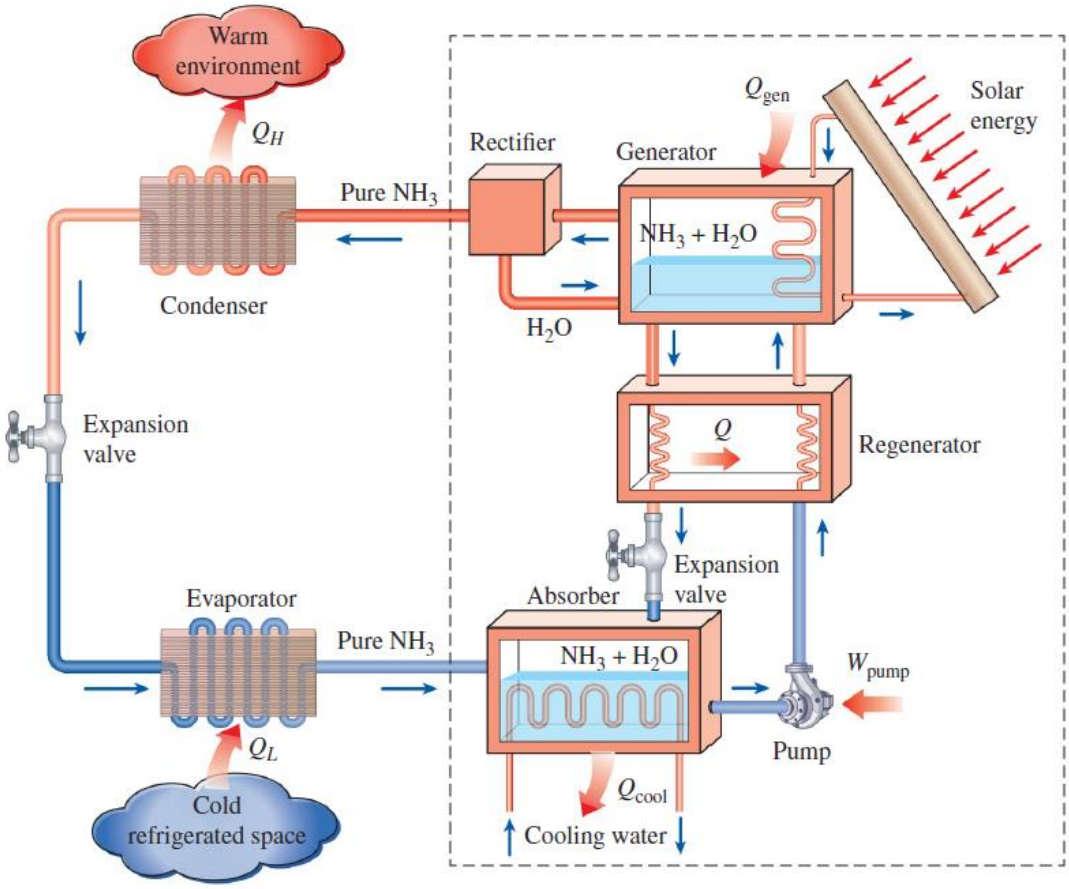

Figure A.2 Ammonia Vapor Absorption Refrigeration Cycle [51]

The hot and pressurized ammonia then passes through a condenser rejecting some of the heat to the atmosphere. This temperature at the exit would still be higher than the atmospheric temperature. Then, refrigerant is allowed to pass through an expansion valve

where the pressure is reduced to the evaporator pressure causing the temperature to drop less than the cold space. This facilitates the heat exchange between the cold space and the refrigerant NH_3. When NH_3 leaves the evaporator, it enters the absorber and the cycle repeats [51]. In the vapor chilling, steam is generally used as the thermal energy source in the generator as it is usually available from a combined gas turbine power plant or from heat recovery steam generator (HRSG).

A.3 Actual Combustion Reaction at Mean Operating Conditions

The following chain of reactions were found to occur in the subsequent zones of the combustors at TIT=1200 K, r=25, x=2.5, ϕ_0=50%, Φ=0.85, α=0.2, T_0=305 K, water heater surface area = 50 m^2, while remaining design parameters fixed as given in Table 6.

Combustion chamber:

$$[Fuel_{CC}] + [Air_{PZ,CC}] \rightarrow [Products_{PZ,CC}] + [Air_{IZ,CC}] \rightarrow [Products_{IZ,CC}] + [Air_{DZ,CC}] \rightarrow [Air_{RH}] \quad (A.1)$$

Reheater:

$$[Air_{PZ,RH}] + [Fuel_{RH}] \rightarrow [Products_{PZ,RH}] + [Air_{IZ,RH}] \rightarrow [Products_{IZ,RH}] + [Air_{DZ,RH}] \rightarrow [Products_{exhaust}] \quad (A.2)$$

The equation in exact amount of moles for the combustion chamber is found to be

$$[0.01246(0.96CH_4 + 0.02C_2H_6 + 0.006C_3H_8 + 0.003C_4H_{10} + 0.011N_2)] + [0.1424(0.7803N_2 + 0.2099O_2 + 0.00933Ar + 0.0047CO_2) + 0.02098H_2O] \rightarrow [0.01234CO_2 + 0.04613H_2O + 0.1113N_2 + 0.004731O_2 + 0.0004877CO + 1.77e -$$

$$7NO_2 + 8.88e-6NO + 1.8e-6(0.96CH_4 + 0.02C_2H_6 + 0.006C_3H_8 + 0.003C_4H_{10} + 0.011N_2) + 0.001329] + [0.1111(0.7803N_2 + 0.2099O_2 + 0.00933Ar + 0.0047CO_2) + 0.01636H_2O] \rightarrow [0.01282CO_2 + 0.06249H_2O + 0.198N_2 + 0.02781O_2 + 9.75e-6CO + 1.77e-7NO_2 + 8.88e-6NO + 0.002366Ar] + [0.2222(0.7803N_2 + 0.2099O_2 + 0.00933Ar + 0.0047CO_2) + 0.03272H_2O] \rightarrow [0.01283CO_2 + 0.09521H_2O + 0.07444O_2 + 0.3714N_2 + 5.57e-7CO + 1.77e-7NO_2 + 8.88e-6NO + 0.004439Ar] \quad (A.3)$$

Giving the mole fractions for the air going into the reheater as

$$y_{N_2} = 0.8019; y_{O_2} = 0.1608; y_{CO_2} = 0.02771; y_{Ar} = 0.009585; y_{CO} = 1.2e-6; y_{NO_2} = 3.8e-7; y_{NO} = 1.9e-5 \quad (A.4)$$

Giving the combustion equation in reheater as

$$[0.01163(0.96CH_4 + 0.02C_2H_6 + 0.006C_3H_8 + 0.003C_4H_{10} + 0.011N_2)] + [0.1424(0.8019N_2 + 0.1608O_2 + 0.009585Ar + 0.02771CO_2 + 1.2e-6CO + 3.8e-7NO_2 + 1.9e-5NO) + 0.03569H_2O] \rightarrow [0.01606CO_2 + 0.05916H_2O + 0.1393N_2 + 0.004555O_2 + 0.0007253CO + 6.98e-8NO_2 + 3.5e-6NO + 3.4e-6(0.96CH_4 + 0.02C_2H_6 + 0.006C_3H_8 + 0.003C_4H_{10} + 0.011N_2) + 0.001329] + [0.09651(0.8019N_2 + 0.1608O_2 + 0.009585Ar + 0.02771CO_2 + 1.2e-6CO + 3.8e-7NO_2 + 1.9e-5NO) + 0.01984H_2O] \rightarrow [0.01945CO_2 + 0.07901H_2O + 0.2167N_2 + 0.01971O_2 + 0.00001478CO + 1.067e-7NO_2 + 5.36e-6NO + 0.002589Ar] + [0.193(0.8019N_2 + 0.1608O_2 + 0.009585Ar + 0.02771CO_2 + 1.2e-6CO + 3.8e-7NO_2 + 1.9e-5NO) + 0.03969H_2O] \rightarrow [0.02481CO_2 +$$

$$0.1187H_2O + 0.05073O_2 + 0.3715N_2 + 1.07e-6CO + 1.804e-7NO_2 + 9.06e-6NO + 0.004439Ar] \quad (A.5)$$

Overall reaction in combustion chamber would then be

$$0.01246(0.96CH_4 + 0.02C_2H_6 + 0.006C_3H_8 + 0.003C_4H_{10} + 0.011N_2) + 0.4757(0.7803N_2 + 0.2099O_2 + 0.00933Ar + 0.0047CO_2) + 0.07006H_2O \rightarrow 0.01283CO_2 + 0.09521H_2O + 0.07444O_2 + 0.3714N_2 + 5.57e-7CO + 1.77e-7NO_2 + 8.88e-6NO + 0.004439Ar \quad (A.6)$$

And for the reheater would be

$$0.01163(0.96CH_4 + 0.02C_2H_6 + 0.006C_3H_8 + 0.003C_4H_{10} + 0.011N_2) + 0.4631(0.8019N_2 + 0.1608O_2 + 0.009585Ar + 0.02771CO_2 + 1.2e-6CO + 3.8e-7NO_2 + 1.9e-5NO) + 0.09521H_2O \rightarrow 0.02481CO_2 + 0.1187H_2O + 0.05073O_2 + 0.3715N_2 + 1.07e-6CO + 1.804e-7NO_2 + 9.06e-6NO + 0.004439Ar \quad (A.7)$$

A.4 Gulder's Approximate Formula

The flame temperature in the combustor could be approximated by

$$T_{ad} = A\sigma^{\alpha}.\exp(\beta(\sigma+\lambda)^2).\pi^x\theta^y\psi^z \quad (A.8)$$

For which

$$x = a_1 + b_1\sigma + c_1\sigma^2; \qquad y = a_2 + b_2\sigma + c_2\sigma^2; \qquad z = a_3 + b_3\sigma + c_3\sigma^2$$

$$\sigma = \phi \qquad \phi \leq 1$$

$$\sigma = \phi - 0.7 \qquad \phi > 1$$

$$\pi = \frac{p_{in}}{p_0}\ ; \qquad \theta = \frac{T_{in}}{T_0}; \qquad \psi = \frac{H}{C}\ in\ fuel; \tag{A.9}$$

$A, \alpha, \beta, \lambda, a_1, b_1, c_1, a_2, b_2, c_2, a_3, b_3, c_3$ are constants tabulated by Gulder [99].

References

[1] "Riyadh - Saudi Arabia Travel Weather Averages (Weatherbase)." [Online]. Available: http://www.weatherbase.com/weather/weather.php3?s=83404&refer=&units=us. [Accessed: 18-Apr-2017].

[2] A.-A. S. H. Hasnain S. M., Smiai M. S., Al-Ibrahim A. M., "Analysis of Electric Energy Consumption in an Office Building in Saudi Arabia," *Am. Soc. Heating, Refrig. Air-Conditioning Eng. Trans.*, vol. 106, pp. 173–184, 2000.

[3] "Gas Turbines in Saudi Arabia." [Online]. Available: www.us-sabc.org/files/public/powergen2012presentation.pdf%0A. [Accessed: 19-Apr-2017].

[4] "Saudi Electricity Company annual report. (2014). Electricity: growth and development in the Kingdom of Saudi Arabia."

[5] M. A. Darwish, H. K. Abdulrahim, A. A. Mabrouk, and A. S. Hassan, "Cogeneration Power-Desalting Plants Using Gas Turbine Combined Cycle," in *Desalination Updates*, InTech, 2015.

[6] V. Ganesan, *Gas Turbines*, Third. Tata McGraw-Hill Education, 2010.

[7] "How Gas Turbine Power Plants Work | Department of Energy." [Online]. Available: https://energy.gov/fe/how-gas-turbine-power-plants-work. [Accessed: 18-Apr-2017].

[8] "Density vs. Temperature." [Online]. Available: http://www.ce.utexas.edu/prof/kinnas/319LAB/Book/CH1/PROPS/densgif.html.

[Accessed: 18-Apr-2017].

[9] A. P. Santos and C. R. Andrade, “Analysis of Gas Turbine Performance with Inlet Air Cooling Techniques Applied to Brazilian Sites,” *J. Aerosp. Technol. Manag.*, vol. 4, no. 3, pp. 341–354, 2012.

[10] M. M. Alhazmy and Y. S. H. Najjar, “Augmentation of gas turbine performance using air coolers,” *Appl. Therm. Eng.*, vol. 24, no. 2–3, pp. 415–429, 2004.

[11] “Turbine Inlet Air Chilling | TIAC | Gas Turbine Inlet Cooling Systems.” [Online]. Available: http://www.stellar-energy.net/what-we-do/solutions/turbine-inlet-air-chilling.aspx. [Accessed: 19-Apr-2017].

[12] “GE Inlet air cooling.” [Online]. Available: http://site.ge-energy.com/businesses/ge_oilandgas/en/literature/en/downloads/inletair_cooling.pdf. [Accessed: 19-Apr-2017].

[13] “How Evaporative Cooling Works Evaporative air conditioning uses only water and moving air to cool using the principles of evaporation...[col=200].” [Online]. Available: http://www.breezair.com/us/why-evaporative/how-evaporative-works. [Accessed: 19-Apr-2017].

[14] R. S. Johnson, “The Theory and Operation of Evaporative Coolers For Industrial Gas Turbine Installations,” *J. Eng. Gas Turbines Power*, vol. 111, no. 2, pp. 1–9, 1989.

[15] “what-is-fog-cooling.” [Online]. Available: https://www.google.com.sa/_/chrome/newtab?espv=2&ie=UTF-8. [Accessed: 19-Apr-2017].

[16] K. N. Abdalla and Z. A. M. Adam, “Enhancing gas turbine output through inlet air

cooling," *Sudan Eng.Soc.J*, vol. 52, no. 4–6, pp. 7–14, 2006.

[17] M. Ameri and S. H. Hejazi, "The study of capacity enhancement of the Chabahar gas turbine installation using an absorption chiller," *Appl. Therm. Eng.*, vol. 24, no. 1, pp. 59–68, 2004.

[18] I. S. Ondryas, "Go beyond evaporative coolers to stretch gas-turbine output," *Power*, vol. 135, no. 7, pp. 27–29, 1991.

[19] A. M. Bassily, "Effects of evaporative inlet and aftercooling on the recuperated gas turbine cycle," *Appl. Therm. Eng.*, vol. 21, no. 18, pp. 1875–1890, Dec. 2001.

[20] N. GašparoviC and J. G. Hellemans, "Gas turbines with heat exchanger and water injection in the compressed air," *Arch. Proc. Inst. Mech. Eng. 1847-1982 (vols 1-196)*, vol. 185, no. 1970, pp. 953–962, Jun. 1970.

[21] A. H. Lefebvre and D. R. Ballal, *Gas turbine combustion : alternative fuels and emissions*. Taylor & Francis, 2010.

[22] B. Brunekreef and S. T. Holgate, "Air pollution and health," *Lancet*, vol. 360, no. 9341, pp. 1233–1242, 2002.

[23] A. Seaton, D. Godden, W. MacNee, and K. Donaldson, "Particulate air pollution and acute health effects," *Lancet*, vol. 345, no. 8943, pp. 176–178, Jan. 1995.

[24] B. R. Gurjar, L. T. Molina, and C. S. P. Ojha, *Air pollution : health and environmental impacts*. CRC Press, 2010.

[25] "Environmental Protection Agency 40 CFR Part 60 Standards of Performance for Stationary Gas Turbines; Standards of Performance for Stationary Combustion Turbines; Proposed Rule," *Fed. Regist.*, vol. 77, no. 168, 2012.

[26] Environmental Protection and Control Department, "Royal Comission

Environmental Regulations," Saudi Arabia, 2015.

[27] I. Dincer and M. Rosen, *Exergy: energy, environment and sustainable development*. 2012.

[28] A. Bejan, "Fundamentals of exergy analysis, entropy generation minimization, and the generation of flow architecture," *Int. J. Energy Res.*, vol. 26, no. 7, pp. 545–565, 2002.

[29] J. Szargut, D. Morris, and F. Steward, *Exergy analysis of thermal, chemical, and metallurgical processes*. 1987.

[30] M. A. Rosen, "Second-Law Analysis : Approaches and Implications," vol. 429, no. October 1998, pp. 415–429, 1999.

[31] M. J. Moran and E. Sciubba, "Exergy Analysis : Principles and Practice," *J. Eng. Gas Turbines Power*, vol. 116, no. April, pp. 285–290, 1994.

[32] A. Al-Ibrahim and A. Varnham, "A review of inlet air-cooling technologies for enhancing the performance of combustion turbines in Saudi Arabia," *Appl. Therm. Eng.*, 2010.

[33] B. Dawoud, Y. H. Zurigat, and J. Bortmany, "Thermodynamic assessment of power requirements and impact of different gas-turbine inlet air cooling techniques at two different locations in Oman," *Appl. Therm. Eng.*, vol. 25, no. 11, pp. 1579–1598, 2005.

[34] M. M. Alhazmy, R. K. Jassim, and G. M. Zaki, "Performance enhancement of gas turbines by inlet air-cooling in hot and humid climates," *Int. J. Energy Res.*, vol. 30, no. 10, pp. 777–797, Aug. 2006.

[35] C. Yang, Z. Yang, and R. Cai, "Analytical method for evaluation of gas turbine

inlet air cooling in combined cycle power plant," *Appl. Energy*, vol. 86, no. 6, pp. 848–856, 2009.

[36] A. M. Al-Amiri and M. M. Zamzam, "Systematic Assessment of Combustion Turbine Inlet Air-Cooling Techniques," *J. Eng. Gas Turbines Power*, vol. 127, no. 1, p. 159, 2005.

[37] A. K. Mohapatra and Sanjay, "Analysis of Combined Effects of Air Transpiration Cooling and Evaporative Inlet Air Cooling on the Performance Parameters of a Simple Gas Turbine Cycle," *J. Energy Eng.*, vol. 141, no. 3, p. 4014015, Sep. 2015.

[38] D. Pandelidis, S. Anisimov, W. M. Worek, and P. Drąg, "Comparison of desiccant air conditioning systems with different indirect evaporative air coolers," *Energy Convers. Manag.*, vol. 117, pp. 375–392, 2016.

[39] S. Sanaye and M. Tahani, "Analysis of gas turbine operating parameters with inlet fogging and wet compression processes," *Appl. Therm. Eng.*, vol. 30, no. 2, pp. 234–244, 2010.

[40] K. H. Kim and K. Kim, "Exergy Analysis of Overspray Process in Gas Turbine Systems," *Energies*, vol. 5, no. 12, pp. 2745–2758, Jul. 2012.

[41] G. Comodi, M. Renzi, F. Caresana, and L. Pelagalli, "Enhancing micro gas turbine performance in hot climates through inlet air cooling vapour compression technique," *Appl. Energy*, vol. 147, pp. 40–48, 2015.

[42] A. K. Mohapatra and Sanjay, "Analysis of parameters affecting the performance of gas turbines and combined cycle plants with vapor absorption inlet air cooling," *Int. J. Energy Res.*, vol. 38, no. 2, pp. 223–240, Feb. 2014.

[43] S. M. S. Mahmoudi, V. Zare, F. Ranjbar, and L. G. Farshi, “Energy and Exergy Analysis of Simple and Regenerative Gas Turbines Inlet Air cooling Using Absorption Refrigeration,” *J. Appl. Sci.*, vol. 9, no. 13, pp. 2399–2407, 2009.

[44] G. Zhang, J. Zheng, Y. Yang, and W. Liu, “A novel LNG cryogenic energy utilization method for inlet air cooling to improve the performance of combined cycle,” *Appl. Energy*, vol. 179, pp. 638–649, 2016.

[45] M. Farzaneh-Gord and M. Deymi-Dashtebayaz, “Effect of various inlet air cooling methods on gas turbine performance,” *Energy*, vol. 36, no. 2, pp. 1196–1205, 2011.

[46] A. Khaliq, K. Choudhary, and I. Dincer, “Energy and exergy analyses of compressor inlet air-cooled gas turbines using the Joule—Brayton refrigeration cycle,” *Proc. Inst. Mech. Eng. Part A J. Power Energy*, vol. 223, no. 1, pp. 1–9, Feb. 2009.

[47] R. K. Jassim, G. M. Zaki, and M. M. Alhazmy, “Energy and exergy analysis of reverse Brayton refrigerator for Gas Turbine power boosting,” *Int. J. Exergy*, vol. 6, no. 2, p. 143, 2009.

[48] A. Khaliq, “Energetic and Exergetic Performance Evaluation of a Gas Turbine–Powered Cogeneration System Using Reverse Brayton Refrigeration Cycle for Inlet Air Cooling,” *J. Energy Eng.*, vol. 142, no. 3, p. 4015029, Sep. 2016.

[49] T. Heppenstall, “Advanced gas turbine cycles for power generation: a critical review,” *Appl. Therm. Eng.*, vol. 18, no. 9, pp. 837–846, 1998.

[50] I. Roumeliotis and K. Mathioudakis, “Evaluation of water injection effect on compressor and engine performance and operability,” *Appl. Energy*, vol. 87, no. 4,

pp. 1207–1216, 2010.

[51] Y. Cengel and M. Boles, *Thermodynamics: an engineering approach*, Eighth Edi. New York: McGraw-Hill, 2015.

[52] Sanjay and B. N. Prasad, "Energy and exergy analysis of intercooled combustion-turbine based combined cycle power plant," *Energy*, vol. 59, pp. 277–284, 2013.

[53] A. K. Shukla and O. Singh, "Performance evaluation of steam injected gas turbine based power plant with inlet evaporative cooling," *Appl. Therm. Eng.*, vol. 102, pp. 454–464, 2016.

[54] A. Khaliq and K. Choudhary, "Thermodynamic performance assessment of an indirect intercooled reheat regenerative gas turbine cycle with inlet air cooling and evaporative aftercooling of the compressor discharge," *Int. J. Energy Res.*, vol. 30, no. 15, pp. 1295–1312, Dec. 2006.

[55] A. Khaliq and K. Choudhary, "Exergy analysis of the regenerative gas turbine cycle using absorption inlet cooling and evaporative aftercooling," *J. Energy Inst.*, vol. 82, no. 3, pp. 159–167, Sep. 2009.

[56] A. Khaliq and I. Dincer, "Energetic and exergetic performance analyses of a combined heat and power plant with absorption inlet cooling and evaporative aftercooling," *Energy*, vol. 36, no. 5, pp. 2662–2670, 2011.

[57] S. M. CORREA, "A Review of NO_x Formation Under Gas-Turbine Combustion Conditions," *Combust. Sci. Technol.*, vol. 87, no. 1–6, pp. 329–362, Jan. 1993.

[58] D. Sullivan and P. Mas, "A Critical Review of NOx Correlations for Gas Turbine Combustors," *ASME Turbo Expo Power Land, Sea, Air*, no. 80005, p. V001T01A002, 1975.

[59] H. Cole and J. Summerhays, “A Review of Techniques Available for Estimating Short-Term NO2 concentrations,” *J. Air Pollut. Control Assoc.*, vol. 29, no. 8, pp. 812–817, 1979.

[60] D. Lee, J. Park, J. Jin, and M. Lee, “A simulation for prediction of nitrogen oxide emissions in lean premixed combustor,” *J. Mech. Sci. Technol.*, vol. 25, no. 7, p. 1871, 2011.

[61] W. R. Bussman and C. E. Baukal, “Ambient conditions impact CO and NOx emissions: Part I,” *Pet. Technol. Q.*, vol. 14, no. 4, pp. 37–41, 2009.

[62] Z. Li, Y. Liu, Z. Chen, Q. Zhu, J. Jia, J. Li, Z. Wang, and Y. Qin, “Effect of the air temperature on combustion characteristics and NO x emissions from a 0.5 MW pulverized coal-fired furnace with deep air staging,” *Energy and Fuels*, vol. 26, no. 4, pp. 2068–2074, 2012.

[63] W. R. Bussman and C. E. Baukal, “Ambient conditions impact CO and NOx emissions: Part II,” *Pet. Technol. Q.*, vol. 14, no. 4, pp. 37–41, 2009.

[64] N. K. Rizk and H. C. Mongia, “Semianalytical Correlations for NOx, CO, and UHC Emissions,” *J. Eng. Gas Turbines Power-Transactions ASME* , vol. 115, no. 3, pp. 612–619, 1993.

[65] S. A. Klein, “Engineering Equation Solver (EES) for Microsoft Windows Operating System: Academic Professional Version,” *F-Chart Software, Madison, WI*. 2012.

[66] A. M. Bassily, “Performance improvements of the intercooled reheat recuperated gas-turbine cycle using absorption inlet-cooling and evaporative after-cooling,” *Appl. Energy*, vol. 77, no. 3, pp. 249–272, 2004.

[67] M. J. Moran, H. N. Shapiro, D. D. Boettner, and M. B. Bailey, *Fundamentals of Engineering Thermodynamics,* 7th ed. John Wiley & Sons, 2011.

[68] M. J. Moran and E. Sciubba, "Exergy Analysis: Principles and Practice," *J. Eng. Gas Turbines Power,* vol. 116, no. 2, pp. 285–290, 1992.

[69] P. Ahmadi, M. A. Rosen, and I. Dincer, "Greenhouse gas emission and exergo-environmental analyses of a trigeneration energy system," *Int. J. Greenh. Gas Control*, vol. 5, no. 6, pp. 1540–1549, 2011.

[70] S. R. Turns and D. R. Kraige, *Properties Tables Booklet for Thermal Fluids Engineering*. New York: Cambridge University Press, 2007.

[71] J. Mcbride and A. Reno, "Coefficients Thermodynamic Properties for Calculating and Transport of Individual Species," *Nasa Tech. Memo.*, vol. 4513, no. NASA-TM-4513, p. 98, 1993.

[72] J. Michael and N. Howard, *Fundamentals of engineering thermodynamics*. 2011.

[73] O. K. Singh, "Combustion simulation and emission control in natural gas fuelled combustor of gas turbine," *J. Therm. Anal. Calorim.*, vol. 125, no. 2, pp. 949–957, Aug. 2016.

[74] "Gas Analysis." [Online]. Available: https://www.enbridgegas.com/assets/docs/Victoria Square Stn No 50139 January.pdf. [Accessed: 22-Apr-2017].

[75] L. R. Glicksman, "Air Water Vapor Mixtures: Psychrometrics," 1996. [Online]. Available: https://ocw.mit.edu/courses/architecture/4-42j-fundamentals-of-energy-in-buildings-fall-2010/readings/MIT4_42JF10_water_vapor.pdf. [Accessed: 26-Apr-2017].

[76] R. W. Hyland and A. Wexter, “Formulations for the thermodynamic properties of the saturated phases of H2O from 173.15 K to 473.15 K,” *ASHRAE Trans.*, vol. 89, pp. 500–519, 1983.

[77] J. M. Smith and H. C. Van Ness, *Introduction to chemical engineering thermodynamics*, Seventh. McGraw-Hill, 2010.

[78] W. Wagner, “The IAPWS Formulation 1995 for the Thermodynamic Properties of Ordinary Water Substance for General and Scientific Use,” *J. Phys. Chem. Ref. Data*, vol. 31, no. 2, p. 387, 1999.

[79] J. R. Cooper, Q. Mary, M. E. Road, and S. I. Associates, “The International Association for the Properties of Water and Steam Revised Release on the IAPWS Industrial Formulation 1997 for the Thermodynamic Properties of Water and Steam 1 Nomenclature 3 Reference Constants 9 Basic Equation for Region 5 10 . 1 Cons,” vol. 97, no. August 2007, 2012.

[80] “Combustors, Afterburners,” 1992. [Online]. Available: https://ocw.mit.edu/courses/aeronautics-and-astronautics/16-50-introduction-to-propulsion-systems-spring-2012/lecture-notes/MIT16_50S12_lec34.pdf. [Accessed: 26-Apr-2017].

[81] H. Saravanamuttoo, G. Rogers, and H. Cohen, *Gas turbine theory*, Fifth. Pearson Education, 2001.

[82] Y. Cengel and R. Turner, *Fundamentals of thermal-fluid sciences*, Second. McGraw-Hill, 2005.

[83] S. Kakac, H. Liu, and A. Pramuanjaroenkij, *Heat exchangers: selection, rating, and thermal design*, Third. CRC Press, 2012.

[84] D. F. Elger, B. A. LeBret, C. T. Crowe, and J. A. Roberson, *Engineering fluid mechanics*, Eleventh. John Wiley & Sons, Inc, 2016.

[85] A. Kumari and Sanjay, "Thermo-environmental Analysis of Recuperated Gas Turbine-Based Cogeneration Power Plant Cycle," *Arab. J. Sci. Eng.*, vol. 41, no. 2, pp. 691–709, 2016.

[86] T. Korakianitis and D. G. Wilson, "Models for Predicting the Performance of Brayton-Cycle Engines," *J. Eng. Gas Turbines Power*, vol. 116, no. 2, pp. 381–388, 1994.

[87] T. L. Bergman, F. P. Incropera, D. P. DeWitt, and A. S. Lavine, *Fundamentals of heat and mass transfer, 2nd edition*, Seventh. John Wiley & Sons, 2011.

[88] K. Wark, *Advanced thermodynamics for engineers*. McGraw-Hill, 1995.

[89] R. S. Benson and W. A. Woods, *Advanced Engineering Thermodynamics*, Second. Pergamon, 1977.

[90] P. Ahmadi, M. A. Rosen, and I. Dincer, "Greenhouse gas emission and exergo-environmental analyses of a trigeneration energy system," *Int. J. Greenh. Gas Control*, vol. 5, no. 6, pp. 1540–1549, 2011.

[91] A. Bejan, *Advanced engineering thermodynamics*, Fourth. Wiley, 2016.

[92] S. de Oliveira, *Exergy: Production, cost and renewability*, First. London: Springer, 2013.

[93] P. Ahmadi and I. Dincer, "Exergoenvironmental analysis and optimization of a cogeneration plant system using Multimodal Genetic Algorithm (MGA)," *Energy*, vol. 35, no. 12, pp. 5161–5172, 2010.

[94] A. H. Lefebvre, "Fuel Effects on Gas Turbine Combustion - Liner Temperature,

Pattern Factor and Pollutant Emissions.," *AIAA/SAE/ASME 20th Jt. Propuls. Conf.*, vol. Cincinnati, no. 11, 1984.

[95] D. B. Olsen, M. Kohls, and G. Arney, "Impact of oxidation catalysts on exhaust NO2/NOx ratio from lean-burn natural gas engines.," *J. Air Waste Manag. Assoc.*, vol. 60, no. October 2014, pp. 867–874, 2010.

[96] S. Han, H. Bian, Y. Feng, A. Liu, X. Li, F. Zeng, and X. Zhang, "Analysis of the relationship between O3, NO and NO2 in Tianjin, China," *Aerosol Air Qual. Res.*, vol. 11, no. 2, pp. 128–139, 2011.

[97] P. L. Hanrahan, "The Plume Volume Molar Ratio Method for Determining NO 2 /NO x Ratios in Modeling—Part II: Evaluation Studies," *J. Air Waste Manage. Assoc.*, vol. 49, no. 11, pp. 1332–1338, 1999.

[98] H. S. Cole and J. E. Summerhays, "A Review of Techniques Available for Estimating Short-Term NO 2 concentrations," *J. Air Pollut. Control Assoc.*, vol. 29, no. 8, pp. 812–817, 1979.

[99] L. Gulder, "Flame Temperature Estimation of Conventional and Future Jet Fuels 6.," vol. 108, no. April 1986, 2016.

[100] "Absorption Cooling Cycle | Refrigerator Troubleshooting Diagram." [Online]. Available: http://www.refrigeratordiagrams.com/air-conditioning/absorption-cooling-cycle.html. [Accessed: 19-Apr-2017].

Vitae

Name	Suleman Mohammed
Nationality	Indian
Date of Birth	1/10/1992
Email	mohd.suleman.hyd@gmail.com
Address	H.No: 17-8-532, Chanchalguda, Hyderabad, India - 500024
Academic Background	MS in Mechanical Engineering (May 2017) King Fahd University of Petroleum and Minerals Bachelor of Engineering (May 2014) Osmania University
Publications	Thermo-environmental analysis of a three zone combustion chamber fueled with natural gas to estimate the concentrations in the exhaust. (To be submitted) Exergo-environmental analysis of a combustion gas turbine cycle subjected to inlet air cooling and evaporative after cooling. (To be submitted)